# Investigating the host-directed therapeutic potential of curdlan-functionalised PLGA nanoparticles in the treatment of intracellular *Mycobacterium tuberculosis*

by
Su-Mari du Plessis


*Thesis presented in partial fulfilment of the requirements for the degree Master of Science in Molecular Biology in Medicine and Health Sciences at Stellenbosch University*

Supervisor: Professor Samantha Sampson
Co-supervisor: Professor Admire Dube

March 2020

## Declaration

By submitting this thesis electronically, I declare that the entirety of the work contained therein is my own, original work, that I am the sole author thereof (save to the extent explicitly otherwise stated), that reproduction and publication thereof by Stellenbosch University will not infringe any third party rights and that I have not previously in its entirety or in part submitted it for obtaining any qualification.

March 2020

## Abstract

Despite the availability of antibacterial agents, tuberculosis (TB) remains the leading cause of death by a single infectious agent globally, accounting for millions of deaths annually. The high mortality and morbidity rates are associated with antibiotic resistance and tolerance. Further, *Mycobacterium tuberculosis*, the causative agent of TB, has successfully evolved various strategies to evade an antibacterial immune response. *M. tuberculosis* infection is a continuous interaction between the host and the bacterium. An improved fundamental understanding of how this bacterium can survive within host immune cells has paved the way for the development of host directed therapies (HDT) that utilize a different approach to conventional antibiotics; and such strategies are desperately required for the eradication of TB.

HDT is an approach targeted at the host immune system instead of *M. tuberculosis* itself. By targeting the host immune system, there is potential to restrict the possible acquisition of genetic resistance, since the bacteria itself is not the target. To favour a protective immune response at the molecular level, immunotherapeutic nanoparticles (NPs) are being exploited. NPs are particulate structures at the nanoscale (1 – 1000 nm) with the ability to target specific cells, with such targeting achieved through modification of the surface of the NP with bioactive ligands. By targeting specific cells, the NPs can localize at the pathogen infected site and elicit an antibacterial response through ligand-receptor interactions.

In this study, to target *M. tuberculosis*-infected macrophages (primary host immune cells), poly(lactide-co-glycolide) (PLGA) NPs were functionalised with curdlan, an immune-stimulatory polysaccharide known to target the dectin-1 receptor expressed on macrophages. Curdlan-dectin-1 interactions are known to stimulate the NF-kβ pathway that produces bactericidal factors such as oxidative species and pro-inflammatory cytokines and activate downstream pathways capable of killing intracellular bacilli. Thus, it is hypothesized that the introduction of curdlan-functionalised PLGA (C-PLGA) NPs to *M. tuberculosis* infected macrophages will stimulate the cells, leading to the death of the intracellular bacilli.

Four different formulations were synthesized containing different curdlan loads and these included PLGA, 2%, 5% and 8% w/w C-PLGA NPs. Dynamic light scattering data confirmed the particles to be in the nano-size range with a negative zeta potential. The cytotoxicity of the NPs towards RAW264.7 macrophages was assessed using the MTT assay over 72h. Macrophages infected with *M. tuberculosis* ΔleuDΔpanD::pMV306hsp+lux expressing the bacterial luciferase gene, were used to assess the killing efficacy of the NPs (using luminescence as a proxy for cell numbers, with confirmatory colony forming unit (CFU) plating). While CFU data showed a trend towards reduction in *M. tuberculosis* bacterial numbers compared to untreated control following NP treatment, interpretation of results was cofounded by possible macrophage lysis, and this will require further investigation. Cytokine quantification highlighted the immune stimulating capabilities of the curdlan-functionalised NPs and upregulation of TNF-α was detected after 72h. The findings of this study support the hypothesis that C-PLGA NPs can stimulate *M. tuberculosis* infected macrophages, potentially leading to death of intracellular *M. tuberculosis*. This demonstrates the potential of C-PLGA NPs to be further developed as a HDT for TB.

## Opsomming

Ten spyte van beskikbare antibakteriële middels, bly tuberkulose (TB) die grootste oorsaak van sterftes deur 'n enkele infektiewe agent wêreldwyd en lei tot miljoene sterftes jaarliks. Die hoë mortaliteit en morbiditeit syfers word geassosieer met antibiotika weerstandigheid en verdraagsaamheid. Verder het *Mycobacterium tuberculosis*, die oorsaak van TB, verskeie strategieë ontwikkel om 'n antibakteriële immuunrespons suksesvol te ontduik. *M. tuberculosis* infeksies is 'n deurlopende interaksie tussen die gasheer en die bakterieë. ‘n Goeie begrip oor hoe hierdie bakterieë kan oorleef binne die gasheer se immuunselle het die weg gebaan vir die ontwikkeling van gasheer-gerigte terapie wat 'n ander benadering tot konvensionele antibiotika gebruik.

Gasheer-gerigte terapie is 'n benadering wat direk gerig is op die gasheer se immuunsisteem in plaas van *M. tuberculosis* self. Deur die gasheer se immuunstelsel te teiken, is dit moontlik om die ontwikkeling van genetiese weerstand te beperk, aangesien die bakterieë self nie geteikin word nie. Om die immuunrespons op ‘n molekulêre vlak te kan beheer, word immunoterapeutiese nanopartikels (NPs) ingespan. NPs is baie klein strukture op die nanoskaal (1 – 1000 nm) met die vermoë om spesifieke selle te teiken. Dit word moontlik gemaak deur die oppervlak van die NP met bioaktiewe molekules te verweisig. Dus, deur spesifieke selle te teiken, kan die NPs ‘n gelokaliseerde antibakteriële reaksie ontlok deur middel van ligand-reseptor interaksies.

Om *M. tuberculosis*-geïnfekteerde makrofage te teiken (primêre gasheer sel) word poly(lactide-co-glycolide) (PLGA) NPs geweisig met curdlan, 'n immuun-stimulerende polisakkaried gerig to die dectin-1 reseptor op die oppervlak van makrofage. Curdlan-dectin-1 interaksies stimuleer die NF-kβ weg wat lei tot die vrystellling van verskeie antibakteriële faktore soos oksidatiewe spesies en pro-inflammatoriese molekules en gevolgelik verskeie paaie stroomaf aktiveer wat in staat is om intrasellulêre patogene dood te maak. Die hipotese is dus dat die aanwending van curdlan-geweisigde PLGA (C-PLGA) NPs geïnfekteerde immunselle sal stimuleer, wat lei tot die dood van die intrasellulêre bakterieë.

Vier verskillende NP formulerings is geproduseer met verskillende hoeveelhede curdlan en sluit in PLGA, 2%, 5% en 8% C-PLGA NPs. Dinamiese lig verstrooiing (DLV) data het bevestig dat die NPs van nano-grootte is met 'n negatiewe zeta potensiaal en stabiel voorkom in ‘n oplossing. Die sellulêre toksisiteit van die NPs is geassesseer oor 72 uur op RAW264.7 makrofage deur middel van die MTT toets. Makrofage is geïnfekteer met *M. tuberculosis* ΔleuDΔpanD::pMV306hsp + Lux wat ons in staat stel om die groei inhiberende potensiaal van die NPs te meet deur verandering in luminessensie te gebruik as ‘n aanduiding van seldood gevolg deur die tel van kolonie vormende eenhede (KVE). Terwyl KVE data 'n afname in *M. tuberculosis* selgetalle toon vir die NP behandelde selle in vergelyking met luminessensie is die resultate verwarrend moontlik as gevolg van die makrofage wat liseer en dus sal dit verdere ondersoek vereis. Sitokien kwantifisering het die immuunstimulerende vermoëns van die curdlan-verweisigde NPs uitgelig en ‘n verhoogde uitdrukking van TNF-α is na 72 uur opgespoor. Die bevindinge van hierdie studie ondersteun die hipotese dat C-PLGA NPs ‘n immuunresponse kan stimuleer in *M. tuberculosis* geïnfekteerde makrofage en dus lei tot 'n dood van intrasellulêre patogene. Dit toon die potensiaal van C-PLGA-NPs om verder as 'n gasheer-gerigte terapie vir TB ontwikkel te word.

## Acknowledgments

I would like to sincerely say thank you to the following people that continued to be my ultimate supporters throughout this process:

- To my supervisor, Prof. Samantha Sampson. A "thank you" is not nearly enough to justify what you meant to me and this project but here goes. Thank you for understanding me better than I could understand myself and dealing with the language gap that arose in very inconvenient times. Thank you for always being willing to listen and brainstorm, the knowledge cropped up within you is something incredible. Thank you for being the best example of what a mentor should be, I feel privileged to have been under your wing for the past two years. You are exactly who young scientists want to be when they grow up! Thank you for pushing me, believing in me and sharing your love of dogs with me. I will always be grateful. Thank you for sharing your love for science with the world!

- To my co-supervisor, Prof. Admire Dube. Thank you for always being there to help, assist and brainstorm. Thank you for being one of the most positive people I have ever come across, it rubs off, trust me. Thank you for sharing your love for nanomedicine with me, the passion for this is clearly visible and inspiring.

- To my lab members, thank you for being a part of this project, either directly or not I appreciate it more than you will know.

- To my friends, family and most importantly parents. Thank you for being my backbone and for supporting me and loving me and just being present! You were instrumental in getting me through this degree. Ek is baie lief vir julle!

- I would like to say thank you to my funders, the National Research Foundations (NRF) for their contribution.

## List of Publications

Raymonde B. Bekale, **Su-Mari Du Plessis**, Nai-Jen Hsu, Jyoti R. Sharma, Samantha L. Sampson, Muazzam Jacobs, Mervin Meyer, Gene D. Morse, Admire Dube. *Mycobacterium Tuberculosis* and Interactions with the Host Immune System: Opportunities for Nanoparticle Based Immunotherapeutics and Vaccines.

**Pharmaceutical Research.** 2019. Vol 36. DOI:10.1007/s11095-018-2528-9

## List of symbols and abbreviations

**α** alpha

**γ** gamma

**β** beta

**AA** Arachidonic acid

**AG** Arabinogalactan

**APCs** Antigen presenting cells

**ATP** Adenosine triphosphate

**BCG** Bacillus Calmette-Guerin

**CaM** Calmodulin

**CFU** Colony forming unit

**CLRs** C-type lectin receptors

**CORVET** Core vacuole/endosome tether

**DCs** Dendritic cells

**EEAI** Early endosomal antigen 1

**ER** Endoplasmic reticulum

**HBHA** Heparin binding hemagglutinin adhesion protein

**HIV** Human immunodeficiency virus

**IFN** Interferon

**IL** Interleukin

**IMCs** Immune modulating compounds

**INH** Isoniazid

**ISO** International Organization for Standardization

**LAMP** Lysosome-associated membrane proteins

**LBPA** Lysobisphosphatidic acid

**LM** Lipomannan

**LTBI** Latent tuberculosis infection

***M. tuberculosis*** *Mycobacterium tuberculosis*

**Man-LAM** Mannosylated-lipoarabinomannan

**MAs** Mycolic acids

**MDR-TB** Multi-drug resistant tuberculosis

**mg** Milligram

**MHC** Major histocompatibility complex

**mL** Millilitre

**MPs** Macrophages

**mV** Millivolts

**NLRs** Nod-like receptors

**nm** Nanometer

**NO** Nitric oxide

**NPs** Nanoparticles

**NRP** Non-replicating persistent

**PA** Phosphatidic acid

**PAMPs** Pathogen associated molecular patterns

**PCL** Polycaprolactone

**PDI** Polydispersity index

**PG** Peptidoglycan

**PI5P** Phosphatidylinositol 5-phosphate

**PIM** Phosphatidylinositol mannoside

**PIP3** Phosphatidylinositol 3-phosphate

**PLGA** Poly(lactide-co-glycolide)

**PRRs** Pattern recognition receptors

**PS** Phosphatidylserine

**PtpA** Protein tyrosine phosphatase

**RIF** Rifampicin

**ROS/RNS** Reactive oxygen and nitrogen species

**rpm** Revolutions per minute

**SIP** Sphingosine-1-phosphate

**SPK** Sphingosine kinase

**TB** Tuberculosis

**TDR-TB** Totally-drug resistant tuberculosis

**TLRs** Toll-like receptors

**VPS33B** Vacuolar Protein Sorting 33B

**WHO** World Health Organization

**XDR** Extensively-drug resistant

**XDR-TB** Extensively-drug resistant tuberculosis

**°C** Degrees Celsius

**mg/mL** Milligram per millilitre

**µg/mL** Micrograms per millilitre

**pg/mL** Picogram per millilitre

**µL** Microliters

**w/w** weight for weight

**w/v** weight for volume

**%** Percentage

## List of equations

# List of tables

## Chapter 3



## Chapter 4



# List of figures

## Chapter 1



## Chapter 2



## Chapter 3

**Chapter 4**



## Table of contents

# Chapter 1

# General introduction

The introductory chapter sets the tone for the rest of the thesis and highlights the need for novel therapeutic approaches against Tuberculosis. Chapter 1 also states the problem, contains the hypotheses as well as the aims and objectives on how we intend to achieve our goal.

My contribution: Comprehensive search of relevant literature

## 1.1 Background

### 1.1.1 Tuberculosis and current therapeutic approaches

Despite the widespread availability of various antibiotics, tuberculosis (TB) still poses a significant threat to global health. More than a century after Robert Koch identified *Mycobacterium tuberculosis* as the causative agent of TB, this bacterium is still classified as the deadliest infectious agent globally (Barberis *et al.*, 2017; WHO, 2019). The World Health Organization (WHO) estimates that in 2017 alone, there were a reported 10 million cases of TB and that 1.6 million people passed away due to the disease (WHO, 2018). An overwhelming 87% of all TB cases accounted for globally can be attributed to just 30 countries. These countries include India (27%), China (9%), Indonesia (8%), the Philippines (6%), Pakistan (5%), Nigeria (4%), Bangladesh (4%) and South Africa (3%) (WHO, 2018). Notably, these high burden countries are predominantly located on continents infamous in large parts for overcrowding, poverty, poor nutrition and high levels of Human Immunodeficiency Virus (HIV) infections. The aforementioned issues are some of the key contributing factors related to higher TB incidence rates with the most influential element being HIV co-infection. People living with HIV have a 20-40 fold increased risk of developing TB compared to healthy individuals (Dheda *et al.*, 2016). Consequently 464 633 of the reported cases in 2017 were amongst people living with HIV and the majority of these patients were already on antiretroviral therapy (WHO, 2018). Therefore, it is important that TB and HIV get treated as two sides of the same coin to ensure achievement of “End TB” strategies.

The current standard treatment approach for susceptible TB consists of a regimen with four anti-TB drugs extending over a 6-month period. During the initial 2-month intensive phase patients take isoniazid (INH), rifampicin (RIF), ethambutol (EMB) and pyrazinamide (PZA) followed by a 4-month continuation period taking only INH and RIF (Tiberi *et al.*, 2018). This regimen has been in use for around 30 years and according to the latest data collected on treatment outcomes, this regimen still proves to be effective with a global success rate of 82% in 2016. However, the treatment success rate drops to a mere 55% in the case of multi-drug resistant (MDR) and rifampicin resistant (RR)-TB infections (WHO, 2018). Once antibiotic resistance is detected a patient no longer qualifies for the above mentioned shorter regimen and the standard treatment duration extends on average to around 18 months using at least 4 active drugs (Louw *et al.*, 2017; Tiberi *et al.*, 2018). Medical practitioners will build a patient-specific regimen based on susceptibility test outcomes using a categorized list of second line antibiotics constructed by the WHO. The WHO recommends that the regimen contains a later-generation fluoroquinolone (levofloxacin, moxifloxacin, gatifloxacin) and an injectable aminoglycoside (amikacin,

capreomycin, kanamycin) in combination with other core drugs such as ethionamide or prothionamide, cycloserine or terizidone, linezolid, and clofazimine (Tiberi *et al.*, 2018). If further resistance is detected then non-core drugs can be added such as bedaquiline and delamanid, two of the most recently non-core drugs approved by the Food and Drug Administration (FDA) (2017) and common candidates within shorter anti-TB trials currently underway (Tiberi *et al.*, 2018).

Shorter regimens for the treatment of resistance TB have been evaluated extensively and until recently the "Bangladesh" regimen was the preferred approach consisting of 9 antibiotics administered over a 9-12 month period. However, the STREAM trial compared the "Bangladesh" regimen with longer conventional resistant treatments and found that the shorter outdated "Bangladesh" regimen was non-inferior and showed similar toxicity than the longer regimens containing injectables (Seung and Hewison, 2019). The aforementioned STREAM trial did not contain bedaquiline at that time and STREAM stage 2 studies are currently in phase 3 of clinical trials, assessing a 6 and 9 month bedaquiline-containing regimen (RESIST-TB, 2019; Seung and Hewison, 2019). The effectiveness of bedaquiline has been reported on previously in a retrospective cohort study that compared drug resistant bedaquiline-containing regimens with conventional regimens in South Africa and found that the addition of bedaquiline had an overall lower risk of mortality (Schnippel *et al.*, 2018). Effectiveness of shorter bedaquiline-containing regimens are further supported by the NiX-TB study that have recently showed promising results for the use of bedaquiline in combination with pretomanid, and linezolid to treat extensively drug-resistant (XDR)-TB and MDR-TB patients within a 6 to 9 month period with regards to both efficacy and safety (RESIST-TB, 2019). Various other short regimen studies with and without bedaquiline are currently entering phase 3 of clinical trials including (RESIST-TB, 2019): i) TB-PRACTECAL study (bedaquiline + pretomanid + existing and re-purposed anti-TB drugs), and ii) the ZeNix study (linezolid + bedaquiline + pretomanid).

It is important to note that usage of these non-core drugs are kept to a minimum and drugs such as para-aminosalicylic acid and carbapenems with clavulanate are only prescribed in the case of XDR-TB infections in an attempt to preserve drug efficacy and limit the acquisition of antibiotic resistance (Tiberi *et al.*, 2018). Preservation of effective antibiotics is crucial since *M. tuberculosis* strains have been isolated that have shown resistance towards all know anti-TB antibiotics including bedaquiline; informally referred to as totally drug-resistant (TDR) strains (Louw *et al.*, 2017).

### 1.1.2 Antibiotic resistance and tolerance

The low success rate of anti-TB regimens can to some extent be ascribed to i) genetically acquired and intrinsic antibiotic resistance as well as ii) phenotypically induced antibiotic tolerance (Torrey *et al.*, 2016). The prolonged prescription in combination with drug-induced negative side effects often leads to patients not adhering to their instructed regimen and in turn creates an environment that promotes the acquisition of resistance mutations (genetically acquired and intrinsic antibiotic resistance) (Gülbay *et al.*, 2006; Louw *et al.*, 2017; Nasiruddin *et al.*, 2017). Antibiotic treatment over extended periods of time imposes strong selective pressure on *M. tuberculosis.* Selective pressure leads to the accumulation of independently acquired chromosomal mutations that render the bacilli drug resistant and aid in pathogen proliferation and transmission. *M. tuberculosis* forms highly clonal populations and is believed to solely transfer their *de* novo acquired mutations through bacterial division and not by horizontal gene transfer due to their lack of extrachromosomal plasmids (Zainuddin *et al.*, 1990). In addition to acquired chromosomal resistance, *M. tuberculosis* harbors various intrinsic resistance mechanisms that include i)

passive resistance through restricted cell wall permeation and more specialized mechanisms such as ii) the production of drug modifying and inactivating enzymes, iii) molecular mimicry, and iv) the presence of various efflux pumps (Smith *et al.*, 2013; Louw *et al.*, 2017).

*M. tuberculosis* is known to sporadically enter a phenotypically drug tolerant state (persister cells) in a stressful environment which is triggered by a downshift in metabolic processes (Gengenbacher *et al.*, 2012; Sikri *et al.*, 2013; Prax *et al.*, 2014). The ability to form persister cells is not a genetically inherited trait and is largely identified by a slow or non-growing population with a lower metabolic rate, a reduction in intracellular adenosine tri-phosphate (ATP) levels and an increase in lipid metabolism (Smith *et al*, 2013; Mouton *et al.*, 2016). These metabolically quiescent persister cells play a key role in clinically diagnosed latent TB infections (LTBI) characterized by an asymptomatic state and considered to be a major contributing factor in the relapse of TB disease (Zhang *et al.*, 2014). Under control of an effective immune response the host can successfully maintain the bacilli in equilibrium *in vivo* and the persister population can survive for lengthy periods. Although persister cells can be widely localized within the host; generally, a granulomatous structure forms as a result of the delicate balance between host and bacterial factors and forms a visual representation of the pathological outcome of TB (Ndlovu *et al.*, 2016; Pagan *et al.*, 2018). As long as the immune response can effectively contain the bacilli a person can remain asymptomatic; however, any reduction in immune efficacy will enable the persisters to revert back to actively replicating cells eventually tipping the equilibrium in favor of bacterial proliferation and the manifestation of active TB disease **(Figure 1.1)**. Granuloma formation can be seen both as advantageous and unfavorable for the host since although the immune system can asymptomatically contain the bacilli for years it also actively restricts drug penetration (Barry *et al.*, 2009) and acts as a safe harbor for *M. tuberculosis*.

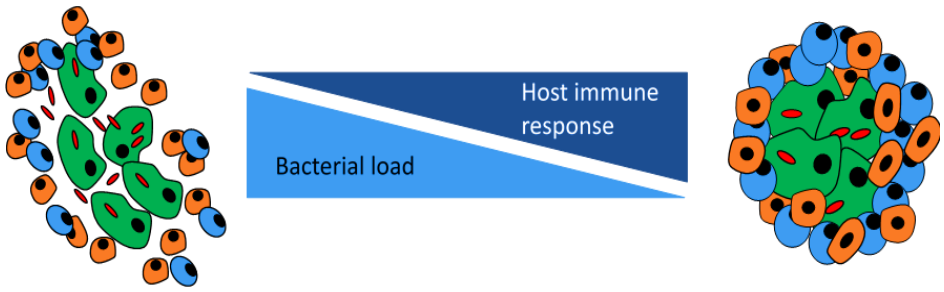


**Figure 1.1. The subtle balance between LTBI and active TB disease.** The shift in the equilibrium between LTBI and active TB disease depends on the ability of the immune system to effectively contain the bacilli. Slight alterations in the efficacy of the immune system will tip the scale in favor of bacterial replication that will lead to active TB disease manifestation and eventual bacilli transmission. Image adapted from Delogu *et al.* (2013).

The switch from complete eradication to mere containment is in part to blame on *M. tuberculosis'* well evolved immune suppression mechanisms that inhibit the normal execution of stimulated bactericidal pathways (Pieters, 2008; Cambier *et al.*, 2014; Weiss *et al.*, 2015).

### 1.1.3 Host-pathogen interaction and immune evasion

Internalization of *M. tuberculosis* into macrophages initiates an immune response mediated through ligand-receptor interactions. Primary immune recognition cells bind to pathogen associated molecular patterns (PAMP's), in particular mannosylated-lipoarabinomannan (Man-LAM), lipomannan (LM) and phosphatidylinositol mannoside (PIM), present on the bacilli through pathogen recognition receptors (PRR's) such as Toll-like receptors, nucleotide oligomerization domain (NOD)-like receptors and C-type lectins (Kleinnijenhuis *et al.*, 2011; Amaral *et al.*, 2016). PAMP and PRR interactions activate various intracellular pathways that elicit context depended protective and pathological responses.

Initial ligand-receptor interactions stimulate invagination and phagosome formation with the associated activation of intracellular bactericidal pathways. Important characteristics of these pathways include increased acidification and intracellular $Ca^{2+}$ levels with high quantities of reactive oxygen and nitrogen species (ROS/RNS) and the secretion of various inflammatory cytokines and chemokines (Gengenbacher *et al.*, 2012). Such specialized immune responses should theoretically be sufficient to control *M. tuberculosis.* However, these bacilli have successfully adapted to manipulate the host immune response to ensure survival and disease transmission. Although bacterial growth may be suppressed, these evolutionary adaptations prevent complete eradication by the immune system. Manipulation of the immune system occurs through mechanism that include masking of PAMP molecules, the exploitation of certain surface lipids that leads to the recruitment and uptake into growth permissive macrophages, and the secretion of molecules that prevent important maturation steps (Pieters, 2008; Cambier *et al.*, 2014; Weiss *et al.*, 2015).

### 1.1.4 Host directed therapeutic nanoparticles

Advanced discoveries into host-pathogen interactions and stimulated immune pathways give us the insights necessary for the development of effective immunotherapeutic compounds that take a different approach to conventional treatment. Instead of targeting the pathogen directly, host directed strategies are aimed at the immune system, i.e. targeting cells such as macrophages, and the stimulation of a protective immune response thus reducing inflammation and tissue damage (Kolloli *et al.*, 2017). The main challenge of host directed immunotherapy, especially with regards to TB, is to convert a bacteriostatic response resulting from successful immune inhibition back to a bactericidal protective response (Churchyard *et al.*, 2009). Immunotherapeutic nanoparticles (NPs) have the potential to overcome ineffective immune responses by stimulating immune cell receptors and triggering an intracellular reaction. NPs are particulate (1–1000 nm) delivery systems whose surface can be functionalised with bioactive molecules **(Figure 1.2)** that enable them to modulate an immune response on the cellular level. Host directed therapy (HDT) NPs are an appealing alternative form of medicine due to their potential to avoid promoting the acquisition of resistance-causing mutations as the immune system is modulated and the bacilli are not the direct target (Tobin, 2015; Kolloli *et al.*, 2017). Furthermore, they may support shortened treatment regimens (Dube *et al.*, 2013).

The NP core can be composed of a variety of materials and in this study we will exploit the high degree of biodegradability and biocompatibility of the polymer, poly(lactide-co-glycolide) (PLGA) (Makadia *et al.*, 2011; Mei *et al.*, 2015) to ensure the synthesis of non-toxic particles. Curdlan, a 1,3-β-glucan molecule, will be attached onto the surface of the PLGA NP to elicit immune stimulation **(Figure 1.2)**. Curdlan is a known agonist of the Dectin-1 receptor, primarily expressed on the surface of macrophages.

This ligand-receptor interaction stimulates a Syk/CARD9 signaling pathway that enhances phagocytic capabilities and the expression of pro-inflammatory genes as well as the increased production of oxidative species (Dube *et al.*, 2013; Tukulula *et al.*, 2015; Wagener *et al.*, 2018).

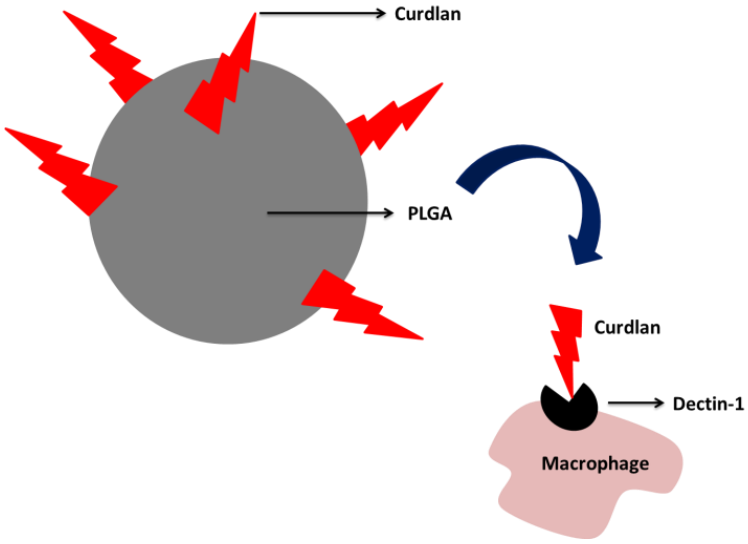


**Figure 1.2. The expected ligand-receptor interaction between curdlan and dectin-1.** The synthesized NPs will be composed of a PLGA polymer core functionalised with the bioactive molecule curdlan. The curdlan will bind to the dectin-1 receptor on macrophages and stimulate various anti-bacterial processes such as phagocytosis, production of pro-inflammatory cytokines and oxidative burst (Dube *et al.*, 2013; Tukulula *et al.*, 2015).

Here, the synthesis and physio-chemical characterization of curdlan-functionalised PLGA particles are reported on as well as the assessment of their anti-bacterial efficacy using a murine macrophage cell line containing *Mycobacterium tuberculosis*. Results obtained through this study will form the groundwork for more in depth-characterization assays necessary to fully assess NP function and efficacy.

## 1.2 Problem statement

*Mycobacterium tuberculosis* remains a deadly infectious agent, responsible for significant mortality worldwide. Although a variety of anti-TB drugs are widely available, treatment success is complicated by the ability of the bacilli to suppress protective immune responses. Further, the necessity for a lengthy treatment regimen with undesirable side-effects, frequently leads to patients being non-compliant and exacerbates the problem of antibiotic resistance. There is therefore an urgent need for alternative treatments for TB. Host directed therapeutic NPs show promise as an effective treatment strategy for TB, since surface functionalization incorporates cell specificity and the desired stimulated immune response that can bypass resistance mechanisms employed by the bacterium.

## 1.3 Hypotheses

It is hypothesized that the introduction of curdlan-functionalised PLGA nanoparticles to *M. tuberculosis* infected macrophages will stimulate the cells, leading to the death of *M. tuberculosis* within the macrophages.

## 1.4 Aims and Objectives

### Aim 1: To synthesize and characterize curdlan–functionalised PLGA (C-PLGA) NPs.

Curdlan-functionalised poly(lactide-co-glycolide) nanoparticles (C-PLGA NPs) will be synthesized using a single emulsion evaporation technique (Shim *et al.*, 2006; McCall *et al.*, 2013; Sirianni *et al.*, 2013; Yadav *et al.*, 2016). The NPs will be functionalised with different amounts of curdlan, i.e. 2%, 5% and 8% (w/w) and a control with no curdlan will be included. The physicochemical properties of the NPs (size, polydispersity index and zeta potential) will be characterized through dynamic light scattering (DLS) analysis and the surface morphology will be determined by scanning electron microscopy (SEM).

### Aim 2: To determine the cytotoxicity of C-PLGA NPs on RAW264.7 macrophages.

The 3- (4,5-dimethylthiazol-2-yl)-2,5-diphenyltetrazolium bromide (MTT) cytotoxicity assay will be used to assess the toxicity of the different NPs in the murine macrophage cell line, RAW264.7. NP toxicity will be assessed using three different NP concentrations of 1 mg/mL, 2.5 mg/mL and 5 mg/mL. In total twelve NP samples will be tested.

### Aim 3: To assess the ability of C-PLGA NPs to kill *Mycobacterium tuberculosis* within RAW264.7 macrophages.

The killing efficacy of the NPs (at a concentration proven to be non-toxic), will be assessed on *M. tuberculosis*-containing macrophages. RAW264.7 macrophages will be infected with a double leucine and pantothenate auxotrophic *M. tuberculosis* strain (*M. tuberculosis*::*ΔleuDΔpanD*) encoding the *LuxABCDE* gene. *LuxABCDE* gene expression allows for auto-luminescence of the bacilli and enabling use of luminescent readings as a real time proxy for cell numbers. The macrophages will be infected with *M. tuberculosis* at an MOI of 10:1 after which the NPs will be introduced to the macrophages and luminescence will be tracked over a 3 day period using a microplate reader.

### Aim 4: To characterize the stimulated immune response.

A customized mouse Multiplex cytokine assay will be performed to determine the cytokine expression profile induced by the NPs. A cytokine panel consisting of three pro-inflammatory and three anti-inflammatory cytokines relevant to TB that include TNF-α, IFN-γ, IL-12, IL-4, IL-10, and IL-1β will be assessed (Kleinnijenhuis *et al.*, 2011; Dube *et al.*, 2013) .

## 1.5 Potential impact of the study

The results of this study will provide insights into the possible application of immunotherapeutic NPs in the eradication of *M. tuberculosis*. In future, this could lead to the discovery of a novel anti-TB therapy. By elucidating the immune response elicited through NP administration we can gain a comprehensive understanding of the complex relationship that exists between pathogen invasion and the innate immune

response necessary for pathogen clearance. Additionally, it can provide us with the knowledge about NP surface functionality and the required adaptions to stimulate an optimal target-specific (either pathogen or tissue type) response.

## 1.6 Thesis overview

### Chapter 2: Published literature review

*Mycobacterium tuberculosis* and Interactions with the Host Immune System: Opportunities for Nanoparticle Based Immunotherapeutics and Vaccines.

Briefly, the review covers host-pathogen interactions, the elicited immune response and the well-developed immune evasion strategies employed by *M. tuberculosis* to overcome such responses. In addition to immune evasion we specify the shortcomings of current conventional approaches against TB and indicate where the use of host directed NPs can be exploited and applied and how nanomedicine can overcome these shortcomings. Finally, the review closes with a comprehensive overview of current NP-based therapeutics already in use and highlights the knowledge gaps and future prospects.

### Chapter 3: Formulation and characterization of C-PLGA nanoparticles

This Chapter describes the synthesis and characterization of NPs. Particle characterization including size, polydispersity index (PDI) and zeta potential data was obtained using dynamic light scattering (DLS) techniques. The surface morphology was established using scanning electron microscopy (SEM) image analysis. An MTT cytotoxicity assay of the NP formulations was performed on RAW264.7 macrophages to investigate the applicable safety of these particles.

### Chapter 4: *In vitro* characterization of nanoparticle activity

This Chapter describes studies to evaluate the ability of NPs to inhibit the growth of intracellular *M. tuberculosis* in RAW264.7 macrophages infected with a luminescent *M. tuberculosis* strain. Luminescence will be tracked over a 3 day period to assess changes in bacterial cell numbers. Additionally, cytokine expression due to particulate macrophage stimulation is assessed by conducting a mouse Multiplex cytokine assay. Customized panels include TNF-α, IFN-γ, IL-12, IL-4, IL-10, and IL-1β. By quantifying these analytes insights will be gained into the inflammatory response elicited by the C-PLGA NPs.

### Chapter 5: Conclusion

In the final Chapter all the results are taken together and the significance of what was discovered is discussed, shortcomings highlighted and future prospects mentioned. Altogether, the results point to the potential of C-PLGA NPs to be applied in the treatment of TB, although further investigation is necessary.

### Chapter 6: References

# Chapter 2

## Literature review

This Chapter represents a published review (reformatted to fit within the thesis) which provides an overview of the interaction that occurs between *M. tuberculosis* and the macrophage and highlights the immune response elicited through such interactions. Furthermore, it addresses the shortcomings of current anti-TB therapeutics and highlights the various adaptive mechanisms used by *M. tuberculosis* to successfully manipulate the host immune system. This highlights where NPs can be exploited as a possible treatment approach and how nanomedicine can overcome the shortcomings of current treatment against TB and possibly other intracellular infections such as Human immunodeficiency virus (HIV). The review highlights current knowledge and applications of NPs as treatment for infectious diseases, their application as a possible vaccine approach and what lies ahead for nanomedicine in the future.

My contribution: Equal contribution as joint first author together with Raymonde Bekale from the University of the Western Cape (UWC).

Identification of relevant literature

Wrote and edited draft attempts

Drafted schematic of **Figure 2.2**.

---

# Mycobacterium Tuberculosis and Interactions with the Host Immune System: Opportunities for Nanoparticle Based Immunotherapeutics and Vaccines

Raymonde B. Bekale[*1], Su-Mari Du Plessis[*2], Nai-Jen Hsu[3], Jyoti R. Sharma[4], Samantha L. Sampson[2], Muazzam Jacobs[3,4,5], Mervin Meyer[6], Gene D. Morse[7], and Admire Dube[1]

[1]Discipline of Pharmaceutics, School of Pharmacy, University of the Western Cape, Cape Town, South Africa

[2]NRF-DST Centre of Excellence for Biomedical Tuberculosis Research, South African Medical Research Council Centre for Tuberculosis Research, Division of Molecular Biology and Human Genetics, Faculty of Medicine and Health Sciences, Stellenbosch University, Cape Town, South Africa

[3]Division of Immunology, Department of Pathology, Institute of Infectious Disease and Molecular Medicine, Faculty of Health Sciences, University of Cape Town, Cape Town, South Africa

[4]National Health Laboratory Service, Johannesburg, South Africa

[5]Immunology of Infectious Disease Research Unit, South African Medical Research Council, Cape Town, South Africa

[6]DST/Mintek Nanotechnology Innovation Centre (NIC), Biolabels Unit, Department of Biotechnology, University of the Western Cape (UWC), Cape Town, South Africa

[7]AIDS Clinical Trials Group Pharmacology Specialty Laboratory, New York State Center of Excellence in Bioinformatics and Life Sciences, School of Pharmacy and Pharmaceutical Sciences University at Buffalo, Buffalo, New York, USA

* These authors contributed equally to this work

Published: February 2019 in Pharmaceutical Research.; 36(1): 8. doi:10.1007/s11095-018-2528-9.

## 2.1 Abstract

Tuberculosis (TB) caused by *Mycobacterium tuberculosis* remains a deadly infectious disease. The thin pipeline of new drugs for TB, the ineffectiveness in adults of the only vaccine available, i.e. the Bacillus Calmette-Guerin vaccine, and increasing global antimicrobial resistance, has rein vigorated interest in immunotherapies. Nanoparticles (NPs) potentiate the effect of immune modulating compounds (IMC), enabling cell targeting, improved transfection of antigens, enhanced compound stability and provide opportunities for synergistic action, via delivery of multiple IMCs. In this review we describe work performed in the application of NPs towards achieving immune modulation for TB treatment and vaccination. Firstly, we present a comprehensive review of *M. tuberculosis* and how the bacterium modulates the host immune system. We find that current work suggest great promise of NP based immunotherapeutics as novel treatments and vaccination systems. There is need to intensify research efforts in this field, and rationally design novel NP immunotherapeutics based on current knowledge of the mycobacteriology and immune escape mechanisms employed by *M. tuberculosis*.

**Keywords.** immunotherapeutic nanoparticles; immunotherapy for tuberculosis; *Mycobacterium tuberculosis*; nanoparticle based host directed therapy; nanoparticles and vaccination

## 2.2 Introduction

Tuberculosis (TB) remains a deadly infectious disease. In 2017, about 10 million people became ill with TB and there were 1.6 million deaths from this disease. Over 60% of cases arose from seven countries with India leading the count, followed by Indonesia, China, The Philippines, Pakistan, Nigeria and South Africa (WHO, 2017). Worldwide, about 1.7 billion people are estimated to be living with asymptomatic TB infection. To underscore the seriousness with which governments consider this pandemic, in September 2018, a high level United Nations General Assembly meeting was held with the goal of discussing unified approaches to ending TB pandemic by the year 2035 (Amani, 2018; Fauci, 2018)).

TB is primarily acquired following inhalation of aerosolized *Mycobacterium tuberculosis* (*M. tuberculosis*) bacilli and the majority of TB cases are pulmonary in nature (WHO, 2017). Drug treatment of TB is intensive, requiring daily intake of a cocktail of ‘first-line’ antibiotics for at least 6 months to achieve a cure. In cases where *M. tuberculosis* has become resistant to the drugs isoniazid (INH) and rifampicin (RIF) (known as multi-drug resistant tuberculosis (MDR-TB)), treatment using ‘second-line’, more toxic drugs which include injectables, for up to 18 months is required (Tiberi *et al.*, 2018). The increasing global incidence of MDR-TB (defined as resistance to a fluoroquinolone and one injectable drug such as amikacin) has resulted in greater attention placed on the judicious use of antibiotics, and

towards the development of new drugs with novel mechanisms of action to avoid generation of drug resistant *M. tuberculosis* strains. However, despite these efforts, drug resistance remains un-curtailed and more severe forms of resistance known as extensively drug resistant tuberculosis (XDR-TB) have been detected (Abate *et al.*, 2016; WHO, 2017).

*M. tuberculosis* is primarily an intracellular pathogen and the macrophage is the major host cell (Amaral *et al.*, 2016). The bacterium possess an innate ability to suppress the antimicrobial response of the macrophage. The survival strategies of *M. tuberculosis* within macrophages, which are detailed in this review, primarily involve prevention of phagosome maturation and an attenuation of pro-inflammatory responses (Kusner, 2005; Dube *et al.*, 2016).The current body of knowledge of the survival strategies employed by *M. tuberculosis* within the immune system, coupled with decreasing effectiveness of conventional antibiotics and a rise in drug resistant strains has led to revived interest in developing immunotherapies for TB. Within this context, immunotherapies encompass approaches in which compounds with immune modulating activity are administered in order to 'activate' immune cells to become a hostile environment for intracellular *M. tuberculosis*. A number of immune modulating compounds (IMCs) are at various stages of development and range from lipids and polysaccharides, cytokines and drugs such as metformin and albendazole (Guler *et al.*, 2015; Abate *et al.*, 2016). Engineered nanoparticles (NPs) have been employed to effectively deliver IMCs to immune cells and this application is discussed further in this review.

Vaccination is one of the most effective strategies for disease prevention. Unfortunately, the only vaccine available against *M. tuberculosis*, i.e. the Bacillus Calmette-Guerin (BCG) vaccine, has very limited effect against adult pulmonary TB (Khademi *et al.*, 2018). Therefore, developing novel, effective vaccination strategies alongside new treatment modalities is a promising strategy to eradicate TB globally. Numerous vaccine candidates for TB are currently in the clinical trial pipeline (Frick, 2015). However, most vaccines do not show strong immunogenicity and lack innate ability to be delivered to appropriate sites for optimal immune stimulation. In this regard, NPs are being applied to achieve optimum induction of robust innate and adaptive immune responses and to target antigens to immune cells and facilitate transfection and this is discussed later.

The goal of this review is to stimulate intensified research to develop immunotherapeutic NPs for TB treatment and vaccination. To facilitate the reader's entry into this field, we firstly provide a comprehensive review of *M. tuberculosis* and how it modulates the host innate and adaptive immune systems. We then describe current work on the application of immunotherapeutic NPs towards *M. tuberculosis* eradication and vaccination.

## 2.3 The mycobacteriology of *Mycobacterium tuberculosis*

In 1882 Robert Koch successfully isolated and identified *M. tuberculosis* as the causative agent of TB (Cambau *et al.*, 2014). *M. tuberculosis* is one of more than a hundred closely related species within the genus Mycobacterium. This genus is divided into two groups, i.e. non-tuberculous mycobacteria that are made up of non-pathogenic or opportunistic, fast-growing pathogens including *M. smegmatis* and the *M. tuberculosis* complex comprising mainly of slow growing, disease-causing species such as *M. leprae* and *M. tuberculosis* (Forrellad *et al.*, 2013; Sinha *et al.*, 2016). *M. tuberculosis* is a gram-variable, contagious rod shaped pathogen varying in diameter and length between 0.3–0.5 μm and 1.5–4.0 μm, respectively (Mercy Eleanor *et al.*, 2016). These aerobic-to-facultative anaerobes are metabolically very adaptable

and can readily switch from a carbohydrate to a fat diet in an attempt to adjust to the evolving host cell conditions (Cook *et al.*, 2009)

*M. tuberculosis* is surrounded by a characteristically thick and waxy cell envelope containing interconnected polymers of mycolic acids (MAs), arabinogalactan (AG) and peptidoglycan (PG) (Niederweis *et al.*, 2010; Rodriguez-Rivera *et al.*, 2017). This unique envelope renders *M. tuberculosis* hydrophobic; a trait primarily attributed to the presence of the MAs which are long chain fatty acids of up to 90 carbon atoms in length (Marrakchi *et al.*, 2014). The hydrophobic membrane acts as a permeability barrier towards various hydrophilic and lipophilic compounds making *M. tuberculosis* inherently resistant to antibiotics (Hett *et al.*, 2008; Niederweis *et al.*, 2010; Merget *et al.*, 2013; Rodriguez-Rivera *et al.*, 2017). However, the inherent resistance cannot solely be attributed to the impermeable membrane since experiments have shown that drugs are able reach cytotoxic levels within cells (Hett *et al.*, 2008). This stresses the important contribution of other virulence factors such as efflux pumps and drug degrading enzymes towards the intrinsic resistance of *M. tuberculosis* (Hett *et al.*, 2008; Niederweis *et al.*, 2010; Louw *et al.*, 2017).

An additional pathway in which *M. tuberculosis* proves to be problematic towards the cure of TB, is its ability to enter a non-replicating persistent (NRP) state enabling it to survive within the host until conditions are more favourable (Hett *et al.*, 2008; Gengenbacher *et al.*, 2013). Persister cells are a simple descriptive term used for tubercle bacilli within the NRP state and these cells are phenotypically and reversibly tolerant towards antibiotics (Mouton *et al.*, 2016). Most conventional antibiotics are designed to target cellular functions important for microbial growth and proliferation in actively replicating cells. However, NRP cells are thought to be metabolically quiescent characterised by a thickening of cell walls, a decrease in protein synthesis and transcription rates, and a low metabolic state with ATP levels up to 5-fold lower compared to actively replicating cells (Rittershaus *et al.*, 2013). This automatically eliminates common antibiotic targets which renders these cells tolerant towards various antibiotics if they remain within the NRP state. Only a small number of bacterial cells enter the NRP state and Keren *et al.* (2004) reported that the persister fraction of an inoculum exposed to antibiotics was only around 1%. This low generation frequency together with their transient nature is the reason knowledge of persister cells is limited and the exact mechanisms by which they enter and exit this state is still unclear (Lewis, 2010). Various factors are alleged to induce persister cell formation including presence of an acidic environment, growth-limiting by-products such as acetate and nutrient and oxygen depletion (Wayne *et al.*, 2001). Persisters are believed to be the cause of latent TB infections (LTBI) that is defined by a non-contagious, clinically asymptomatic state (Mouton *et al.*, 2016). Approximately 5–10% of persons infected with *M. tuberculosis* will eventually develop primary active TB and 90–95% will remain latently infected, not because the bacilli gets eradicated but is effectively controlled within granulomatous structures (Gideon *et al.*, 2011). LTBI is a major obstacle in the control of TB due to the chance of disease activation once the cells exit the NRP state and proliferate. Consequently, latently infected persons are the pool of future infections. The possibility of persister cells being present ensures that anti-TB treatment regimens extend over long periods of time aggravating an already rigorous antibiotic course.

## 2.4 Current TB therapy and drug resistance

Treatment is administered as a ‘cocktail’ of several antibiotics, each targeting various mycobacterial functions at relatively high doses as a preventative measure against acquisition of resistance. Treatment of drug-susceptible TB is a 6 month regimen based on a minimum of 4 first-line antibiotics (INH, RIF,

ethambutol and pyrazinamide) during the initial 2-month intensive phase (Tiberi *et al.*, 2018). The course for drug-resistant TB extends to around 18 months of 4 core drugs (later-generation fluoroquinolone such as moxifloxacin, an injectable aminoglycoside such as amikacin plus ethionamide or prothionamide, terizidone or cycloserine, linezolid and clofazimine) with an intensive phase of at least 8 months. Elevated doses of the antibiotics are used and cause severe side effects including ototoxicity, hepatotoxicity, hyperuricemia and neuropsychiatric problems (Gülbay *et al.*, 2006). The current lengthy treatment regimens and side effects are a major cause of patient non-compliance and consequently failure of TB treatment and the manifestation of drug resistance (Abate and Hoft, 2016).

*M. tuberculosis* rapidly acquires resistance to antibiotics **(Figure 2.1)** and it is estimated that this rate is similar for both bacterial cells in both active and NRP state. Therefore it is proposed that mycobacterial mutations occur in a time-dependent manner instead of a replication dependent manner (Rittershaus *et al.*, 2013). Contrary to most bacterial species, resistance is not attributed to horizontal gene transfer and is completely reliant on independently acquired chromosomal mutations and non-chromosomal events such as the production of drug modifying and inactivating enzymes, along with the presence of a MA-rich membrane and efflux pumps (Smith *et al.*, 2013; Louw *et al.*, 2017). Fitness costs frequently accompany these resistance mutations through secondary mutations on different loci; however, *M. tuberculosis* remains fully virulent and successfully fixes resistance mutations in consecutive populations (Smith *et al.*, 2013).

The contribution of antibiotic resistance towards the TB epidemic has led to the restricted use of the most recently discovered anti-TB drugs (i.e. bedaquiline and delamanid) to retain efficacy and to maintain low levels of resistance. Clinical studies are also on-going to optimize use of existing TB drugs by investigating various dose and treatment duration options (Savic *et al.*, 2017; Velásquez *et al.*, 2018).

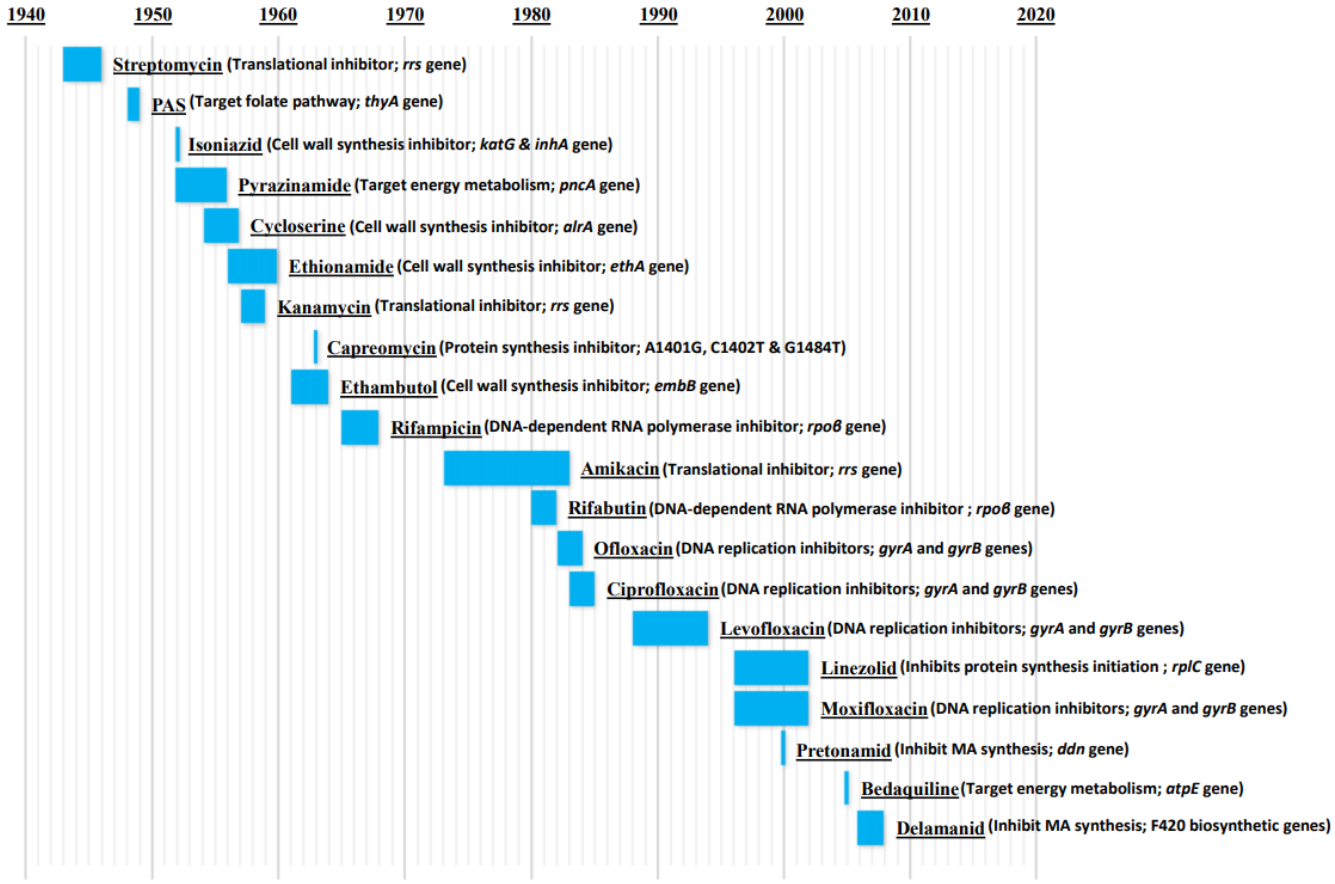


**Figure 2.1.Timeline illustrating period (in years) between antibiotic discovery and resistance acquisition.** The brackets list the mode of action of the antibiotic and the primary genes involved in acquired resistance to the specific antibiotic. Image adapted from Calitz *et al.* (unpublished).

## 2.5 The interaction of *M. tuberculosis* with the macrophage and mechanisms of survival

*M. tuberculosis* is primarily transmitted via inhalation of aerosolized bacilli and establishes infection within the lung. Bacilli are detected by resident immune cells including alveolar macrophages, dendritic cells (DCs) and neutrophils. An innate immune response is initiated through selective binding to pattern recognition receptors (PRRs) such as Toll-like receptors (TLRs), C-type lectin receptors (CLRs), and Nod-like receptors (NLRs) (Opitz *et al.*, 2013; Amaral *et al.*, 2016).

PRRs recognize polysaccharide-like structures present on *M. tuberculosis* known as pathogen associated molecular patterns (PAMPs), specifically mannosylated-lipoarabinomannan (Man-LAM), lipomannan (LM) and phosphatidylinositol mannoside (PIM) (Amaral *et al.*, 2016). PAMP motifs are highly conserved within species and are used as unique identifiers of an invading pathogen. The fate of ingested *M. tuberculosis* in immune cells can alternate between complete eradication, latent containment within a granuloma or the successful suppression of immune functioning and consequent transmission by *M. tuberculosis.*

### 2.5.1 Phagosome maturation and phagolysosome formation

PAMP recognition of PRRs leads to phagocytic uptake of *M. tuberculosis* by macrophages (MPs) (Silva Miranda *et al.*, 2012). Engagement of PRRs initiates formation of pseudopod-like structures around the bacterium that seal at the tips and form an intracellular vesicle known as a phagosome (Levin *et al.*, 2016). The subsequent maturation stages are characterised by fusion of the phagosome with various endosomal and lysosomal compartments that alters its protein and enzymatic composition and initiates the desired antimicrobial activity. Key stages include the early phagosome, late phagosome and eventual formation of the phagolysosome (Levin *et al.*, 2016).

*M. tuberculosis* can successfully prevent phagosome maturation and persist within vesicles characterised by continuous association with Rab5, the absence of PI3P and sphingosine kinase (SPK), low V-ATPase levels, a near neutral pH, and the active retention of coronin-1. Early phagosomes fuse with early endosomes and acquire Rab5, which recruits the hVPS34 kinase that together with other molecules, leads to the cyclic accumulation of PI3P on the phagosomal membrane. PI3P is a membrane trafficking regulatory lipid believed to be an important docking site for various proteins specifically the early endosomal antigen 1 (EEA1) and the class C core vacuole/endosome tether (CORVET) complex; these are central role players in membrane fusion and the ensuing phagosome maturation and phagolysosome formation stages (Chua *et al.*, 2004; Pieters, 2008; Pauwels *et al.*, 2017).

However, reports have shown that PI3P is absent on the phagosomal membranes containing live *M. tuberculosis* but is continuously present on those that harbour dead cells (Jayachandran *et al.*, 2007). *M. tuberculosis* prevents accumulation of PI3P through direct interference with the hVPS34 kinase responsible for PI3P production or through the secretion of SapM, a PI3P hydrolysing enzyme (Jayachandran *et al.*, 2007; Pieters, 2008). The transition from an early phagosome to a late phagosome is characterised by replacement of Rab5 with Rab7, the acquisition of lysosomal enzymes delivered in transport vesicles and the accumulation of lysosome-associated membrane proteins (LAMP1 and 2) necessary for phagolysosome formation (Weiss *et al.*, 2015). The late phagosome becomes a more hydrolytic and oxidative compartment suited for cargo degradation. Rab7 is important for centripetal movements and mediates the switch from a CORVET complex to the homotypic fusion and vacuole-sorting (HOPS) complex important for late endosomal fusion (Levin *et al.*, 2016; Pauwels *et al.*, 2017). *M. tuberculosis* produces PtpA, a protein tyrosine phosphatase, which dephosphorylates and inactivates the host protein Vacuolar Protein Sorting 33B (VPS33B), a regulator of membrane fusion. Inactive VPS33B cannot generate GTP-activated Rab7 hence blocking phagosome maturation and PL fusion (Pieters, 2008; Weiss *et al.*, 2015; Levin *et al.*, 2016; Pauwels *et al.*, 2017).

Following *M. tuberculosis* ingestion, V-ATPase is rapidly recruited to the phagosomal membrane gradually acidifying the intraphagosomal compartment through inward pumping of protons (H+) (Pauwels *et al.*, 2017). *M. tuberculosis* selectively excludes V-ATPase from the phagosomal membrane and arrests the internal acidification process at a pH of approximately 6.4; much higher than the intended pH ($\leq 5$) of the late phagosome necessary for downstream functioning of various phagosomal proteases and lysosomal enzymes (Gengenbacher *et al*,, 2012; Weiss *et al.*, 2015; Queval *et al.*, 2017). Exactly how *M. tuberculosis* excludes V-ATPase is an ongoing debate, but Queval *et al.* (2017) demonstrated possible strategies *M. tuberculosis* exploits to target the V-ATPase complex. Their studies have shown that the CISH protein is actively recruited to *M. tuberculosis* containing phagosomes and actively leads to the ubiquitination and subsequent degradation of V-ATPase (Queval *et al.*, 2017). Additionally, Wong

*et al.* (2011) also showed a direct link between PtpA and its ability to bind directly to the H subunit of the V-ATPase complex. Binding to the unit actively prevents the trafficking of this enzyme to *M. tuberculosis* -containing phagosomes. A low pH in mature phagosomes is important to ensure optimal enzymatic functioning of degrading lysosomal enzymes such as cathepsin D that are delivered once the phagosome fuses with the lysosome.

Calcium ($Ca^{2+}$) mobilization is associated with microbial ingestion. Increases in cytosolic $Ca^{2+}$ levels are marked by the binding of $Ca^{2+}$ with calmodulin (CaM) that activate CaMKII (Malik *et al.*, 2003; Kusner, 2005). This signalling cascade leads to the activation of hVPS34 that catalyses PI3P production and the consequent binding of EEA1 to PI3P, promoting membrane fusion and phagosome maturation (Kusner, 2005). Firstly, *M. tuberculosis* can suppress sphingosine kinase (SPK) therefore blocking the increase in macrophage cytosolic $Ca^{2+}$ levels (Malik *et al.*, 2003). Macrophage ingestion of inactivated *M. tuberculosis* cells activates SPK resulting in the translocation of the enzyme to the phagosome membrane. SPK phosphorylates sphingosine, yielding sphingosine-1-phosphate (S1P) that induces an increase in $Ca^{2+}$ from endoplasmic reticulum (ER) stores (Malik *et al.*, 2003). Secondly, in contrast to the prior mentioned inhibiting effects, *M. tuberculosis* can also effectively exploit the increase in $Ca^{2+}$ levels to prolong survival. *M. tuberculosis* actively retains coronin-1 on the phagosomal membrane leading to the $Ca^{2+}$dependent activation of calcineurin and consequently, the direct prevention of phagosome-lysosome fusion (Jayachandran *et al.*, 2007). Notably, Jayachandran *et al*. (2007) showed that coronin-1 dependent $Ca^{2+}$ mobilization is independent of SPK. This might be due to the differences observed in internalization between opsonized and non-opsonized *M. tuberculosis* which activates different downstream signalling pathways.

The final stage of bacterial destruction is the fusion of the late phagosome with lysosomal compartments mediated by various soluble NSF attachment protein receptors (SNAREs) (Pauwels *et al.*, 2017). The resulting phagolysosome becomes acidic (pH 4.5) and the degradative capacity is enhanced through acquisition of various hydrolytic enzymes such as cathepsin (Weiss *et al.*, 2015; Pauwels *et al.*, 2017). At this stage antimicrobial effects are further elevated through an increased production of reactive oxygen and nitrogen species (ROS/RNS) augmented by the NADPH oxidase (NOX) complex, recruited to the phagosome membrane throughout the maturation process, and the inducible nitric oxide synthase (iNOS) (Gengenbacher *et al.*, 2012; Levin *et al.*, 2016; Pauwels *et al.*, 2017). NOX, in particular NOX2, transfers electrons from NADPH to intra-phagosomal oxygen forming superoxide anions. These anions dismutate to form hydrogen peroxide and other toxic ROS. In addition, iNOS generates nitrate and nitrite that reacts with nitrous acid at a low pH producing nitric oxide and nitrogen dioxide. Nitric oxide and superoxide radicals can finally come together and form the highly toxic peroxynitrite (Gengenbacher *et al.*, 2012). These reactive radicals are important for pathogen eradication; however, *M. tuberculosis* can avert toxicity through the production of proteins involved in detoxification and damage repair. The primary strategy employed by *M. tuberculosis* is the secretion of KatG, a catalase-peroxidase that catabolizes peroxides within the phagosome (Pieters, 2008; Gengenbacher *et al.*, 2012). Oxidative stress can be further subdued by LAM which can scavenge free oxygen radicals (Gengenbacher *et al.*, 2012). In addition, to inhibit phagolysosome fusion, *M. tuberculosis* secretes PknG, a eukaryotic homolog and kinase acting protein, into the cytosol of the macrophage. PknG phosphorylates a currently unknown host molecule that acts as a mediator in membrane fusion hence suppressing lysosomal delivery of the phagosome by the host factor (Pieters, 2008). **Figure 2.2** summarizes the major immune regulatory strategies exploited by *M. tuberculosis*.

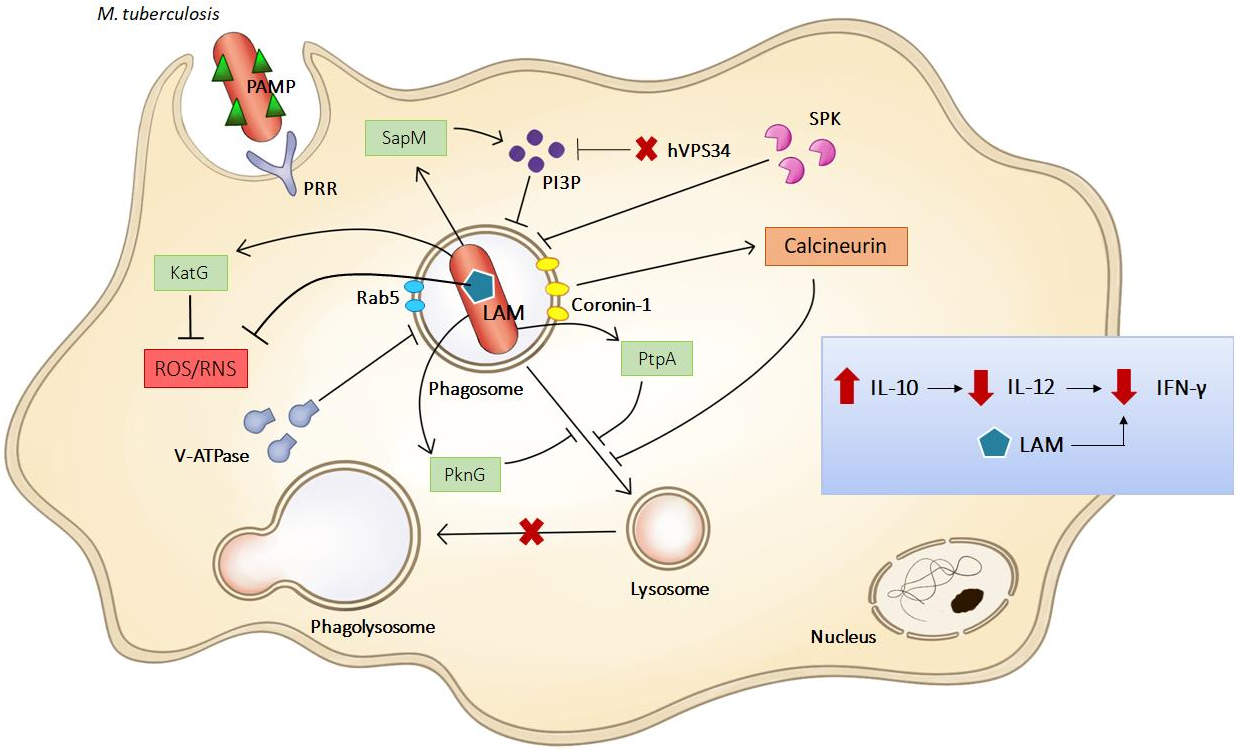


**Figure 2.2. Overview of the major immune regulatory strategies exploited by *M. tuberculosis* within the macrophage.** The bacilli can prolong its survival by actively preventing maturation and fusion of the *M. tuberculosis*-containing phagosome characterised by continuous association with Rab5, absence of PI3P, low V-ATPase levels hence a near neutral pH, the active retention of coronin-1 on the membrane, and a decrease in cytosolic $Ca^{2+}$ levels due to SPK suppression. In addition, *M. tuberculosis* can secrete various proteins including SapM, PtpA, PknG and KatG acting on various stages of the maturation and fusion steps. The mycobacterial polysaccharide, LAM, can directly inhibit IFN-γ secretion. Moreover, *M. tuberculosis*-containing macrophages secrete higher levels of IL-10, a major negative regulator of macrophage activation. IL-10 production inhibits IL-12 secretion and consequently suppresses IFN-γ production.

### 2.5.2 Cytokine mobilization and granuloma formation

Uptake of *M. tuberculosis* by macrophages leads to secretion of various cytokines and chemokines. These cytokines and chemokines act in concert and lead to increased vascular permeability, mediate systemic effects such as fever and the recruitment of various inflammatory cells (Duque *et al.*, 2014). The macrophage cytokine profile is made up of pro-inflammatory cytokines including IFN-γ, TNF-α, IL-2, IL-6, IL-12, IL-18, IL-23 and anti-inflammatory cytokines IL-27 as well as IL-4, IL-10, IL-13 and TGF-β (Duque *et al.*, 2014; Wang *et al.*, 2014). The different cytokine groups activate different macrophage phenotypes differentiating between a degrading pro-inflammatory macrophage with a Th1 cell cytokine environment or a macrophage phenotype characterised by a "resting" state with low microbicidal effects and a Th2 cytokine profile (anti-inflammatory). Macrophage activation through pro-inflammatory cytokines is necessary to obtain effective bactericidal properties. However, it is important that these pro-inflammatory cytokines are produced in appropriate amounts to prevent cytotoxic effects within the host. This is an important consideration in designing immunotherapies and is discussed in later sections. *M.*

*tuberculosis* LAM inhibits IFN-γ secretion, an important macrophage activating cytokine (Meena *et al.*, 2010). In addition to LAM, internalization of *M. tuberculosis* induces an increased production of IL-10, an anti-inflammatory cytokine associated with IFN-γ suppression. O'Leary *et al.* (2011) reported that macrophages infected with live *M. tuberculosis* secreted approximately 2X more IL-10 in comparison to macrophages infected with dead/inactivated *M. tuberculosis*. Addition of an anti-IL-10 antibody led to enhanced phagosome maturation highlighting the importance of IL-10 in mycobacterial pathogenicity and survival (O'Leary *et al.*, 2011). An increased production of IL-10 leads to the decreased production of IL-12 and reduced recruitment of macrophage activating cytokines (O'Leary *et al.*, 2011; Dube *et al.* 2016). By successfully inhibiting macrophage activation, *M. tuberculosis* consequently arrests the phagosome maturation process as well as the subsequent degradative pathways.

Cytokine and chemokine production leads to the recruitment of various cell populations to the site of the *M. tuberculosis*-containing macrophages including epithelioid cells, Langhans giant cells, mononuclear phagocytes, fibroblasts, and T and B lymphocytes (Gengenbacher *et al.*, 2012; Silva Miranda *et al.*, 2012). These immune regulatory cells form a highly organised structure known as a granuloma. Necrotic macrophages are generally located within the center of the granulomatous structure surrounded by interconnected layers of multinucleated giant cells, apoptotic macrophage, foam cells, dendritic cells, and neutrophils (Pagan *et al.*, 2018). The outermost layer of the structure is surrounded by a layer of T cells, B cells, and natural killer cells known to be major producers of IFN-γ and recognize specific peptides bound to major histocompatibility complexes (Pagan *et al.*, 2018). The granuloma is a hallmark of most *M. tuberculosis* infections and creates an immune micro-environment that enables the host to control the infection, mediated by a fine balance between pro- and anti-inflammatory cytokine production. TNF-α and IFN-γ are considered to be important pro-inflammatory cytokines involved in the functioning and formation of the granuloma with IL-10 being the major negative regulator (Silva Miranda *et al.*, 2012). In 90–95% of infected patients, the subsequent formation of a solid granuloma is a telling sign that the immune system is effectively containing *M. tuberculosis* and the bacilli in general enters the NRP state resulting in a latent, asymptomatic infection. Should the cytokine balance be tipped, the bacilli may reactivate, forming caseous lesions and the development of active symptomatic TB (Gengenbacher *et al.*, 2012). The likelihood of this balance being disrupted in favour of active disease development increases for patients with compromised immune systems as in the case of human immunodeficiency virus (HIV) co-infection. Once the balance is tipped, the granuloma becomes increasingly necrotic, characterised by caseation, eventually leading to the active transmission of *M. tuberculosis* bacilli (Silva Miranda *et al.*, 2012).

## 2.6 The adaptive immune response to *M. tuberculosis* infection

Despite the initial attempt to eliminate the bacilli by cells of the innate immune system, prolonged host protection from active disease requires the generation of adaptive immune response that are initiated and driven by the activated antigen presenting cells (APCs), i.e. macrophages and dendritic cells (DCs) (Wolf *et al.*, 2008; Harari *et al.*, 2011). The coordination between innate and adaptive immune responses is comprised of cellular, cytokine and chemokine components which are necessary for effective control of bacilli replication and dissemination.

### 2.6.1 Antigen presentation

Antigen presentation by APCs is a crucial step that links the innate and adaptive immunity and involves distinctive mechanisms. For major histocompatibility complex (MHC) class II presentation, *M. tuberculosis* peptide antigens are presented by APCs to antigen-specific CD4+ T cells, which are thought to be the most important protective response for control of intracellular infection (Caruso *et al.*, 1999). For MHC-I presentation, all nucleated cells are able to present *M. tuberculosis* peptide antigens to antigen-specific CD8+ T cells. This mechanism allows infected cells with cytosolic peptide antigens to be killed through Fas/Fas-L induced apoptosis or granule-mediated function (Canaday *et al.*, 2001). The stimulation of T cells in the context of MHC molecules activates adaptive immunity and induces IFN-γ secretion and cytolytic CD8 T cell activity. However, as described earlier, *M. tuberculosis* employs several evasion strategies to circumvent the phagosome-lysosome fusion pathway, and thereby prevents antigen processing and presentation to T cells.

Unlike macrophages, DCs are considered professional APCs and act as initiators of specific T cell immunity against *M. tuberculosis* infection (Tallieux *et al.*, 2003; Prendergast *et al.*, 2013). Depletion of DCs delays onset of *M. tuberculosis* specific CD4+ T cells priming that compromises host immunity in conjunction with uncontrolled bacilli replication (Tian *et al.*, 2005). After bacilli uptake, DCs present antigens to T cells following migration to the draining lymph node in an IL-12 and TNF-α dependent manner. Upon arrival in lymph nodes, DCs become functionally mature, characterized by upregulation of MHC-II, CD40, CD80, and CD86, to effectively stimulate naïve T cells (Khader *et al.*, 2006; Keeton *et al.*, 2014). Although a complex regulatory process, TNF-α is known to be an important factor that facilitates DC maturation towards specific T cell priming (Caux *et al.*, 1992; Sallusto *et al.*, 1994). Interestingly, while persistent TNFRp55 expression leads to potential defective T cell responses during chronic *M. tuberculosis* infection (Dambuza *et al.*, 2016), sustained TNF-α expression by DCs enhances maturation and generates a much more robust T cell response (Zhang *et al.*, 2003). Thus, DCs are positioned to serve as an important link between innate and adaptive immunity and may act as useful targets for immunotherapy and vaccine development (Griffiths *et al.*, 2016; Ahmad *et al.*, 2017).

### 2.6.2 T cell responses in adaptive immunity

The adaptive immune response is initiated in the peripheral lymphoid organs, and consists of cell-mediated immunity by T cells and humoral immunity by B cells. Research in the area of immunity to *M. tuberculosis* has largely focused on T cells due to their critical role in the elimination of bacteria during primary infection, followed by their ability to generate *M. tuberculosis* specific and memory responses to protect from subsequent infections. The importance of CD4+ T cells against *M. tuberculosis* is supported by the clinical association of increased susceptibility to TB in HIV infected patients (Selwyn *et al.*, 1989; Lahey *et al.*, 2013). This is supported by murine studies with antibody depletion of CD4+ T cells or the use of gene-deficient mice (Caruso *et al.*, 1999; Scanga *et al.*, 2000), which show that the loss of CD4+ T cells significantly increases susceptibility to *M. tuberculosis* infection. Following priming, synthesis of IL-2 promotes naïve T cell proliferation and differentiation into different subsets of effector T cells, particularly CD4+ Th1 cells and type 1 cytokine responses that are crucial for protection against *M. tuberculosis*. The major effector function of CD4+ T cells is considered to be the production IFN-γ which is pivotal for host protection. The critical role of IFN-γ in *M. tuberculosis* infection was demonstrated in various experimental studies (Cooper *et al.*, 1993; Flynn *et al.*, 1993) and confirmed in children with genetic deficiencies of IFN-γ (Jouanguy *et al.*, 1997). Moreover, TNF-α from

*M. tuberculosis* -specific CD4+ T cells has been explored for its use as a biomarker for diagnosis of active TB disease (Harari *et al.*, 2011). The contribution of T cell derived TNF-α to immune defense against *M. tuberculosis* has been investigated using T cell-specific TNF-α deficient mice and shown that, while myeloid TNF-α is required for initial control of bacterial replication, T cell-derived TNF-α is essential to sustain protection during chronic TB infection (Dongowski *et al.*, 2012). Interestingly, in contrast, TNF-α from T cells was found to be largely redundant in cerebral immunity against TB infection (Hsu *et al.*, 2017).

### 2.6.3 Humoral immunity by B cells

It is generally accepted that while cell-mediated immune response is the effector branch of adaptive immunity to defend intracellular pathogens, the extracellular counterparts are protected by the humoral immune response, in which B cells are activated to secrete antibodies. Like T cell responses, the antibody responses are antigen specific and have different ways to mediate the clearance of pathogens, such as neutralization and opsonization. Although the understanding of adaptive immune response against *M. tuberculosis* relies pre-dominantly on the studies of cell-mediated immunity, increasing evidence supports the role of B cell and humoral immunity in the defense against *M. tuberculosis* infection (Chan *et al.*, 2014; Achkar *et al.*, 2015). Serological detection tests indicate that *M. tuberculosis* infection induces humoral immune responses to a wide variety of mycobacterial antigens (Steingart *et al.*, 2009). Studies have also shown that the BCG vaccine can elicit antibody responses to various mycobacterial antigens (Brown *et al.*, 2003; De Vallière *et al.*, 2005), and contribute to immune protection against mycobacteria. Moreover, in vitro and animal studies using antibodies to *M. tuberculosis* antigens have shown enhanced protection with increased survival and reduced bacterial burden (Pethe *et al.*, 2001; Williams *et al.*, 2005). Recent immunization studies with mycobacterial capsular arabinomannan conjugates have demonstrated antibody and T cell responses that contribute to protective immunity against *M. tuberculosis* (Prados-Rosales *et al.*, 2017). These findings provide evidence for the potential role of humoral immunity in TB vaccine development strategies.

## 2.7 Immunotherapeutic NPs and *M. tuberculosis* eradication

NPs have been used to stimulate macrophages to achieve eradication of intracellular *M. tuberculosis*. Greco *et al.* (2012) developed an immunotherapeutic liposome comprised of phosphatidylserine (PS) on the outer membrane and phosphatidic acid (PA) in the inner membrane (Janus faced liposomes). PS was included in the NP design to inhibit cellular production of pro-inflammatory cytokines and enhance anti-inflammatory cytokine secretion. PA is a lipid IMC involved in phagolysosome maturation (Greco *et al.*, 2012). Hence the strategy was to achieve *M. tuberculosis* killing using PA and avoid the pathology associated with over production of pro-inflammatory cytokines using PS. From the same research group, Poerio *et al.* (2017) synthesized similar liposomes having PS in the outer layer, however, additional lipids in the inner layer were investigated for ability to lead to mycobacterial killing, i.e. PA, PI3P, phosphatidylinositol 5-phosphate (PI5P), lysobisphosphatidic acid (LBPA), S1P and arachidonic acid (AA). These lipids were selected due to their known ability to promote phagosome maturation (Poerio *et al.*, 2017).

Greco *et al*. demonstrated that the presence of PA on the liposomes enhanced intracellular mycobacterial (*M. tuberculosis* H37Rv) killing in THP-1 macrophages and in human bronchoalveolar lavage cells through promotion of $Ca^{2+}$-mediated phagolysosome maturation and increased ROS production (Greco

*et al.*, 2012). Further, the desired balance in the immune response was demonstrated. Production of pro-inflammatory cytokines IL-1β, IFN-γ and TNF-α was dampened, while TGF-β production was enhanced. Similarly, Poerio *et al*. demonstrated enhanced phagosome acidification (to a pH of up to 5.5) when PS/PA, PS/ PI3P and PS/PI5P NPs were incubated with BCG infected THP-1 macrophages. These NPs also promoted ROS production and ultimately enhanced mycobacterial killing in macrophages (Poerio *et al.*, 2017).

Intranasal administration of the PS/PA liposomes to *M. tuberculosis* infected BALB/C mice was shown to result in a 100-fold reduction in pulmonary bacterial burden after 4 weeks, in comparison to a 2-fold reduction from orally administered INH. Combined administration of the PA liposomes and INH also proved effective. A tenfold reduction in serum levels of TNF-α, IL-1β and IFN-γ was observed with PA liposome treatment alone or in combination with isoniazid (Greco *et al.*, 2012). These studies demonstrate that cellular induction of phagosome maturation and ROS production, while suppressing pro-inflammatory cytokine secretion is a viable strategy to killing intracellular mycobacterium species. NPs in this instance allowed co-delivery of the IMCs to macrophages, allowing presentation of one type of IMC (i.e. PS) to the macrophage surface receptors and the presentation of multiple IMCs within the macrophage.

An IMC functionalised polymeric NP was developed by Dube *et al*. (Dube *et al.*, 2013). The polysaccharide IMC, i.e. 1,3-β-glucan, was adsorbed onto the chitosan shell and the NP core comprised the polymer poly(lactide-co-glycolide) (PLGA). RIF was also loaded into the NP core, and could be released in a sustained manner. 1,3-β-glucan activates dectin-1 on macrophage surfaces subsequently activating various downstream signal transduction pathways which promote pro-inflammatory gene expression as well as intracellular ROS/RNS production. Pro-inflammatory cytokines known to be produced through Dectin-1 activation include IL-12 (Chan *et al.*, 2009; Goodridge *et al.*, 2009). Apart from gene induction, Dectin-1 signalling also increases intracellular $Ca^{2+}$, following phosphorylation of various intracellular phospholipases (Xu *et al.*, 2009)(Xu *et al.*, 2009). Given these pharmacological effects, Dectin-1 activation by 1,3-βglucan can potentially reverse the immune suppressive effects of *M. tuberculosis* in MPs. A significant increase of IL-12p70, TNF-α, INF-γ and ROS were reported, following incubation of these NPs with healthy human alveolar-like macrophages. Levels of anti-inflammatory cytokines IL-4 and IL-10 remained unchanged (Dube *et al.*, 2013). In later work, linear chain 1,3-β-glucan, i.e. curdlan, was chemically conjugated onto PLGA producing IMC functionalised PLGA polymer which could form NPs (Tukulula *et al.*, 2015). The curdlan-PLGA NPs could stimulate THP-1 macrophages as evidenced by enhanced phosphorylated ERK production, an upstream mediator of ROS/RNS. These studies demonstrate the stimulation of APCs using β-glucan functionalised NPs, however, further studies in *M. tuberculosis* infected cells are required, as well as studies to determine an acceptable balance between macrophage activation secretion and bacterial killing. Recently, Hwang *et al*. (2018) conjugated single stranded β-glucan onto silica NPs. These NPs also encapsulated INH which could be released in a sustained manner. However, these NPs were observed to minimally activate peripheral blood mononuclear cell (PBMCs) as both the silica NPs and INH loaded silica/ glucan NPs stimulated the PBMCs at similar levels to control (Hwang *et al.*, 2018).

## 2.8 NP systems for vaccination against *M. tuberculosis*

Various NP based vaccine candidates have been evaluated in animal models and show encouraging results. Ballester *et al*. (2011) conjugated the DNA vaccine expressing antigen 85B (Ag85B) onto

pluronic-stabilized sulphide NPs. The NPs alongside the immuno-stimulatory oligonucleotide CpG were delivered to mice and it was demonstrated that vaccination with NP-Ag85B via the pulmonary route substantially reduced lung bacterial burden (Ballester *et al.*, 2011). These findings therefore suggest that pulmonary immunization with NPs can serve as an effective strategy for the design of future TB vaccines. There is a sufficient evidence to prove that in comparison to other sites, mucosal vaccination via the respiratory tract provides improved immune protection against pathogenic bacteria (Chen *et al.*, 1995; Giri *et al.*, 2006). However, mucosal adjuvants are challenged with respect to ability to generate robust cellular immune responses via this route which has curtailed their progression to the clinic (Stylianou *et al.*, 2014). The induction of immune responses by mucosal immunization requires the co-administration of appropriate adjuvants that can initiate and support the effective collaboration between innate and adaptive immunity (Belyakov *et al.*, 2009). BCG-primed mice were shown to have an enhanced immune response following intranasal delivery of Ag85B-HBHA (heparin binding hemagglutinin adhesion protein) by carnauba wax NPs (Stylianou *et al.*, 2014). BHA is a mycobacterial protein utilized by *M. tuberculosis* to achieve adherence to alveolar epithelium (Pethe *et al.*, 2001) and this property was exploited by linking to the highly immunogenic and protective Ag85B (Kaufmann, 2000; Langermans *et al.*, 2005; Gartner *et al.*, 2008). Human clinical trials were performed demonstrating that Ag85B and early secretory antigen target (ESAT-6) adjuvanted with IC31 could generate long-lasting Th1 cell responses (van Dissel *et al.*, 2010; van Dissel *et al.*, 2011). Additional work to deliver Ag85B and ESAT-6 using liposomes (CAF01) as adjuvant was performed in humans. CAF01 is a liposome composed of dimethyldioctadecyl-ammonium stabilized with a glycolipid immunomodulatory trehalose 6,6-dibehenate which is a synthetic variant of cord factor located in the mycobacterial cell wall. The vaccine system has been demonstrated to be safe and efficacious in humans (Hussein *et al.*, 2018). Clinical testing of this formulation is ongoing.

To enhance the magnitude of the immune response, Yu *et al.* (2012) applied Fe3O4-glutamic acid-polyethyleneimine (PEI) NPs as a delivery system to co-deliver Ag85A with ESAT-6 of *M. tuberculosis* and IL-21.The results indicated that the NP based vaccine induced a strong immune response (in comparison to administration of Ag85A-ESAT-6-IL-21 alone) and significantly reduced growth of *M. tuberculosis* in the lungs of mice. The authors attributed the enhanced immune response to improved cellular delivery and consequent transfection by the NPs (Yu *et al.*, 2012).

One of the more common materials that have been used for vaccine delivery is PLGA (Kirby *et al.*, 2008; Carlétti *et al.*, 2013; Rose *et al.*, 2015) In one example, Bivas-Benita *et al.* (2009) loaded the TB antigen Rv1733c onto the surface of PLGA-PEI NPs. Intratracheal intubation of the NPs led to enhanced T cell responses. These NPs were able to stimulate and induce maturation of DCs (evidenced by up-regulation of surface expression of the molecules CD40, CD80, CD83 and CD86 in culture) and IFN-γ induction in mice. Liposomes have also been recognized as efficient immunoadjuvants and delivery systems (O'Hogan *et al.*, 2003; Khademi *et al.*, 2018). A peptide DNA-liposome conjugated vaccine was investigated by Rosada *et al.* (2008). By entrapping DNA-hsp65 vaccine within cationic liposomes, these particles could elicit a strong Th1 pattern of immune response (following intranasal administration) that resulted in bacilli reduction and lung preservation in mice (Rosada *et al.*, 2008). The use of liposomes significantly reduced the amount of DNA-hsp65 vaccine required (16 fold reduction) while maintaining optimum levels of immune response. In the first decade of 2000's, Okada *et al*. reported 100% survival in non-human primate model of TB (Cynomolgus monkey) when administered with BCG plus DNA-hsp65 vaccine encapsulated in liposomes (Okada *et al.*, 2007). However, there has been no indication of any clinical testing of this vaccine candidate.

Researchers from South Africa have advanced an NP vaccine formulation to clinical trials, i.e. a synthetic nanoemulsion adjuvant, GLA-SE (a synthetic TLR-4 agonist glucopyranosal lipid adjuvant) formulated in an oil-in-water emulsion and further adjuvanted with TB antigen ID93 (Penn-Nicholson *et al.*, 2018). Based on the reproducible efficacy and enhanced Th1 response exhibited by the ID93/GLA-SE formulation, clinical trials to estimate safety and immunogenicity in humans are underway, and recent reports of the Phase I clinical trial indicate very promising results (Penn-Nicholson *et al.*, 2018). The reader is also directed to Khoshnood *et al.* (2018) for a comprehensive review of novel vaccine candidates for TB currently at various stages of pre-clinical and clinical evaluation (Khoshnood *et al.*, 2018).

## 2.9 Summary and future directions

It is encouraging that one of the major global funders of TB biomedical research the United States National Institute of Allergy and Infectious Diseases (NIAID) recently released a research plan towards ending the TB epidemic (Fauci, 2018), which also describes the need to conduct research to improve fundamental knowledge of bacterial biology and host immune mechanisms that eliminate or control the bacterium. These research activities are seen as part of the components of a toolkit for development of host-directed therapies, less toxic drug regimens, new diagnostic tools and vaccines.

To date, limited work has been performed on the application of immunotherapeutic NPs to achieve intracellular eradication of *M. tuberculosis*. Much more work has been performed to apply NPs as delivery systems and adjuvants to achieve effective vaccination, and it is exciting that at least one candidate is currently undergoing clinical evaluation (Penn-Nicholson *et al.*, 2018). An immunotherapeutic NP can have the design of the immunomodulating compounds (IMC) encapsulated within the NP core (providing opportunity for compound protection and controlled release), or incorporated within the NP shell **(Figure 2.3)**. Janus faced NPs are particularly interesting in this regard, as they enable different IMC presentation to various parts of the cells over time (Greco *et al.*, 2012). The IMCs could also be chemically conjugated onto the surface of the NP (Tukulula *et al.*, 2015) and such conjugation could be achieved through linkers to provide triggered release of the IMC, e.g. under certain pH, enzyme or redox conditions. Conjugation will enable precise insight of the amount of IMC delivered to the immune cells; which may prove beneficial in cases where fine tuning of the immune response is required to mitigate toxicity. Using NPs, combination immunotherapy has been described (Greco *et al.*, 2012) and multiple IMCs or an IMC and an antibiotic (Dube *et al.*, 2013) can be delivered to cells with higher efficiency compared to compound delivery in the absence of the NP.

Looking to the future, it is our opinion that studies to evaluate several other types of NPs and IMCs for intracellular TB eradication are required. Future studies should include more mechanistic and immunological assessments in order to gain understanding of NP and immune cell interactions and cell activation processes, NP elimination pathways and kinetics. Rational selection of materials for NP synthesis and IMCs will be required and some of the general NP design considerations presented in **Figure 2.3** could be taken into account.

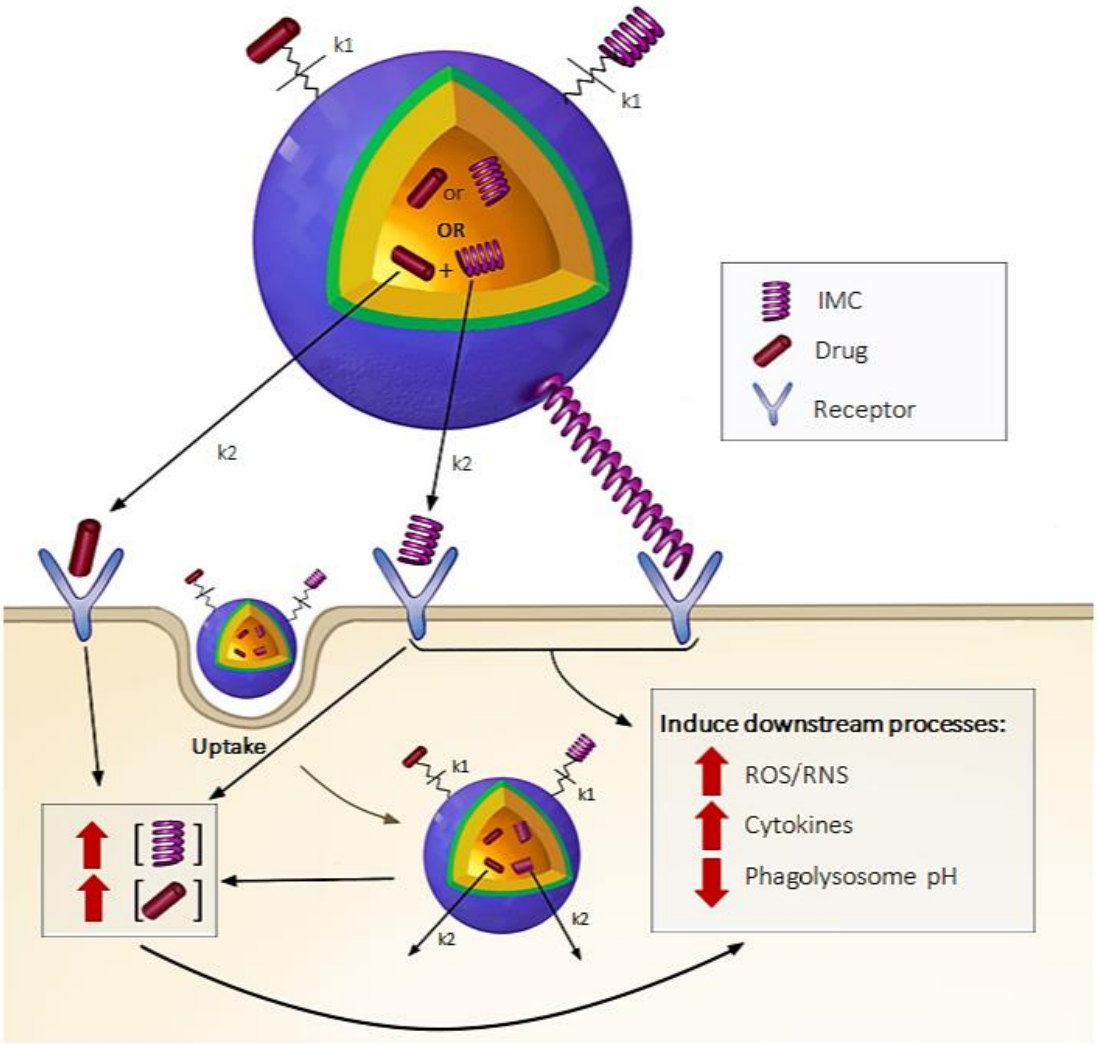


**Figure 2.3. Schematic representation of typical NP design for cellular targeted immune modulation for TB treatment and vaccination.** The IMC may be conjugated onto the particle and remains an intrinsic part of the NP (integration of immune functionality into the NP). The IMC may also be conjugated onto the surface of the NP via linker which allows release under specific conditions. The rate (k1) of release of the IMC can be controlled through linker selection. The IMC may in both cases bind to specific receptor located on target cell surface. The IMC may also be loaded in the core of the NP and released at a controlled rate (k2) and bind to surface receptors or enter cell and interact with intracellular receptors or proteins.

The efficacy of NP immunotherapy approaches to eradicate intracellular *M. tuberculosis* within the granulomatous structure remains to be shown. Existing in vitro granuloma as well as animal models could be used to determine efficacy in this clinically relevant scenario. Typically, in immunotherapy, macrophages have been the target, however, DCs could also be targeted, as they are positioned as a link between the innate and adaptive immunity and thus can act as useful targets for both therapy and vaccination. Toxicity is a concern which should be addressed. Some authors have used combination immunotherapy to dampen the proinflammatory response while activating other antibacterial responses

of the macrophage. This is an interesting approach which should be looked into further with the aim of striking a balance between toxicity and efficacy. TB typically occurs in the context of HIV coinfection. Hence pre-clinical and clinical studies to evaluate these therapies and vaccination approaches should consider the HIV co-infection scenario. For example, how immune activation may lead to immune reconstitution inflammatory syndrome.

Currently, the field of cancer immunotherapy is an area of intense exciting research offering many possibilities for disease treatment. Researchers in infectious disease immunotherapy could derive lessons from the cancer field to drive this emerging field at a faster rate towards the clinic. Indeed, from early stages, research in this field requires global partnerships of multidisciplinary teams involving at least microbiologists, immunologists, material scientists and pharmaceutical scientists. We believe that NP immunotherapies hold the key to highly effective and safe TB treatments and vaccinations. We hope that research in this field will become intensified in the near future.

## 2.10 Acknowledgments and disclosures

Research reported in this publication was supported by the Fogarty International Center of the National Institutes of Health under Award Number K43TW010371-01A1 granted to AD. SLS is funded by the South African Research Chairs Initiative of the Department of Science and Technology and National Research Foundation (NRF) of South Africa, award number UID 86539. The authors acknowledge the SA MRC Centre for TB Research and DST/NRF Centre of Excellence for Biomedical Tuberculosis Research for financial support for this work. The content is solely the responsibility of the authors and does not necessarily represent the official views of the National Institutes of Health, the SA MRC or the NRF. The authors wish to acknowledge Ms. Aaliya Tayob and Dr. Hanri Calitz for sketching figures in this manuscript.

# Chapter 3

# Formulation and characterization of curdlan-functionalised poly(lactide-co-glycolide) nanoparticles

Chapter 3, which is presented in manuscript format, describes the synthesis and characterization of poly(lactide-co-glycolide) (PLGA) nanoparticles (NPs) functionalised with varying ratios of curdlan (2%, 5% and 8% (w/w)). This work forms part of a larger study, and the characterization of the physico-chemical properties of the NPs was also conducted by Ms. Raymonde Bekale and Dr. Sarah D'Souza at the University of the Western Cape (UWC). In this Chapter, the toxicity of the NPs are examined on RAW264.7 murine derived macrophages using the (3- (4,5-dimethylthiazol-2-yl)-2,5-diphenyltetrazolium bromide (MTT) assay. The 4 different NP formulations are applied in three different concentrations of 1, 2.5 and 5 mg/mL. This will highlight the applicable safety of the NPs for further intracellular treatment assays.

My contribution: Synthesis of nanoparticles

Cytotoxicity characterization

Data analysis

---

## 3.1. Materials

### 3.1.1. Consumables

The following solvents and reagents were used for the synthesis of the NPs:

Poly(D-L-lactide-co-glycolide) with a lactide:glycolide ratio of 50:50 (PLGA, $M_W$ 30-60 kDa), curdlan (origin: *Alcaligenes faecalis*, $M_W$ 189 kDa)), poly vinyl alcohol (PVA; $M_W$, 13–23 kDa) and sucrose were all obtained from Sigma-Aldrich. The two solvents, dichloromethane (DCM) and dimethyl sulfoxide (DMSO) were purchased from Laborem and Merck, respectively. All the reagents and solvents were of analytical grade and used as instructed by supplier unless stated otherwise.

The following cell line and reagents were used for assessing toxicity:

RAW264.7 murine macrophages (ATCC TIB-71) cultured in D10 (Dulbecco's modified Eagle's medium (DMEM) supplemented with 10% Fetal Bovine Serum (FBS) both of which were obtained from ThermoFisher) and the passage number continuously maintained below 30. Phosphate-Buffered Saline (PBS) were obtained from ThermoFisher and the MTT (3- (4,5-dimethylthiazol-2-yl)-2,5-diphenyltetrazolium bromide) together with the DMSO solution was purchased from Sigma-Aldrich.

### 3.1.2. Equipment

The following equipment was used:

Analytical balance (Mettler®, model PE 6000); Stuart magnetic stirrer (Staffordshire, UK); QSONICA Probe sonicator (QSONICA); BÜCHI Rotary evaporator (BÜCHI, Labotec); Eppendorf 5804 Benchtop Centrifuge (Marshall Scientific); Bath sonicator (SCIENTECH, Labotec); Upright ultralow -80 °C freezer (NU-9668E, NuAire); Freeze dryer (Virtis, Freeze mobile model 125L); Malvern Zetasizer NanoZS90 (Malvern); Sputter coater (Emitech K550X); Scanning electron microscope (Auriga HR-SEM F50, Zeiss); Thermo Steri-Cycle $CO_2$ incubator (Marshall Scientific), FLUOstar Omega plate reader (BMG LABTECH).

## 3.2 Methods

### 3.2.1 Preparation of C-PLGA NPs.

Four different NP formulations were prepared by means of regulating the mass ratio of the C-PLGA co-polymer (containing 10% w/w of curdlan on the C-PLGA NP) mixed with the pure PLGA polymer (Tukulula *et al.*, 2015). The C-PLGA co-polymer was obtained from the laboratory of Prof. Dube at UWC following conjugation of curdlan to PLGA using a published protocol with 10% w/w curdlan particles (Tukulula *et al.*, 2015). The amounts (mg) of PLGA polymer and C-PLGA co-polymer that were weighed to synthesize the NPs containing the desired amounts of curdlan (2%, 5% and 8% (w/w)) were determined using **Equation 3.1** and are presented in **Table 3.1**. PLGA only NPs were also included as the fourth formulation. The desired NP formulations were decided on in an attempt to investigate a wide enough range of curdlan loads. The maximum load of curdlan synthesized were 8% w/w C-PLGA and beyond 8% the co-polymer becomes difficult to dissolve within a solvent necessary for NP synthesis. Thus a range between 0 and 8% w/w curdlan were chosen.

$$Step\ 1{:}\ \%\ Curdlan\ content = \frac{C\text{-}PLGA\ mass\ (mg) \times 10\%}{20\ mg\ of\ total\ polymer}$$

$$Step\ 2{:}\ Non\text{-}conjugated\ PLGA\ mass\ (mg) = 20\ mg\ of\ total\ polymer\ -\ C\text{-}PLGA\ mass\ (mg)$$

**Equation 3.1**

**Table 3.1. The varying % curdlan loads of each respective particle.** The desired curdlan content on the NP surface was achieved by blending the various masses of C-PLGA co-polymer with PLGA polymer. The total mass of polymer(s) used in the synthesis process was 20 mg.

| **Theoretical curdlan content % (w/w)** | **Mass ratio of PLGA:C-PLGA** | |
|---|---|---|
| | **PLGA** | **C-PLGA** |
| 0% (PLGA only) | 20 mg | 0 mg |
| 2% | 16 mg | 4 mg |
| 5% | 10 mg | 10 mg |
| 8% | 4 mg | 16 mg |

The single emulsion-evaporation technique, with adaptions from Shim *et al.* (2006), McCall *et al.* (2013), Sirianni *et al.* (2013), and Yadav *et al.* (2016) was used to synthesize the C-PLGA NPs **(Figure 3.1)**. These fundamentally include use of sucrose as cryoprotectant (Shim *et al.*, 2006) and finding the ideal parameters under which the PLGA NPs should be synthesised and characterised, as discussed below (McCall *et al.*, 2013; Sirianni *et al.*, 2013 and Yadav *et al.*, 2016). Briefly, to synthesize the NPs, amounts of C-PLGA and PLGA were weighed according to the calculated masses **(Table 3.1)** and were dissolved in DMSO and DCM, respectively, using a probe sonicator to ensure complete dissolution. The two solutions were combined in a glass vial under magnetic stirring (1500 rpm), and thereafter added dropwise to a PVA (0.5% (w/v); solution over 2 minutes under probe sonication (3 minutes, 55%, 70 Watt).

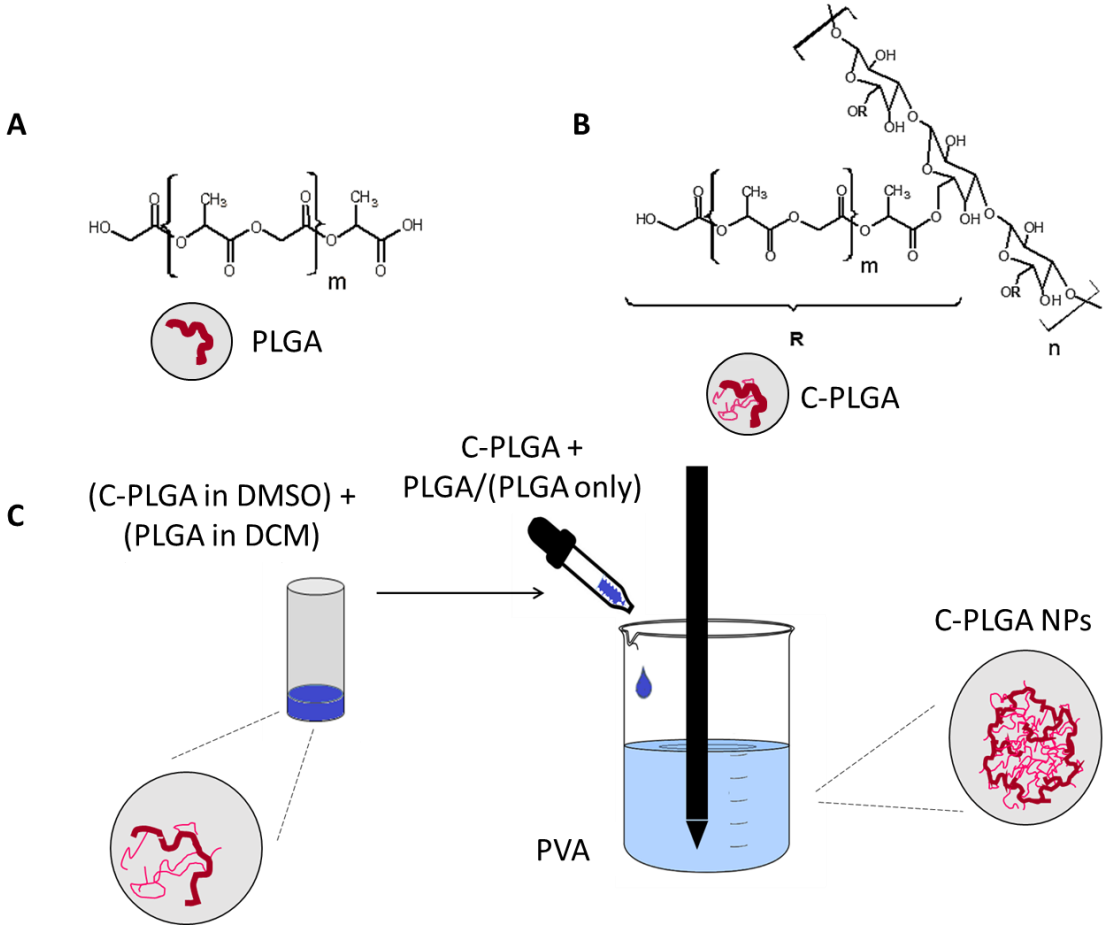


**Figure 3.1. The single emulsion NP synthesis process. A)** Chemical structure of PLGA and a diagrammatic depiction of the polymer. **B)** Chemical structure of the C-PLGA co-polymer and a diagrammatic depiction thereof. The chemical structure highlights the binding site between curdlan and the PLGA polymer to form the resulting C-PLGA co-polymer. **C)** Illustration depicting the first few steps in the synthesis process and the diagrammatic representation of the resulting C-PLGA NP. Adapted from Tukulula *et al.* (2015).

The resultant emulsion was transferred into a round bottomed flask and the organic solvents (DMSO, DCM) were removed through evaporation in a rotary evaporator (BÜCHI RII) (35ºC, 20 minutes). The resulting NPs were collected by centrifugation (10 000 rpm, 20 minutes) and washed either once (1X wash) or twice (2X wash) with distilled water in an ultrasonic bath (10 minutes, intensity 5) (SCIENTECH, Labotec). Both 1X and 2X wash NPs are reported on with the 1X wash NPs likely containing more residual PVA compared to the 2X wash NPs. Sucrose (1% w/v) was added to the final volume as a cryoprotectant and the NPs were lyophilized over a 2 day period. The final product was collected and stored at room temperature within a desiccator.

### 3.2.2 Characterizing the physiochemical properties of the C-PLGA NPs.

The lyophilized NPs were resuspended in distilled water (1 mg/mL) using an ultrasonic bath (10 minutes, intensity 5) (SCIENTECH, Labotec) and the suspension transferred into disposable 12 mm square polystyrene cuvettes. A Malvern NanoZS was used to measure the size and polydispersity index (PDI) of the NP suspension within the cuvette at a 90° scattering angle using dynamic light scattering (DLS) principles at 25 °C. DLS is a non-invasive technique that determines NP size based on the speed by which the particles move within a suspension due to Brownian motion. The smaller the particle, the quicker the Brownian motion and vice versa (Stetefeld *et al*., 2016). Together with the size and PDI measurements, the NanoZS was also used to analyze the zeta potential of the NP suspension. Averages of triplicate repeats were reported for all the above-mentioned characterization steps. Scanning electron microscopy (SEM) was used to assess the morphology of the NPs. The NP pellet was smeared on an aluminium stub with a carbon adhesive and left in a fume cupboard overnight to dry at room temperature. The dry pellet was coated with a thin film of palladium at 40 mA for 1 minute using a sputter coater and then observed under the microscope.

### 3.2.3 Assessing the toxicity of C-PLGA NPs in RAW264.7 macrophages

Macrophage (RAW264.7) viability after C-PLGA NP exposure was measured using the MTT assay; a calorimetric assay frequently used for the assessment of drug toxicity towards host cells. The assay exploits the ability of metabolically active eukaryotic cells to reduce the thiazolyl blue tetrazolium salt into water insoluble formazan crystals. The amount of crystals formed correlates with cell metabolism. Reduction occurs predominantly through the actions of dehydrogenase enzymes as well as other lesser known reducing agents such as ascorbic acid and cysteine (Stockert *et al.*, 2012; Riss *et al.*, 2017). The addition of DMSO dissolves the formazan crystals, forming a violet-blue color with an absorbance maximum near 570 nm. Absorbance values were translated into cell survival measurements and expressed as percentage cell viability relative to untreated controls (Equation .2).

$$\%\ \boldsymbol{cell\ viability} = \frac{\boldsymbol{OD\ of\ treated\ wells}}{\boldsymbol{OD\ of\ untreated\ wells}} \times \mathbf{100}$$

**Equation 3.2**

#### 3.2.3.1 Nanoparticle preparation

Each of the four different NP formulations were introduced in three different concentrations of 1 mg/mL, 2.5 mg/mL and 5 mg/mL to the macrophages. In total, 12 different NP samples were prepared and used for *in vitro* cytotoxicity evaluation **(Figure 3.2)**. The NPs were weighed in 1.5 mL eppendorf tubes, dispersed in sterile D10 (Dulbecco's modified Eagle's medium (DMEM) supplemented with 10% (v/v) heat-inactivated fetal bovine serum) and probe sonicated (QSONICA, Newton, USA) to ensure complete dispersion of the NPs (1 minute; 50% power). The NP solutions were UV sterilized for 30 minutes before being introduced to the macrophages.

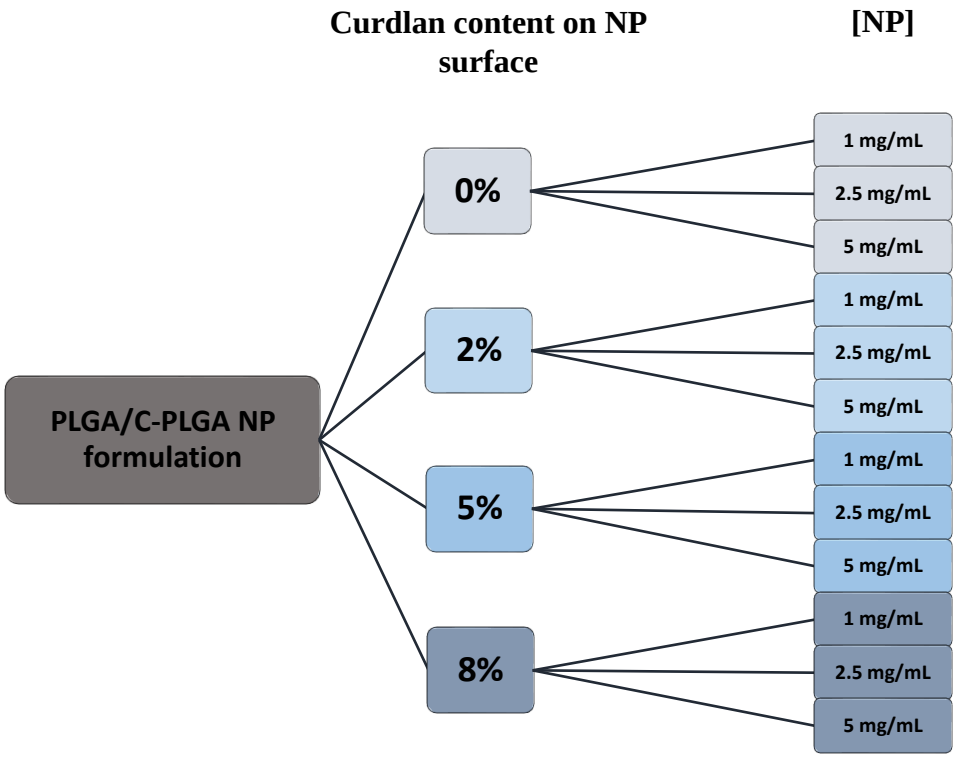


**Figure 3.2. The 12 different NP samples formulated and tested for induced cellular toxicity on RAW264.7 macrophages.** The particle range consisted of the PLGA NPs (0% w/w curdlan) and C-PLGA NPs containing 2%, 5% and 8% w/w curdlan. Each of the final samples was tested at three different concentrations ([NP]) on the macrophages of 1 mg/mL, 2.5 mg/mL and 5 mg/mL in quadruplicate technical repeats.

#### 3.2.3.2 MTT cytotoxicity assay

RAW264.7 (ATCC TIB-71) cells were seeded at $2.5\times10^4$ cells per well within a black, clear bottom, 96-well tissue culture plate containing 100 µL D10. Cells were cultured within plates for 24h at 37 °C, 5% $CO_2$ before the NPs were added. The media was replaced with 50 µL of fresh D10 and 50 µL of the desired NP formulation suspended in D10 and thereafter incubated at 37 °C, 5% $CO_2$ for a further 24h, 48h and 72h, respectively. Each NP formulation was added at the three different NP concentrations and each concentration was tested in quadruplicate **(Figure 3.3)**. NP toxicity was assessed on the 2X wash NPs due to the ease with which these NPs could disperse within water or D10 solutions to the 1X wash NPs.

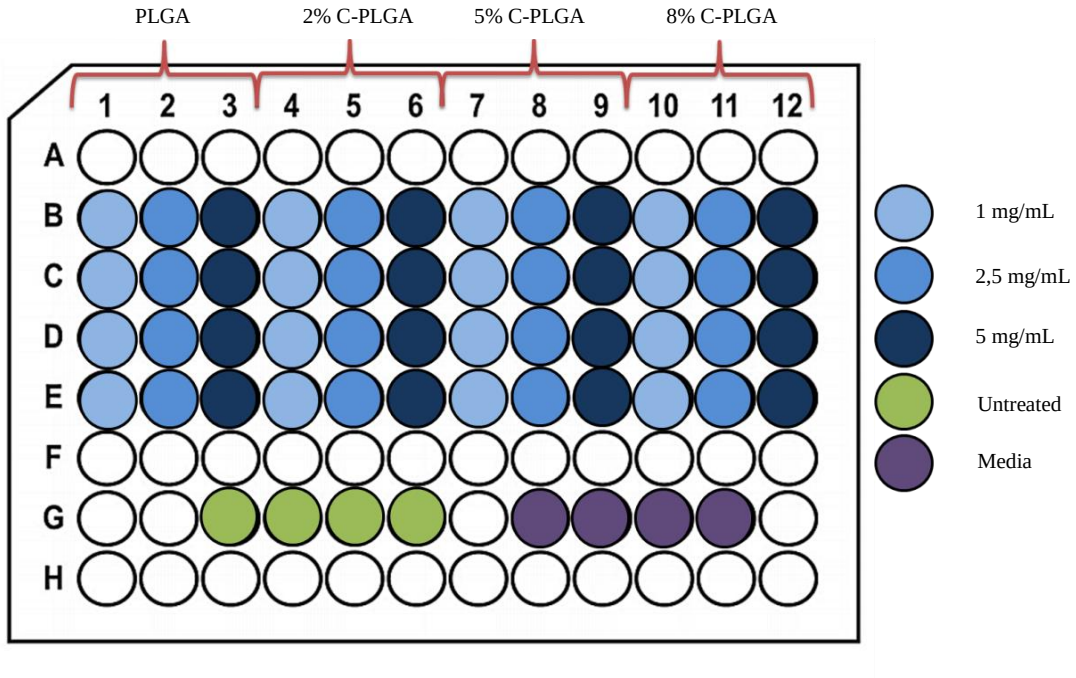


**Figure 3.3. Experimental layout for MTT assay in a 96-well tissue culture plate.** The plate was replicated for the three different time points and analyzed on each respective day. NP concentrations were tested in technical quadruplicates and 3 biological replicates were performed for each experiment performed. A p value ≤ 0.05 were considered to be statistically significant between the different treatments.

On the day of the assay, the cells were washed once with PBS and 100 µL of the fresh MTT solution was added to the treated wells and incubated for 4h at 37 °C, 5% $CO_2$. The MTT solution was dissolved in PBS (5 mg/mL) and filter-sterilized (2 µm) to remove contaminants as well as undissolved MTT clumps. Following the incubation period, the MTT solution was replaced with 200 µL DMSO and absorbance was read at 570 nm using a microplate analyzer. Cytotoxicity was tested over a 3 day period and a microplate was sacrificed on each respective day. Toxicity was assessed in quadruplicate technical repeats and three biological repeats. The absorbance values obtained were translated into percentage (%) cell viability as explained through Equation .1. This provided an indication of percentage cell viability relative to the untreated control over time for each of the treatment formulations.

### 3.2.5 Statistical analysis

DLS and MTT data were analysed using GraphPad Prism v7.05 and expressed as the mean ± standard deviation (n=3). Differences between the means were analysed by performing a One-way analysis of variance (ANOVA) and a Two-way ANOVA for the DLS and MTT data, respectively. Observable differences were considered to be statistically significant if the calculated p-value was less than 0.05. If a statistically significant difference was identified, a Post hoc test was performed to specify between which formulations the difference lie.

## 3.3 Results and discussion

### 3.3.1 C-PLGA nanoparticle preparation and characterization

As a first step in this study, PLGA NPs and C-PLGA NPs containing varying curdlan content (2%, 5% and 8% (w/w)) were successfully synthesized. This was achieved by effectively controlling the ratios of C-PLGA co-polymer to PLGA polymer during the synthesis process. Following NP synthesis, a series of analytical techniques were used to characterize the particles, and confirm that they possessed the desired characteristics.

To assess particle size, Dynamic light scattering (DLS) data were obtained using the Malvern NanoZS **(Table 3.2; Figure S3.1, S3.2)**. In general, it was found that the size of the NPs was not influenced by the amount of wash steps involved and that the average NP size remained relatively similar throughout, although 1X wash NPs were predicted to be more stable in suspension given their higher average zeta potential values.

**Table 3.2. The physico-chemical properties of the different C-PLGA NP formulations for both the 1X and 2X wash methodologies.** Data represents triplicate repeats presented as mean ± standard deviation. Samples were analysed using a Malvern Zetasizer NanoZS90 at 25 ˚C. A one-way ANOVA was conducted on each of the different parameters followed by a Tukey's multiple comparisons test and a $P < 0.05$ considered to be statistically significant. *Indicate a statistically significant difference.

| | 1X Wash | | | 2X Wash | | |
|---|---|---|---|---|---|---|
| **Nanoparticle** | **$D_H$ (nm)** | **PDI** | **Zeta potential (mV)** | **$D_H$ (nm)** | **PDI** | **Zeta potential (mV)** |
| | Mean ± SD | Mean ± SD | Mean ± SD | Mean ± SD | Mean ± SD | Mean ± SD |
| PLGA | 335.9±9.1 | 0.21±0.04 | -20.9±2.3 | 339.0±12.4 | 0.25±0.01 | -21.9±4.3 |
| 2% C-PLGA | 354.9±21.2* | 0.28±0.06* | -21.3±0.4 | 360.4±30.0 | 0.25±0.04 | -22.4±7.5* |
| 5% C-PLGA | 293±33.3* | 0.21±0.04 | 22.2±2.2 | 313.7±14.5* | 0.28±0.04 | -18.2±5.8 |
| 8% C-PLGA | 290.5±11.2* | 0.16±0.01* | -23±1.7 | 380.1±26.6* | 0.34±0.07 | -6.7±6.0* |

For the 1X wash NPs, the mean hydrodynamic diameter (nm) was found to be between 290.53 ± 11.2 nm and 354.9 ± 21.2 nm with a significant difference observed between the 2% C-PLGA and 5% C-PLGA NPs (P=0.028) as well as the 2% C-PLGA and 8% C-PLGA NPs (P= 0.023). For the 2X wash NPs a size range between 313.7 ± 14.5 nm and 339.0 ± 12.4 nm was observed with a significant difference between occurring between the 5% C-PLGA and 8% C-PLGA NPs (P= 0.026). A two-ANOVA was used to analyze the differences in the physico-chemical properties between the 1X wash and 2X wash and a Sidak's multiple comparisons test indicated that the only significant difference was for the 8% C-PLGA NP; size (P=0.0004), PDI (P=0.0006), zeta potential (P=0.0014). These findings correspond with previously published literature on NPs designed and tested for macrophage-specific stimulation (Tukulula *et al.*, 2015; Abdelghany *et al.*, 2019). Tukulula *et al.* (2015, 2018) designed curdlan-functionalised NPs ranging in size between 286.93 ± 9.9 nm and 486.8 ± 26.6 nm and rifampicin-

encapsulated glucan-PLGA NPs ranging between 264.3 ±4.6 nm and 301.2 ± 5.5 nm (2015) as well as 260.5 ± 12.4 nm and 283.1 ± 7.0 nm (2018). In both of these studies the authors showed that the NPs were effectively taken up by macrophages and that a macrophage-specific immune response was indeed stimulated. Furthermore, Abdelghany *et al*. (2019) synthesized and tested PLGA NPs and alginate-entrapped PLGA NPs loaded with moxifloxacin and amikacin with a size range between 294 ± 2.3 nm and 347 ± 21 nm. Similar to the findings of Tukulula *et al*. (2018), these antibiotic loaded particles were effectively taken up by macrophages and the antibiotics released within. The optimal size for macrophage uptake is still heavily debated, but it is suggested that particulate phagocytosis occurs more rapidly for NPs with an intermediate size average around 200 nm (Sharma *et al.*, 2010; Fenaroli *et al.*, 2014). Interestingly, PLGA NPs within this intermediate size average have been shown to localize within macrophages and in the lungs of mice once administered intravenously at the tail (Fenaroli *et al.*, 2014). A possible explanation for the preferential intermediate size might be an evolutionary adaption from the host. Particles smaller than 200 nm are considered to be small enough to be removed as foreign objects from the host into the lymphatic system whereas particles between 200 and 500 nm need to be transported within immune cells such as macrophages and consequently get phagocytosed (Danhier *et al.*, 2012).

DLS techniques report on the size of NPs within a suspension. However, it is possible to obtain the size of NPs in a dry state using SEM image analysis. Although we do not report here on NP size based on SEM we did observe that the NPs appear to be smaller on the SEM images compared to being in dispersion. This is expected since NPs within a suspension are hydrated and the hydrodynamic diameter obtained from DLS analysis includes measurement of a layer of solvent around the particles (Bhattacharjee, 2016). The main purpose of the SEM analysis was to gain insights into the morphology of our synthesized particles. SEM results demonstrated that all our NPs are spherical (Figure 3.4), this includes the 2% and 5% C-PLGA NPs (not shown). This is generally expected of polymer NPs that tend to naturally undertake a spherical geometry in an attempt to minimize the surface tension (Vauthier and Ponchel, no date) Spherical structures are inclined to be smaller with lower surface tension than their non-spherical counterparts.

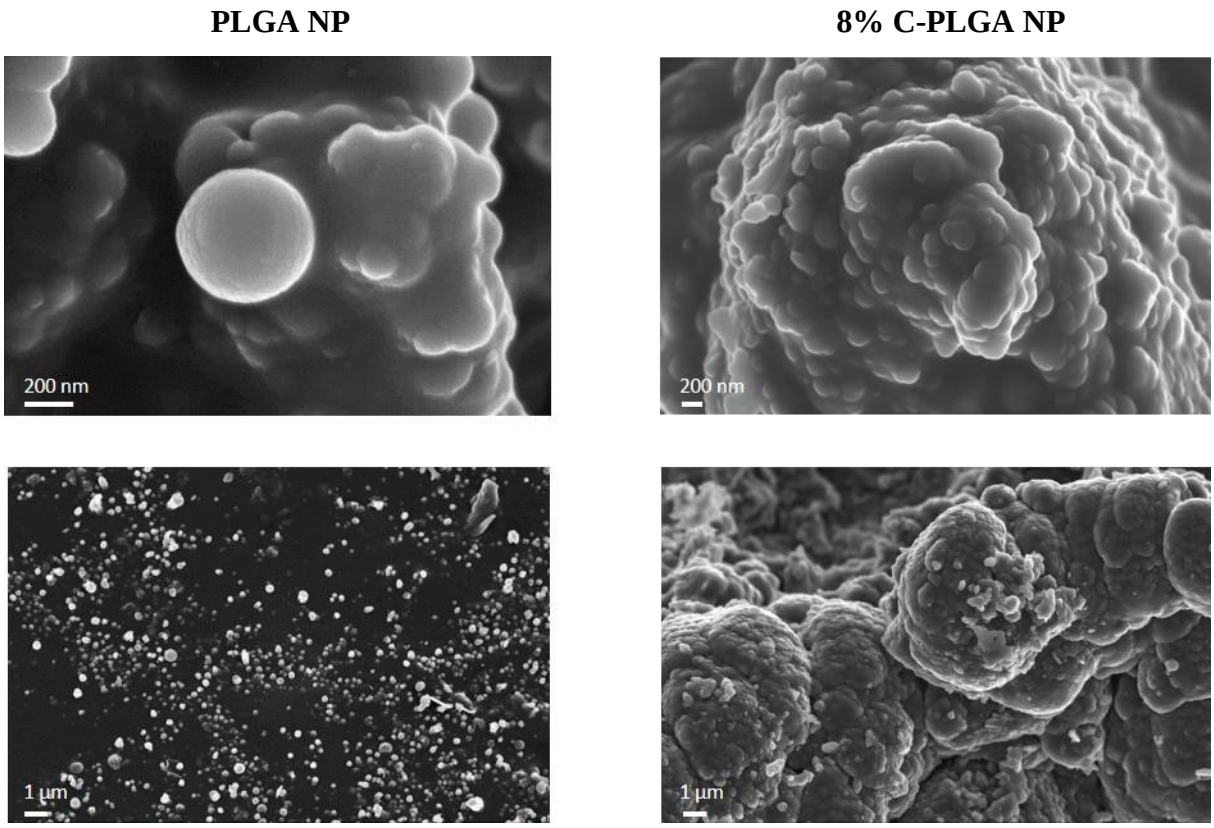


**Figure 3.4. Representative SEM images of PLGA NPs and 8% C-PLGA NPs confirming a spherical conformation.** Surface morphology was determines using a scanning electron microscope. The top panel was taken at a 200 nm and the bottom panel at a 1 µm range. All 4 of our different NP formulations proofed to have a spherical conformation and although not reported here, the 2% and 5% C-PLGA NP had a similar appearance.

In addition to size, the zeta potential (surface charge) and PDI of the NPs all influence macrophage uptake and thus NP efficacy. The zeta potential refers to the net electrical charge on the particle surface and determines the stability of a NP suspension with zeta potential values close to ± 30 mV considered to reflect high stability of particle (Bhattacharjee, 2016; Zazo *et al.*, 2016). Furthermore, the charge influences interactions with the environment within the host, including with proteins, tissue and cells (Zazo *et al.*, 2016). Our NPs did not fall within the intended theoretical range, but for the purpose of this study they were stable; for the 1X wash NPs we observed a zeta potential range between -20.9 ± 2.3 mV and -23 ± 1.7 mV and for the 2X wash NPs a wider range of zeta potential values between -6.7 ± 6.0 mV to -22.4 ± 7.5 were reported with a statistically significant difference being detected between the 2% C-PLGA and 8% C-PLGA NPs (P=0.049). In general, the closer the values are to 0 mV, the more unstable the suspension is. However, it is possible for very stable samples to show low zeta potential values due to factors beyond the scope of this study such as van der Waals forces that need to be accounted for (Bhattacharjee, 2016). Overall, the 1X wash NPs were expected to be more stable and the 2X wash 8% C-PLGA NP were expected to be the least stable of all the formulations with a zeta potential value of -6.7 ± 6.0 mV. This low, unstable zeta potential highlights the relationship that exist between the surface charge and PDI. Surface charge can influence agglomeration that will consequently lead to higher PDI values. This is seen with the 8% C-PLGA NP that presented with the highest reported PDI value. A high

surface charge indicates that there are strong repulsion forces between the NPs within a dispersion and this would be expected to minimize agglomeration, and consequently the size distribution of the NPs (Li *et al.*, 2016).

The PDI is a dimensionless parameter used to define the size distribution of NPs of colloids (Danaei *et al.*, 2018). A colloid can either be monodispersed (PDI range 0.0 – 0.2) that indicates a uniform size distribution within a sample or be polydispersed (PDI range 0.4 – 1) that indicates a non-uniform size distribution due to factors such as agglomeration of particles or protein binding. The former is preferable. All our samples were monodispersed (PDI<0.4) with the 1X wash PDI values ranging between 0.16±0.01 and 0.28±0.06, with a significant difference seen between the 2% C-PLGA and 8% C-PLGA NPs (P=0.049), and the 2X wash NPs having PDI values ranging between 0.25±0.01 and 0.34±0.07. The intricate relationship between NP size, PDI, zeta potential and shape is clearly highlighted by the 2X wash 8% C-PLGA NP. The weak surface charge (-6.7±6.0 mV) lead to more agglomeration as seen by the high PDI value (0.34±0.07) and SEM image which could contribute towards detection of larger NP sizes (380.1±26.6 nm).

Taken together, the physicochemical characterization data indicated that we were able to synthesize stable NPs within the desired size range for further safety and efficacy analysis.

### 3.3.2 Cytotoxicity assay

According to the International Organization for Standardization (ISO), any compound resulting in a cell viability reduction below 80% is considered toxic towards the host (Basha *et al.*, 2019). According to this standard we assessed the toxicity of 4 different NP formulations administered at 3 different concentrations **(Figure 3.5)** over a 72h period. We found all of them to be not cytotoxic towards RAW264.7 macrophages with the average values of three biological repeats remaining above 80% cell viability. This corresponds with previously published literature about the safety of polymeric NPs and in particular NPs synthesized from PLGA (Makadia *et al.*, 2011; Dube *et al.*, 2013; Tukulula *et al.*, 2015; Chen *et al.*, 2018).

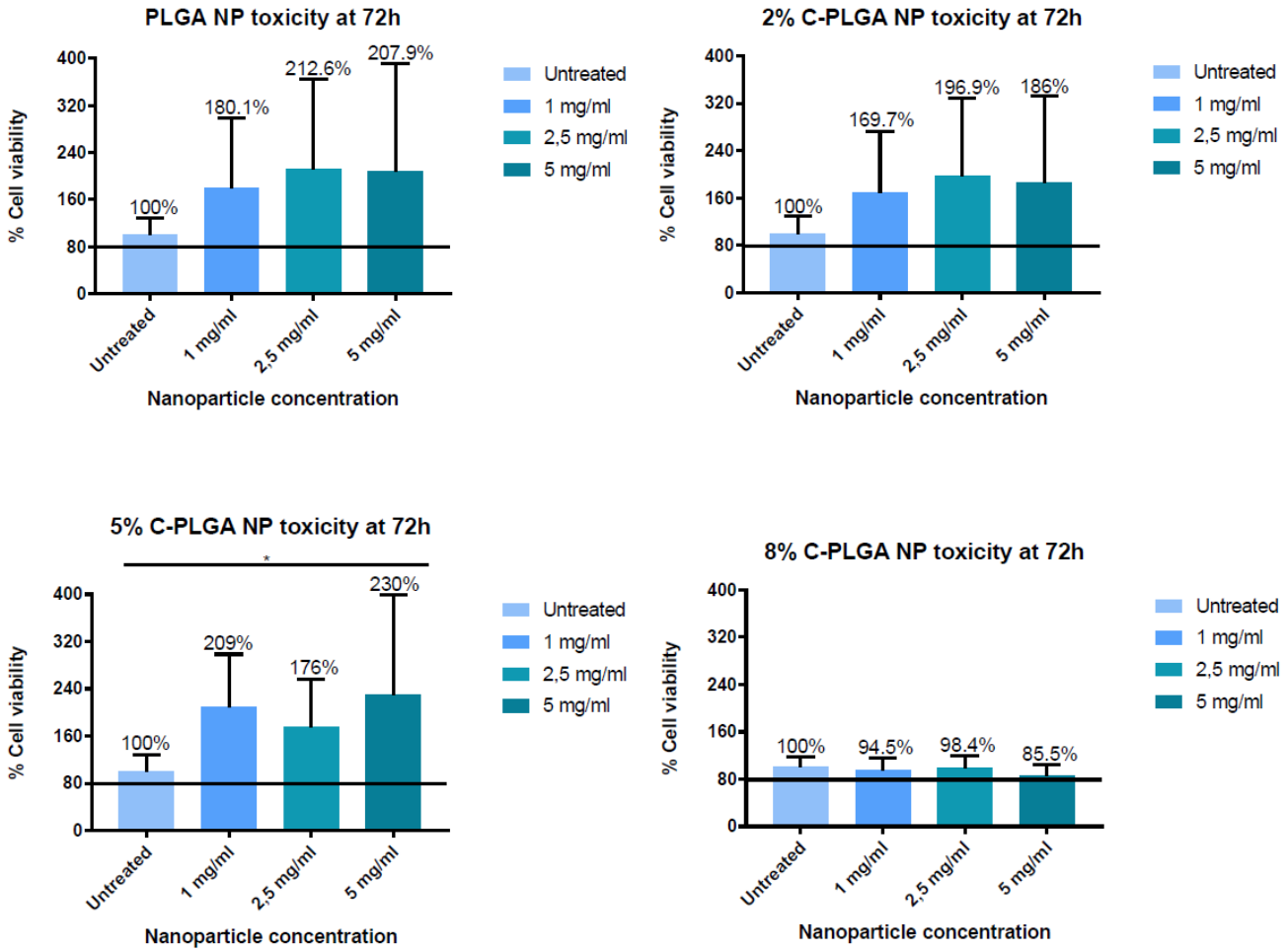


**Figure 3.5. MTT cytotoxicity assessment of different C-PLGA NP formulations administered in 3 different concentrations on murine RAW264.7 macrophages after 72h.** A one-way ANOVA was conducted to compare the means of the administered NP concentrations at 72h for each of the respective 2X wash C-PLGA NP formulations (PLGA, 2%, 5%, and 8% C-PLGA). Each formulation was tested in quadruplicate and the results are representative of triplicate biological repeats and expressed as the mean ± SD. A Tukey's multiple comparisons post-hoc test was applied and a value of $P<0.05$ was considered to be statistically significant. Numbers on bars indicate the mean percentage cell viability corresponding with the Y-axis. *Indicate a statistically significant difference. Horizontal line through bars represent 80% toxicity cut-off as determined through ISO standards.

No clear dose dependent trend was observed and variability in cell viability (as evidenced by the standard deviation values) was present. The variability was especially prevalent for the PLGA, 2% and 5% C-PLGA NPs and not for the 8% C-PLGA NP. This can possibly be due to the instability observed for the 8% C-PLGA NP (zeta potential=-6.7±6.0 mV; PDI=0.34±0.07) that contributed to a high degree of agglomeration of NPs suspended in D10. The presence of a lot of aggregates could suggest that fewer single particles could interact with the macrophages and be engulfed due to their large size thus remaining as clumps in the media.

Interestingly, for the PLGA, 2% and 5% C-PLGA NPs it was observed that the addition of the particles resulted in viability values higher than 100% suggesting stimulation of macrophage proliferation. This

is not uncommon and Li *et al.* (2016) found in a study utilizing gold nanoparticles that NP treatment caused proliferation of Human Periodontal Ligament Stem Cells (hPDLSCs), reaching cell viability values above 150% for the 60 nm NPs administered at a concentration of 28 μm. In this study, cell proliferation was observed where larger NP aggregates exceeded the receptor-mediated endocytosis threshold and nonspecifically adsorbed onto the surface of the cells (Hoshyar *et al.*, 2016; Li *et al.*, 2016). However, this explanation could be misinterpreted with regards to our particles as the NPs used in their study were approximately 60 nm in size and our NPs are almost 5X larger. In our case the increase in cell viability observed could be due to macrophage activation that leads to an increase in metabolic activity within the cells. When these results are translated to *in vivo* models, it can be speculated that heightened macrophage proliferation at the site of infection could enhance the recruitment of adaptive immune cells and consequently lead to a more powerful pathogen-specific inflammatory immune response. However, it is important to keep in mind that excessive inflammation can cause 'cytokine storm' at the site of the infection which can become clinically deleterious (Chiang *et al.*, 2018). In line with stimulated macrophage proliferation, Tukulula *et al*. (2015) observed the same trend as reported here where THP-1 macrophages proliferated when treated with C-PLGA NPs likely due to cell stimulation. This could be explained by an in increase in the production of pro-inflammatory cytokines; therefore, to assess and confirm the theory of macrophage stimulation and subsequent proliferation we quantify and report on inflammatory cytokine production within Chapter 4. Notably, the NPs might not specifically induce cell proliferation but stimulate mitochondrial activity that increases the presence of important hydrogenase enzymes. As mentioned previously, the MTT assay depends on metabolically active cells to reduce the tetrazolium salt into formazan crystals. However, enhanced metabolic activity does not primarily indicate cell proliferation thus depicting false positive growth. A major shortcoming of the MTT assay is that this assay does not accurately represent cell numbers and these findings might be misinterpreted and further investigation into the macrophage response is necessary.

## 3.4 Conclusion

We have successfully synthesized stable, spherical PLGA and 2%, 5% and 8% C-PLGA NPs within the desired size range as characterized by DLS techniques and SEM image analysis. The safety and biocompatibility of the particles were tested and confirmed on RAW264.7 macrophages. In the following chapter we assess the killing efficacy of these particles on *M. tuberculosis*-infected RAW264.7 macrophages and report on cytokine production as a result of the stimulated immune response.

# Chapter 4

# Characterization of Intracellular nanoparticle activity

In this chapter the ability of curdlan–functionalised poly(lactide-co-glycolide) nanoparticles (C-PLGA NPs) to inhibit the intracellular growth of *Mycobacterium tuberculosis* was assessed. RAW264.7 murine macrophages were infected with a luminescent strain of *M. tuberculosis* that enables us to track cell viability over time. An attenuated strain suitable for use within a BSL-2 setting was used. Alterations in luminescence provide a real time quantitative proxy of changes in bacterial cell numbers. A Luminex multiplex assay is conducted to detect the presence of 6 pro-inflammatory cytokines to determine if sufficient immune stimulation occurs through the C-PLGA NP-receptor interaction that will possibly contribute towards the eradication of bacilli.

My contribution: Assessment of Intracellular NP efficacy

Supernatant collection and preparation for Luminex assay

Colony forming unit determination

Data analysis

---

## 4.1. Materials

### 4.1.1. Consumables

Liquid mycobacterial cultures were grown in 7H9-OGT – 7H9 (Becton Dickinson), supplemented with 10% oleic acid–albumin–dextrose– catalase (OADC; Becton Dickinson, NJ, United States), 0.2% (v/v) glycerol (Sigma-Aldrich), 0.05% (v/v), Tween-80 (Sigma-Aldrich). Solid cultures were grown on 7H10 agar (Becton Dickinson, NJ, United States). Additional supplements included pantohenate (24 μg/mL), leucine (50 μg/mL), kanamycin (25 μg/mL) (Sigma-Aldrich), hygromycin (50 μg/mL) (Invitrogen). RAW264.7 macrophages (ATCC TIB-71) were cultured and maintained in Dulbecco's modified Eagle's medium (DMEM) (ThermoFisher) supplemented with 10% Fetal Bovine Serum (FBS) (ThermoFisher). Secreted cytokines were analysed using a customized mouse Multiplex R&D luminex kit (WhiteSci).

### 4.1.2. Equipment

Thermo Steri-Cycle $CO_2$ incubator (Marshall Scientific), Labotec water bath (Labotec), Labotec Orbital shaking incubator (Labotec), Bath sonicator (SCIENTECH, Labotec), Probe sonicator (QSONICA), Labnet Prism microcentrifuge (Labnet), Spectrophotometer (Thomas Scientific), Labotec Orbital Shaking incubator (Labotec), FLUOstar Omega plate reader (BMG LABTECH), Bio Plex platform (Bio Plex™, Bio Rad Laboratories).

## 4.2. Methods

### 4.2.1. Bacterial strains and culture.

**Table 4.1** describes the *M. tuberculosis* strains utilized in this study. Mycobacterial cells were cultured in 7H9 supplemented with 10% OADC, 0.2% (v/v) glycerol, 0.05% (v/v) Tween-80 (7H9-OGT), and the necessary antibiotics for plasmid maintenance (kanamycin (25 µg/mL), hygromycin (50 µg/mL)). Additionally, *M. tuberculosis* Δ*leuD*Δ*panD* liquid cultures were supplemented with leucine (50 µg/mL) and pantothenate (24 µg/mL) and incubated at 37 °C with shaking at 180 rpm. Reporter strains expressing the bacterial luciferase operon of plasmid pMV306hsp + LuxCDABE (Andreu *et al.*, 2010) were previously obtained through electroporation as describe by Snapper *et al.* (1990). Bioluminescence from *LuxCDABE* gene expression was used to measure the changes in bacterial numbers for both the *M. tuberculosis* Δ*leuD*Δ*panD*::pMV306hsp+lux strain and *M. tuberculosis* Δ*leuD*Δ*panD* wild-type (WT) reference strain. Solid cultures of *M. tuberculosis* Δ*leuD*Δ*panD::*pMV306hsp+lux were grown on 7H10 agar containing leucine (50 µg/mL) and pantothenate (24 µg/mL) Plasmid pMV306hsp + LuxCDABE was obtained from Addgene; reference number 26155.

**Table 4.1. Strains and plasmids used in the study.**

| Strain/plasmid | Description | Source |
|---|---|---|
| *M. tuberculosis* Δ*leuD*Δ*panD* | Double leucine and pantothenate auxotroph $Hyg^R$ | (Sampson *et al.*, 2004) |
| *M. tuberculosis* Δ*leuD*Δ*panD*::pMV306hsp+lux | *M. tuberculosis* Δ*leuD*Δ*panD* transformed with plasmid pMV306hsp + LuxCDABE Episomal $Kan^R$ | pMV306hsp + LuxCDABE (Andreu *et al*., 2010) Addgene plasmid number 26155 |

$Kan^R$, kanamycin resistant, $Hyg^R$, hygromycin resistant

### 4.2.2. Assessing the intracellular killing efficacy of C-PLGA NPs

RAW264.7 cells were seeded at a concentration of $5\times10^4$ cells per well in a white solid bottom, 96-well tissue culture plate and incubated overnight at 37°C, 5% $CO_2$ **(Figure 4.1)**. Macrophage cells were infected with *M. tuberculosis* Δ*leuD*Δ*panD*::pMV306hsp+lux and *M. tuberculosis* Δ*leuD*Δ*panD* at an MOI of 10:1. Sampson *et al.* (2004) and Mouton *et al.* (2019) have thoroughly characterized and compared *M. tuberculosis* Δ*leuD*Δ*panD* with non-attenuated *M. tuberculosis* H37Rv and provided comprehensive evidence to support the use of this attenuated strain as a model organism in TB research. In preparation for the infection, the mycobacterial cells were sonicated at 37 kHz for 12 minutes to disperse clumps and filtered through a 40 µm cell strainer. Cells were washed in D10 and the absorbance ($OD_{600}$) adjusted to 1. This was achieved by measuring the OD of the bacterial cultures prior to washing and then resuspending the cell pellet in a volume of D10 that would result in an adjusted $OD_{600} = 1$. The D10 media was continuously supplemented with leucine (50 µg/mL) and pantothenate (24 µg/mL) to support the growth of *M. tuberculosis* Δ*leuD*Δ*panD* cells. Once absorbance was adjusted, 100 µL of cell suspension was added to each well and incubated at 37°C, 5% $CO_2$ for 3h. Following the 3h uptake

period, cells were washed once with PBS and 200 µL D10 containing (1:100) penicillin/streptomycin was added to the wells and incubated at 37°C, 5% $CO_2$ for 1 h to kill any remaining extracellular, unphagocytosed bacteria. Cells were then washed three times with PBS. To the NP treated wells, 100 µL fresh D10 and 100 µL of the desired NP formulation suspended in D10 (supplemented with leucine (50 µg/mL) and pantothenate (24 µg/mL)) was added. NPs were prepared as mentioned in **Chapter 3** and UV-sterilized for 30 minutes before administration. Rifampicin treated wells (2 µg/mL) (positive control), *M. tuberculosis* Δ*leuD*Δ*panD*::pMV306hsp+lux untreated wells (negative control), and *M. tuberculosis* Δ*leuD*Δ*panD* untreated wells (background luminescence control) received 200 µL fresh D10 only (supplemented with leucine (50 µg/mL) and pantothenate (24 µg/mL)). In addition to untreated *in vitro M. tuberculosis* Δ*leuD*Δ*panD*::pMV306hsp+lux, *in vitro M. tuberculosis* Δ*leuD*Δ*panD*::pMV306hsp+lux were also treated with each of the NP formulations as a proof of concept highlighting the need for immune stimulation in the functioning of the particles. Based on the MTT cytotoxicity results it was decided to administer the 4 NP formulations at a concentration of 5 mg/mL since no toxicity was observed at this concentration after 72h. Each treatment was evaluated in quadruplicate (technical repeats) and the experiment itself done in triplicate (biological repeats) **(Figure 4.1)**.

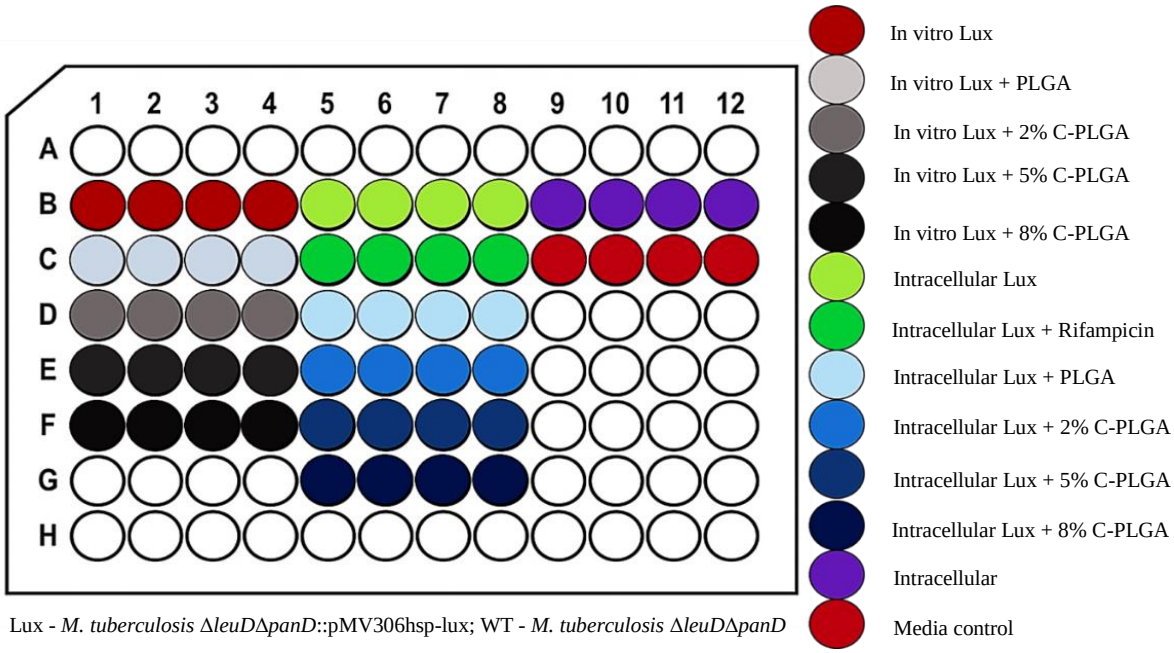


**Figure 4.1. Typical plate layout used to assess the growth inhibitory potential of C-PLGA NPs.** RAW264.7 macrophages were seeded at $5x10^4$ cells/well and infected *with M. tuberculosis* Δ*leuD*Δ*panD*::pMV306hsp-lux and *M. tuberculosis* Δ*leuD*Δ*panD* wild-type at an effective MOI of 10:1. PLGA and 2%, 5%, and 8% C-PLGA NPs were administered at 5 mg/mL and luminescence readings were obtained at 24h, 48h and 72h. Intracellular controls included rifampicin (2 µg/mL) treated *M. tuberculosis* Δ*leuD*Δ*panD*::pMV306hsp+lux (positive control), untreated *M. tuberculosis* Δ*leuD*Δ*panD*::pMV306hsp+lux (negative control), and untreated *M. tuberculosis* Δ*leuD*Δ*panD* (background luminescence control). In addition to NP treated *in vitro M. tuberculosis* Δ*leuD*Δ*panD,* untreated *M. tuberculosis* Δ*leuD*Δ*panD* was added to indicate the unrestricted growth of the bacilli. Each treatment was tested in quadruplicate (technical repeats) and the experiment was repeated three times (biological repeats).

Bioluminescence of the bacterial luciferase operon on the pMV306hsp+LuxCDABE provides a real time proxy of bacterial cell numbers and was used to measure the intracellular bacterial load at 24h, 48h and 72h. A FLUOstar microplate reader was used and the luminescence gain setting automatically adjusted to 3600. The mean luminescence of the WT *M. tuberculosis* Δ*leuD*Δ*panD* cells was subtracted from each of the respective wells to obtain the plotted relative light units (RLU'S). Confirmatory colony forming unit (CFU) plating was done after 72h on 7H10 agar supplemented with 10% OADC, 0.2% (v/v) glycerol, 1eucine (50 μg/mL) and pantothenate (24 μg/mL). Briefly, after removal of the supernatant, macrophages were lysed with $dH_2O$ and serial dilutions of the lysates plated and incubated at 37 ˚C for 21 days.

### 4.2.3 Quantification of cytokines by multiplex luminex assay

A customized mouse Multiplex Immunoassay (R&D Systems, WhiteSci) was used to simultaneously quantify the following analytes: Interferon-gamma (IFN-γ), tumor necrosis factor-alpha (TNF-α), interleukin (IL)-1β, IL-4, IL-10, and IL-12. The assay was performed according to the manufacturer's instructions and the cytokine concentrations measured on a Bio-Plex platform (Bio Plex ™, Bio-Rad laboratories).

Briefly, cell culture supernatants of the macrophage only controls, untreated macrophages containing *M. tuberculosis* Δ*leuD*Δ*panD*::pMV306hsp-lux, and *M. tuberculosis* Δ*leuD*Δ*panD*::pMV306hsp-lux treated with each of the 4 different NP formulations (PLGA, 2%, 5% and 8% C-PLGA) were collected. The cell supernatants were collected in Spin-X centrifuge tubes and possible extracellular bacilli were removed by centrifugation (1 minute, 10 000 rpm) and the flow-through was stored at -20 ˚C.

### 4.2.4 Statistical analysis

Luminescence data were analysed using GraphPad Prism v7.05 and expressed as the mean ± standard deviation (n=?). Differences between the bioluminescence means were analyzed with a two-way ANOVA and a one-way ANOVA was used for both CFU and cytokine excretion analysis. Observable differences were considered to be statistically significant if the calculated p-value was less than 0.05. If a statistically significant difference was identified, a Post hoc test would be performed to specify between which formulations the difference lie.

For luminex analysis on the Bio-Plex platform, the transformed mean fluorescent intensity values of each cytokine was used to determine the correlation coefficient ($r^2>0$) for the standard curves and the median fluorescent intensities was determined by the Bio-Plex manager software. A standard curve ranging from 12 – 3060 pg/ml for IFN-γ, 3 – 788 pg/ml for TNF-α, 249 – 60453 pg/ml for IL-1β, 62 – 15110 pg/ml for IL-4, 12 – 3029 pg/ml for IL-10 and 43-10295 pg/ml for IL-12 was used in the assay. Analytes containing below Out Of Range (<OOR) values (concentrations too low to be detected) were omitted for further interpretation.

## 4.3 Results and discussion

### 4.3.1 Assessing the intracellular killing efficacy of C-PLGA NPs

The MTT assay demonstrated no cytotoxicity for all four 2X wash NP formulations at a concentration up to 5 mg/mL after 72h **(Figure 3.5)**. It was speculated that a higher concentration of NPs present in the

suspension could increase the likelihood of cell stimulation leading to mycobacterial killing, and hence 5 mg/mL was selected for the killing assays. Since no obvious difference was observed in the physico-chemical properties of the 1X wash and 2X wash NPs, we decided to utilize 1X wash NPs to assess the effect of NPs on intracellular mycobacteria. *In vitro* cultured *M. tuberculosis* Δ*leuD*Δ*panD::*pMV306hsp-lux **(Figure 4.2A, S4.1A)** and intracellular *M. tuberculosis* Δ*leuD*Δ*panD*::pMV306hsp-lux **(Figure 4.2B, S4.1B)** were treated with 5 mg/mL of the PLGA, 2%, 5% and 8% w/w C-PLGA NPs and the expression of bioluminescence was tracked over a 3 day period using a microplate reader. A rifampicin (2 μg/mL) treated positive control was included to provide an indication of what is expected if bacterial cell death is occurring. Rifampicin was chosen due to its important role as one of the frontline anti-TB drugs. Additionally, untreated, negative controls were incorporated into our intracellular and *in vitro* experiments.

#### 4.3.1.1 Assessing mycobacterial killing using bioluminescence readings

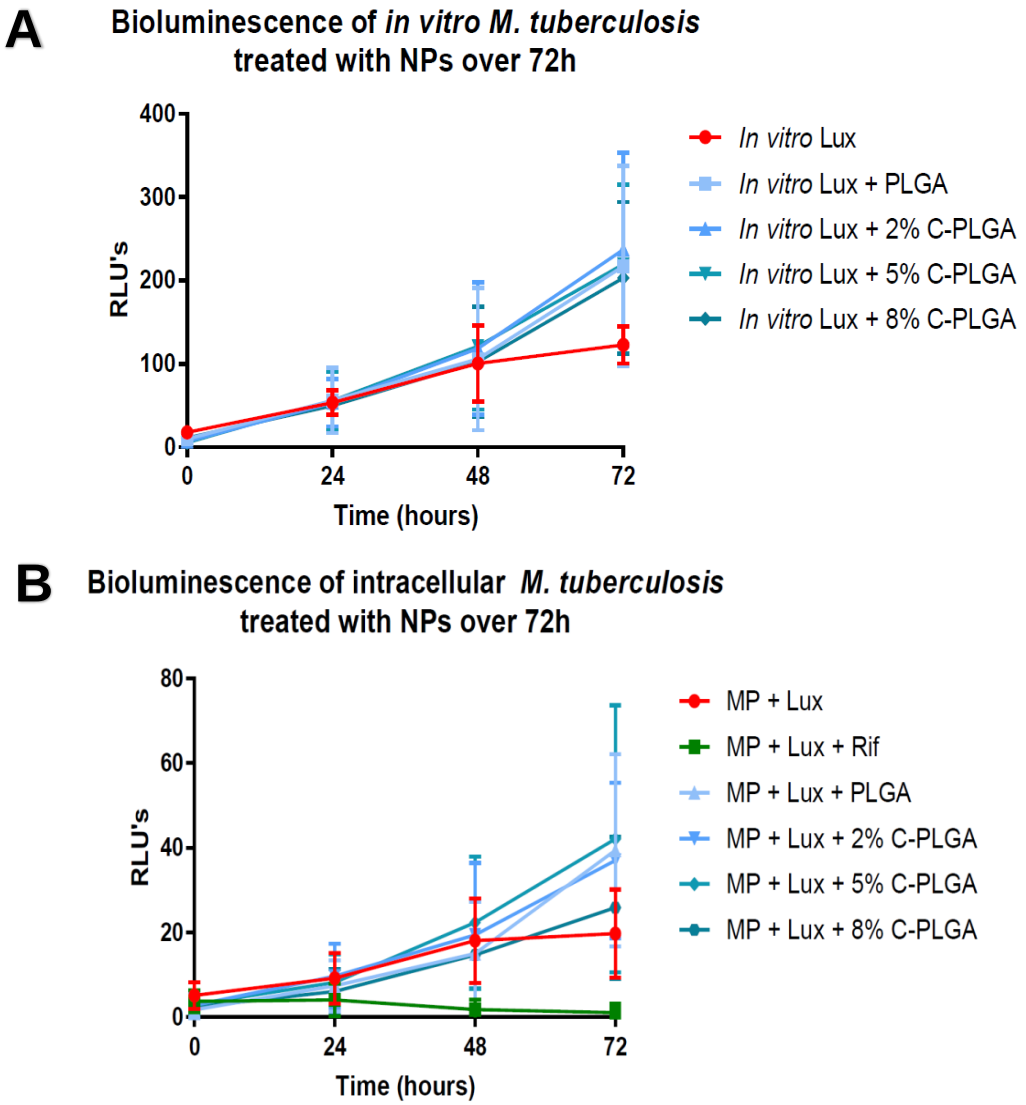


**Figure 4.2. Effect of NPs on *M. tuberculosis* cell numbers over time.** *In vitro*- cultured *M. tuberculosis* Δ*leuD*Δ*panD*::pMV306hsp-lux (A) cell numbers were compared with intracellular *M. tuberculosis* Δ*leuD*Δ*panD*::pMV306hsp-lux within RAW264.7 macrophages (B), by tracking luminescence over 72h. The intracellular and *in vitro* cultures were treated with 1X wash PLGA, 2%, 5% and 8% C-PLGA NPs at a concentration of 5 mg/mL. Untreated controls were incorporated as well as rifampicin (2 µg/mL) treated controls for the intracellular mycobacterial cells. Data is expressed as the mean of three biological repeats (quadruplicate technical repeats) with error bars indicating ±SD. A two-way ANOVA was conducted between the different treatments followed by Tukey's multiple comparisons test and a $P<0.05$ value was considered to be statistically significant. For the *in vitro* cultures (A) the only statistically significant difference was between the untreated controls and the 2% C-PLGA NP ($P=0.005$) and 8% C-PLGA NP ($P=0.019$) treated cells, respectively. With regards to the intracellular bacilli a statistically significant difference was detected between the rifampicin treated controls and the untreated cells ($P=0.0005$), the PLGA NP ($P<0.0001$), 2% C-PLGA NP ($P<0.0001$), 5% C-PLGA NP ($P<0.0001$) and 8% C-PLGA NP ($P=0.001$) treated cells, respectively. MP - Macrophage; Lux - *M. tuberculosis* Δ*leuD*Δ*panD*::pMV306hsp-lux; Rif - rifampicin

For both the *in vitro* and intracellular bacteria **(Figure 4.2A & B, S4.1A & 4.1B)**, our results show the same growth trend between the NP treated cells and the untreated controls up to 48h but at the 72h time-point the untreated controls plateau and the NP treated wells tended to increase in cell numbers. For the intracellular rifampicin treated control a reduction in RLU's is observed immediately from the 24h time-point as is expected from a bactericidal agent **(Figure 4.2B).**

The main reason for assessing NP efficacy on *in vitro* cultures was to provide a proof of concept on the functioning of host-directed therapeutic NPs. Theoretically no growth inhibitory effect is expected on *in vitro* cultured *M. tuberculosis* Δ*leuD*Δ*panD::*pMV306hsp-lux compared to intracellular *M. tuberculosis* Δ*leuD*Δ*panD::*pMV306hsp-lux. The curdlan on the surface of the NPs is expected to interact with the Dectin-1 receptor on macrophages thus stimulating a macrophage-specific antibacterial effect (Tukulula *et al.*, 2015, 2018). This is supported by our *in vitro* results where no reduction is seen in bacterial luminescence compared to that of the untreated control **(Figure 4.2A, S4.1A)**. It appeared that the addition of NPs lead to heightened expression of bioluminescence for the *in vitro* cultures although the only statistically significant difference detected was between the untreated *M. tuberculosis* Δ*leuD*Δ*panD::*pMV306hsp-lux and bacilli treated with the 2% and 5% C-PLGA NPs, respectively ($P<0.05$).

Contrary to what was expected we did not observe a reduction in bacterial luminescence for the NP treated intracellular cultures compared to the untreated controls and no specific particle was significantly superior to another **(Figure 4.2B, S4.1B)**. A statistically significant difference was detected through a Tukey's multiple comparison post-hoc test was between each of the four NP formulations and the rifampicin treated control ($P<0.05$), respectively. It was confirmed that the NPs themselves do not contribute towards an increase in the detected bioluminescence (data not shown). This suggested that the relatively high RLU's observed for the NP treated wells could be due to the enhanced growth of intracellular bacteria or the lysis of macrophages that release luminescent bacteria into the extracellular space. For the latter, the released intracellular bacteria could then grow unhindered in the media and thus contribute to misleading bioluminescence results.

Prior to assessing the efficacy of the NPs the MTT cytotoxicity assay had been performed for the 2X wash NPs only **(Figure 3.5)**. The assay was not initially carried out for the 1X wash NPs as no apparent physico-chemical difference was observed and the assumption was made that similar cytotoxicity as well as efficacy results would be obtained. However, after observing the unexpected efficacy results, a single biological repeat was completed with the 8% C-PLGA NPs **(Figure 4.3)**. Our results show a time- and dose-dependent toxic effect on the macrophages and a consequent drop in cell viability below 80% compared to the untreated controls. Due to time constraints toxicity testing of the 1X wash NPs was only repeated once and this should be investigated more extensively.

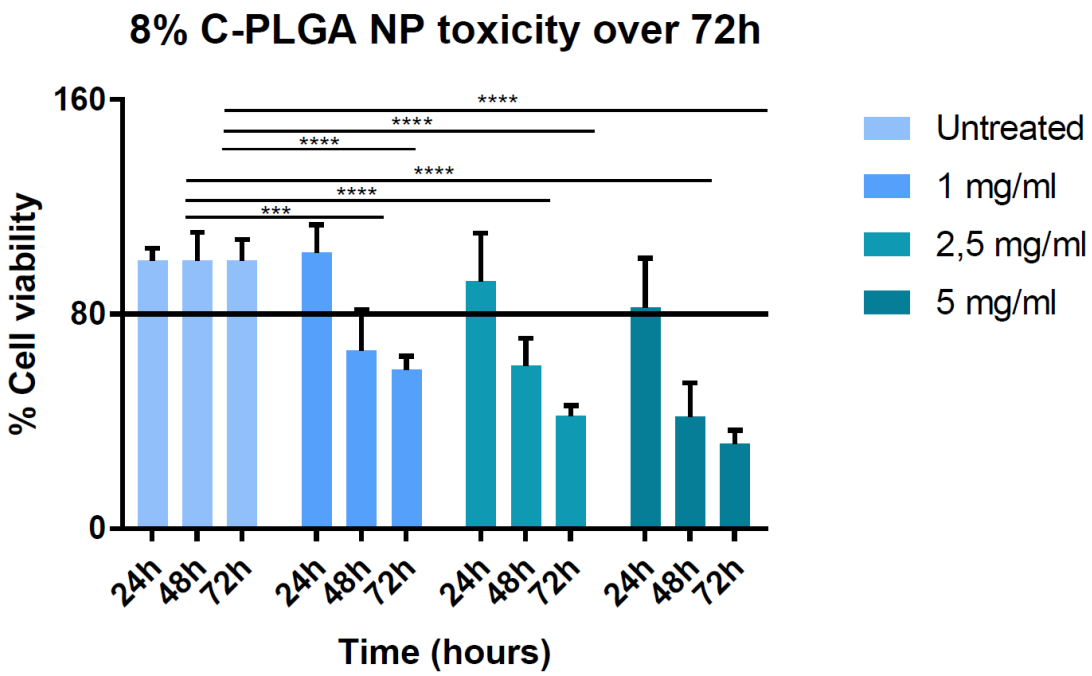


**Figure 4.3**. **MTT cytotoxicity assay with the 1X wash 8% C-PLGA NPs**: RAW264.7 macrophages were seeded at 2,5X10$^4$ cells/well after which 1X wash 8% C-PLGA NPs were administered at 1 mg/mL, 2,5 mg/mL and 5 mg/mL and absorbance obtained over a 3 day period. A two-way ANOVA was conducted to compare the means of the administered NP concentrations at each time-point with the untreated control. Significance was tested with a Tukey's multiple comparisons test and a $P<0.05$ value was considered to be statistically significant. The results are representative of a single biological repeat expressed as the mean of quadruplicate technical repeats ± SD. The NPs show a dose- and time-dependent toxic effect on the macrophages with only the 24h time point remaining above the 80% cell viability cut-off line. From 48h onwards all the treatments show a statistically significant drop in cell viability compared to the untreated controls ($P<0.05$).

The apparent toxicity of the 1X wash NPs might contribute towards lysis of the macrophages thus releasing luminescent bacteria into the extracellular space that contribute towards inaccurately high luminescent readings indicated in figure 4.2B. We assessed this theory by replacing the media of a single infection **(biological repeat 3; Figure S4.1)** at the 72h time-point and repeating the measurement. We found that an obvious drop was observed in RLU's when comparing the measurements at the single time-point before and after media replacement for the NP treated cells **(Figure 4.4)**. A possible explanation for the observed toxicity and release of bacteria might be that 1X wash NPs dispersed with more ease in D10 compared to 2X wash NPs. This could indicate that aggregates might have been present in the 2X wash NP suspension used for initial MTT cytotoxicity assays; for the more evenly suspended 1X wash NPs more particles could be taken up by the macrophages thus stimulating macrophages more effectively.

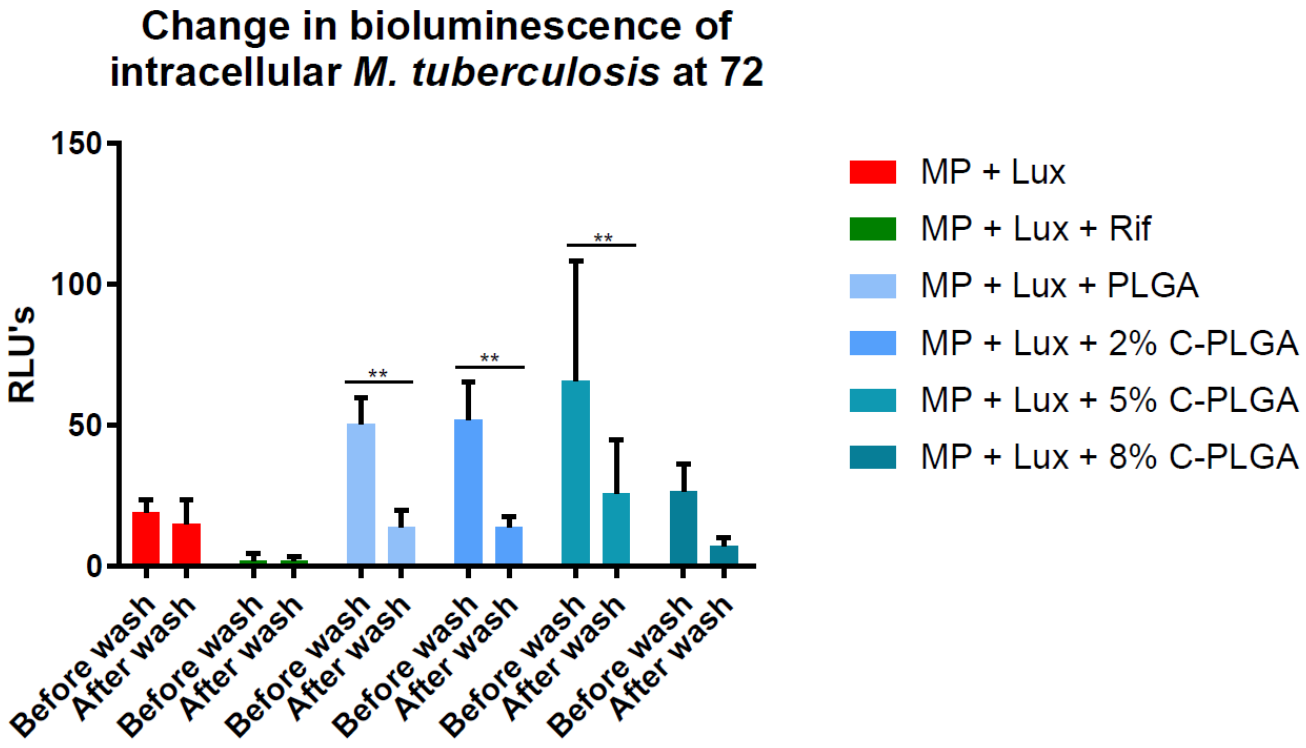


**Figure 4.4. Assessing possible 1X wash NP toxicity-related cell lysis.** RAW264.7 macrophages were infected with *M. tuberculosis* Δ*leuD*Δ*panD*::pMV306hsp-lux at an MOI 10:1. The intracellular cultures were treated with 1X wash PLGA, 2%, 5% and 8% C-PLGA NPs at a concentration of 5 mg/mL. Untreated controls were incorporated as well as rifampicin (2 µg/mL) treated controls. A two-way ANOVA was used to analyze the data and a Sidak's multiple comparisons test identified significant differences ($P<0.05$). *Indicate statistically significant differences. Data expressed as the mean of quadruplicate technical repeats with error bars indicating ±SD. At the 72h time-point, exclusively, the media was replaced with fresh D10 and bioluminescence readings were repeated. An obvious reduction in bioluminescence is present for each of the NP treated wells between the before and after wash columns.

### 4.3.1.2. Assessing mycobacterial killing using CFU plating

Contradictory to detected bioluminescence, confirmatory CFU plating of the 2%, 5% and 8% w/w C-PLGA NP treated intracellular mycobacteria showed a trend towards a reduction in viable cell numbers **(Figure 4.5, S4.2)**. However, a Tukey's multiple comparisons test indicated no clear statistically significant difference between the different NP formulations ($P>0.05$). These distinct results were unexpected since Andreu *et al.* (2013) extensively showed bioluminescence readings to correlate with CFU readouts under various intracellular and *in vitro* conditions including antibiotic treatment. A simple explanation for these distinct findings might be the aforementioned possible toxicity that leads to cell lysis and bacterial release into the extracellular space and hence confounds interpretation of the killing efficacy data. Further investigation is therefore required. However, should the observed difference in killing efficiency between curdlan loaded NPs and the PLGA only NPs prove to be true, it could indicate that possible growth inhibition could be due the speculated curdlan-receptor interaction that stimulates the Syk-dependent activation of the NF-κB pathway; also activated with *M. tuberculosis* uptake

(Wagener *et al.*, 2018). This pathway upregulates the production of oxidative species, $Ca^{2+}$ levels, various important pro-inflammatory cytokines such as TNF-α and IL-12 as well as enhancing the phagocytic tendency of particles compared to unloaded NPs into macrophages (Dube *et al.*, 2014; Tukulula *et al.*, 2015; Wagener *et al.*, 2018).

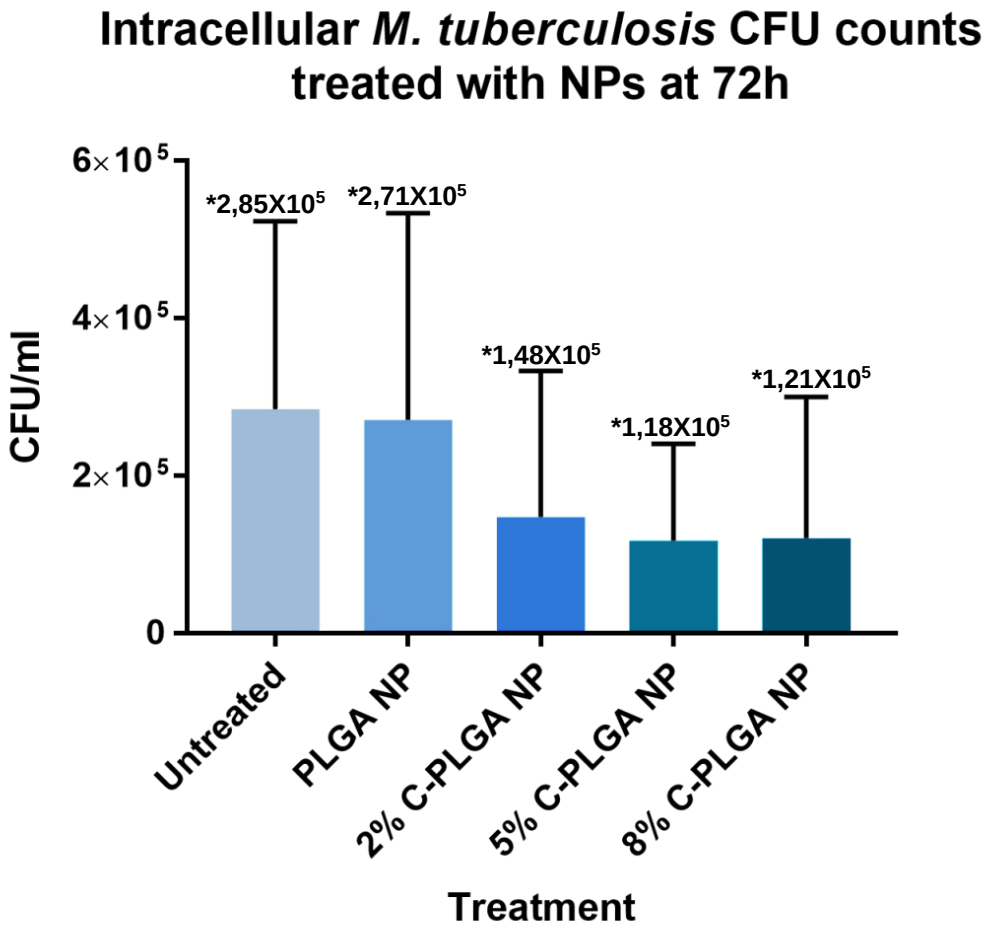


**Figure 4.5. Determination of intracellular *M. tuberculosis* Δ*leuD*Δ*panD*::pMV306hsp-lux burden by CFU plating.** RAW264.7 macrophages were infected with *M. tuberculosis* Δ*leuD*Δ*panD*::pMV306hsp-lux and treated with PLGA, 2%, 5% and 8% C-PLGA NPs for 72h and compared to untreated controls. Macrophages were lysed after 72h and the cells plated on 7H10 agar supplemented with leucine and pantothenate. Agar plates were incubated at 37 ˚C for 21 days. Data represents three biological repeats (quadruplicate technical repeats) with error bars indicating ±SD. A one-way ANOVA was used to analyze the data and a Tukey's multiple comparisons test confirmed no statistically significant differences between the treatments (P>0.05). *Indicate mean CFU of triplicate biological repeats.

### 4.3.2 Cytokine quantification

Stimulation of the NF-κB pathway through curdlan-dectin-1 interactions has been implicated numerous times in the production of important pro-inflammatory cytokines that play a central role in an effective inhibitory immune response against *M. tuberculosis* (Hetland *et al*., 1998; Dube *et al.*, 2013; Zhu *et al.*, 2015; Bouchemal *et al.*, 2019). From our panel of six cytokines that included IFN-γ, TNF-α, IL-1β, IL-4, IL-10, and -IL-12, we found that all the analytes were out of range (<OOR) except TNF-α. TNF-α secretion levels were significantly upregulated (P<0.0001) in the supernatant of the *M. tuberculosis*-infected macrophages treated with 2%, 5% and 8% C-PLGA NPs compared to PLGA only NP treated cells, the untreated controls and unstimulated-uninfected macrophages **(Figure 4.6)**.

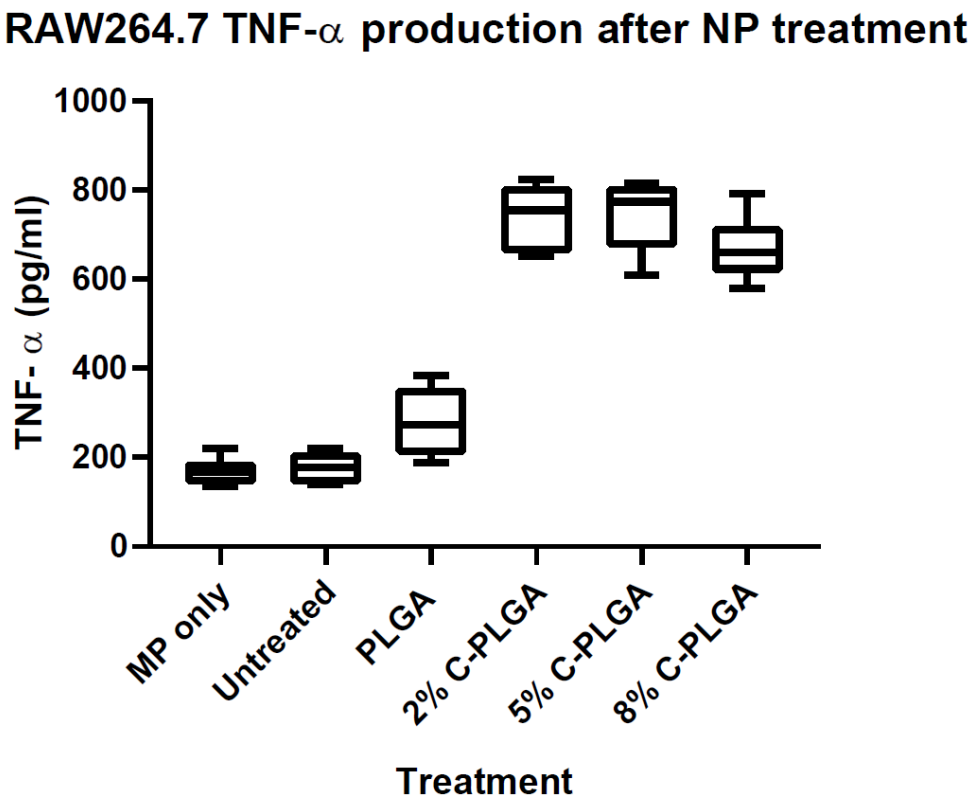


**Figure 4.6. TNF-α cytokine secretion by RAW264.7 murine macrophages due to NP stimulation.** RAW264.7 macrophages were infected with *M. tuberculosis* Δ*leuD*Δ*panD*::pMV306hsp-lux and treated with PLGA, 2%, 5% and 8% C-PLGA NPs at a concentration of 5 mg/mL. The supernatant of the macrophage-only control as well as untreated control was collected together with the NP treated wells after 72h and cytokine levels were quantified with a mouse Multiplex luminex kit. The total cytokine panel consisted out of 6 different cytokines; however, only TNF-α was within a detectable range. Data represents duplicate biological repeats (triplicate technical repeats) and the assay was performed in duplicate. A one-way ANOVA was conducted between the different treatments followed by a Tukey's multiple comparisons test and a P<0.05 value was considered to be statistically significant.

However, no statistically significant difference was observed between the 2%, 5% and 8% w/w C-PLGA NP treated cells indicating that stimulation of cytokine secretion is not dependent on the amount of curdlan loaded onto the particle as much as it is influenced by the presence of curdlan itself. It can be

speculated that this could be due to receptor saturation and that the macrophage could not be further stimulated thus reaching a plateau. The cytokine stimulating effect of curdlan present on the NPs correlated with a reduction in CFU counts for the 2%, 5% and 8% w/w C-PLGA NPs **(Figure 4.5)**. The importance of this pro-inflammatory cytokine in activating macrophages and reducing bacterial burdens is well documented and various studies have shown the aggravation of TB pathological outcomes with the addition of TNF-α neutralizing agents (Churchyard *et al.*, 2009; Cavalcanti *et al.*, 2012). In one of these studies, Lin *et al.* (2010) showed with cynomolgus macaques that treatment with TNF-α neutralizing agents lead to complete disease dissemination by 8 weeks post-infection and that anti-TNF-α agents caused disease reactivation in latently infected subjects.

Our current bacilli killing results based on luminescence and CFU readouts are inconclusive and further investigation is a necessity. However, the detection of TNF-α secretion in the cell supernatant suggest the potential immune modulatory effects of the curdlan which in turn could contribute towards bacterial killing. The direct growth inhibitory effect of curdlan on intracellular *M. tuberculosis* has recently been demonstrated by Negi *et al.* (2019); however, curdlan was exploited on its own without NPs acting as a form of carrier. In a mouse study the authors showed that the growth inhibitory effect observed on intracellular *M. tuberculosis* is due to activation of the STAT-1 and NF-κB pathways that leads to the production of nitric oxide (NO) and various important pro-inflammatory cytokines especially IL-1β, IL-12, TNF-α, and IL-6. Furthermore these authors showed with *in vivo* assessments that treatment with curdlan increases the pool of Th1 and Th17 cells and leads to an increase in memory CD4 T cells (Negi *et al.*, 2019). The killing effect of curdlan is not limited to *M. tuberculosis* alone and their findings are further supported by (Ghosh *et al.*, 2013) who showed similar *in vivo* immunomodulatory effects of curdlan on eliminating Visceral Leishmaniasis. Similar to Negi *et al*., these authors reported significant upregulation of NO as well as Th1 and Th17 associated cytokines such as IL-1β and IL-22 (Ghosh *et al.*, 2013). Stimulation of both a Th1 and Th17 immune response is promising since both these immune reaction are stimulated by *M. tuberculosis* infections (Torrado *et al.*, 2011; Lemmer *et al.*, 2015; Lyadova *et al.*, 2015). A Th1 immune response is associated with protection against TB and Th17 with TB pathology, respectively, thus a fine balance between the two responses is considered important to control the outcome of TB and the consequent overproduction of Th17 related cytokines is linked with severe tissue damage (Torrado *et al.*, 2011; Lyadova *et al.*, 2015). These statements are further supported by the observed elevated TNF-α levels; TNF-α is considered an important co-factor together with IL-1β involved in TH17 immune cell differentiation and elevated expression of TNF-α is associated with an in increase in IL-17 immune cell production (Torrado *et al.*, 2011). Hence, overproduction of TNF-α could indicate TB pathology and tissue damage but more cytokines should be analysed to further assess the exact immune milieu, and determine whether this is likely to deliver a favourable outcome or not. This would help to establish the potential of curdlan as a host directed therapeutic compound to successfully maintain an effective and safe immune response especially since excessive inflammation is one the most unknown and feared outcomes of HDT.

*M. tuberculosis*-specific killing remains to be thoroughly investigated with regards to NPs functionalised with curdlan. A proof of concept study conducted previously by our group highlighted the potential of curdlan-functionalised polycaprolactone (C-PCL) NPs to stimulate a macrophage-specific immune response that lead to the reduction in *M. tuberculosis* cell numbers **(Figure 4.7)**. This effect was only observed for intracellular bacilli and not for *in vitro* cultures thus highlighting the need for host cell stimulation to elicit a killing effect on the bacteria.

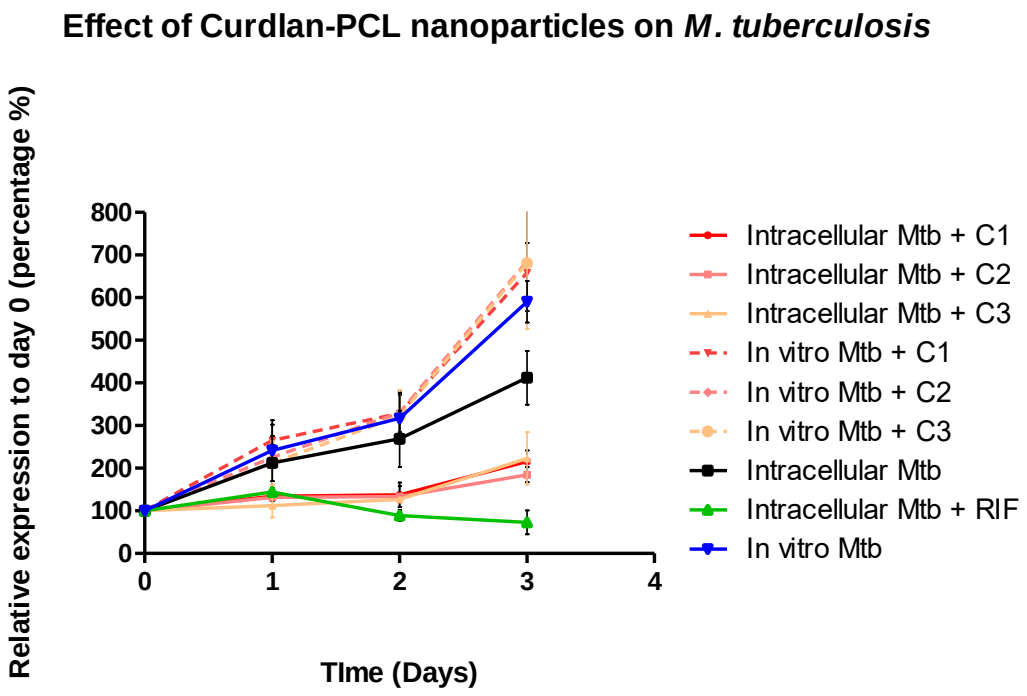


**Figure 4.7. Luminescence expression of C-PCL NP treated intracellular *M. tuberculosis*.** RAW264.7 macrophages were infected with *M. tuberculosis* H37Rv::pMV306hsp-lux and the NPs were administered to intracellular and *in vitro* cultures at 0,1 mg/mL. Rifampicin (2 µg/mL) treated and untreated controls were added as positive and negative controls, respectively. Cell viability was tracked over a 3 day period using luminescence as a proxy for cell numbers. Three different NPs were assessed containing different curdlan loads; C1 – 0,1% w/w C-PCL, C2- 1% w/w C-PCL, 2% w/w C-PCL. (Dr. Jomien Mouton, unpublished).

In literature thus far the majority of studies of functionalised NPs aim to provide insights into the macrophage-specific immune response stimulated through the ligand-receptor interactions. Thus, these studies merely provide insights about the potential of curdlan-functionalised NPs to contribute towards killing intracellular bacilli by illuminating the stimulated antibacterial immune responses. In a study done by (Tukulula *et al.*, 2015) the authors designed C-PLGA NPs and demonstrated the capability of the NPs to stimulate the production of phosphorylated ERK, an upstream mediator of oxidative species such as NO known to be toxic to intracellular bacteria. The macrophage-specific targeting of curdlan NPs are furthermore established in 2018 by Tukulula *et al*. and supported by Basha *et al*. (2019) that exploited curdlan NPs to specifically target anti-TB drugs to macrophages. Hence, in addition to illuminating the target specificity of curdlan they also indicate the potential of these NPs to effectively release drugs at the site of infection.

## 4.4 Conclusion

We have assessed the killing potential of C-PLGA NPs using intracellular *M. tuberculosis* Δ*leuD*Δ*panD*::pMV306hsp-lux. Notably, the cytotoxicity assays **(Chapter 3)** and the killing efficacy assessments **(Chapter 4)** were performed in parallel, thus the complete data for cytotoxicity was not available at the time of initiating the killing efficacy assessments. The subsequently obtained data could explain the unexpected inconsistencies that arose from the luminescence and CFU readouts, possible

cytotoxicity under the conditions used confounded interpretation of the killing assays, and this would require further investigation. However, the potential of curdlan-specific immune stimulation is supported by the upregulation of TNF-α in the supernatant of the 2%, 5% and 8% w/w C-PLGA NP treated cells. This confirms the immune stimulating capabilities of curdlan as highlighted in previously published literature, and supports further investigation of the NPs as a host-directed therapy.

# Chapter 5

## Conclusion, limitations and future recommendations

PLGA, 2%, 5% and 8% w/w C-PLGA NPs were successfully synthesized using the single emulsion solvent evaporation method. DLS analysis confirmed that the particles were in the desired size range and stable and uniform in aqueous suspension No statistically significant differences were observed when comparing the C-PLGA NPs and the PLGA NPs indicating the addition of curdlan up to 8% w/w does not alter these physico-chemical properties of the PLGA NPs and by our measures relative consistency was present throughout. We note though that previous studies have reported on possible batch-to-batch variability. This emphasizes the need to remain consistent throughout the synthesis process, and to take extreme care during the handling and production of NPs. Good record keeping on the quality and state of consumables and reagents, and consistency in the timing and circumstances during NP characterization is essential (Baer, 2018). For future studies, an additional control step to detect possible variability that might arise is the use of X-ray photoelectro spectroscopy (XPS), a sensitive surface analysis method able to identify the slightest alteration between surface properties of different NP batches (Baer, 2018). This might be an important step to incorporate when the yield of NPs needs to be up-scaled from laboratory use to commercial applications. Additionally, the incorporation of XPS could allow for more comprehensive characterization of the surface chemistry of the NPs and investigation of the biological behavior of these particles within the desired environment (Spampinato *et al.*, 2016).

An MTT assay was performed to assess the cytotoxicity of the NPs on RAW264.7 macrophages at NP concentrations of 1, 2.5 and 5 mg/mL. When performed for the 2X wash NPs, all 4 NP formulations stayed within the ISO guidelines and did not lead to a reduction below 80% in cell viability after 72h of treatment at each of the administered concentrations. We observed that the PLGA, 2% and 5% w/w C-PLGA NPs stimulated macrophage proliferation that lead to viability values above 100%; however, high variability was observed (as indicated by the standard deviation). The same proliferation was not observed for the 8% w/w C-PLGA NPs. It is speculated that this could have been due to possible agglomeration in D10 since the 8% w/w C-PLGA NPs appeared to be the least stable of all the formulations with a low average zeta potential value of -6.7 ± 6.0 mV and relatively high PDI value of 0.34 ± 0.07, and therefore a lower particle surface area (in comparison to less aggregated particles) would be present for interaction with the macrophages. Future studies are recommended to determine the particle properties in D10.

Notably, the MTT assay has some limitations, and future studies could benefit from the incorporation of assays that provide more insight into cell numbers, metabolic state and cell death pathways. When using the MTT assay, a change in viability between treated and untreated controls can be over-or underestimated due to experimental manipulations such as pipetting errors leading to inconsistent cell numbers between the wells or unknown parameters including enzymatic reactions that interfere with the assay; these factors should be considered when results are interpreted. An important limitation of the MTT assay is that the reduction of tetrazolium does not accurately reflect cell numbers but is rather an indication of cell metabolism or the rate by which glycolytic NADH is produced (Riss *et al.*, 2017). Cells that are actively growing will have a different metabolic rate than those that are deteriorating, those that have undergone differentiation and those that have grown into a confluent monolayer with not much space remaining for further proliferation. Taking into account that the MTT assay might depict metabolic

activity it is possible that the polymer NPs has the potential to stimulate mitochondrial activity that contributes towards an increase in apparent cell viability readings and the consequent variability observed. An interesting possibility is that there might be heterogeneous macrophage responses, i.e. that NPs are stimulating mitochondrial activity in one cell while other cells are being killed due to toxicity. However, enhanced metabolic activity could overshadow possible toxicity contributing to false positive outcomes. Nevertheless, this will need to be further investigated through the use of available mitochondrial inhibitors that will give a clear indication if the polymer particles are affecting mitochondrial activity or stimulating macrophage proliferation.

Alternatives to be considered for future assessments include ATP assays. These measure the production of ATP as an indicator of viable cells and are considered to be the most sensitive method to detect cell viability (Riss *et al.*, 2017). The CellTiter-GLO® Luminescent Cell Viability Assay has the benefit of generating a stable luminescent reading as a result of immediate cell lysis after the addition of the ATP assay reagent. Another alternative is the RealTime-Glo® MT Cell Viability Assay that depends on the ability of live cells to convert a pro-substrate into a substrate that can be reduced by NanoLuc® Luciferase to produce a luminescent signal. Another option would be the use of live/dead assays with florescent readouts; these lend themselves to flow cytometric measurement, and would therefore provide population-wide readouts on a single cell level. This could provide insight into heterogeneous responses within the macrophage population. Finally, as a more cost-effective option, one could use the Trypan-Blue exclusion assay that exploits the ability of the Trypan blue dye to only enter dead cells. Dead cells will be stained blue and can easily be differentiated from live cells and counted using a light microscope.

Based on the positive MTT assay results, it was decided to administer 1X wash NPs at 5 mg/mL to optimize the prospect of curdlan-macrophage interactions for further experimentation. We infected macrophages with a double auxotrophic strain expressing the bacterial luciferase gene which enabled us to track luminescence over 72h after NP administration (Sampson *et al.*, 2004; Andreu *et al.*, 2010, 2013). After 72h it appeared that the PLGA, 2%, 5% and 8% C-PLGA NPs did not have a growth inhibitory infect on the intracellular bacilli and bacterial luminescence was observed to increase; however, we showed that this might be due to luminescent bacteria released into the extracellular space due to possible macrophage lysis. Unexpected toxicity of the NPs or possible over-stimulation might cause the macrophages to lift off from the microplate surface or induce cell lysis that release viable bacilli. Curdlan-specific stimulation of the macrophages could induce excessive inflammation and the consequent upregulation of TNF-α. Although considered an important inflammatory mediator, in excessive amounts this cytokine can be associated with necrosis, a form of cell death that cause lysis of the macrophage and the release of viable *M. tuberculosis* bacilli in to immediate environment (Cavalcanti *et al.*, 2012). It is important to find an inflammatory balance and an issue frequently arising with HDT is the possible induction of a cytokine storm; an excessive inflammatory response frequently associated with increased levels of TNF-α (Gustafson *et al.*, 2016).

Contrary to bioluminescence readings, confirmatory CFU plating showed that the 2%, 5% and 8% w/w C-PLGA NPs could have an inhibitory effect that corresponds with upregulated TNF-α secretion of these specific NPs compared to untreated and PLGA NP treated cells. Keeping the possibility of cell lysis in mind which would automatically reduce the amount of available cells to plate (since only adherent macrophages are lysed for release of bacteria), this could indicate that the presence of curdlan on the NPs, independent of the percentage (w/w), stimulate a macrophage-specific immune response. Based on what is known about TNF-α, this could potentially contribute to killing of intracellular bacilli.

Upregulation of TNF-α indicates successful immune stimulation through curdlan-macrophage interactions. However, the latter requires further testing to determine whether there is a true reduction in intracellular bacterial numbers, as well as to more thoroughly assess the phenotype of the macrophage following NP treatment. In addition to being a potent pro-inflammatory cytokine, TNF-α is a biomarker frequently associated with containment of TB in latently infected patients (Cavalcanti *et al.*, 2012) and various studies have shown that the treatment with anti-TNF-α agents frequently lead to the reactivation of active TB disease (Jauregui-amezaga *et al.*, 2013; Long *et al.*, 2019). This could contribute towards discrepancies observed between the two cell viability measurements that identify different populations. Bioluminescence uses ATP as a biomarker (Andreu *et al.*, 2012) for cell viability and thus has the capacity to detect viable and uncultivable cells (Venkateswaran *et al.*, 2003). Whether this is the case here will require further investigation.

Building on these results, further optimization and intracellular and *in vivo* characterization is essential. First, translating the results from murine macrophages into mouse studies will give a more clear indication of the impact of NPs within a fully functional *in vivo* immune system. While *in vivo* mouse studies can give a clear indication on what would happen within a complete immune response, this may not reflect certain aspects of human host responses. To gain some insight into the effect of NPs on human macrophages, studies could be performed in the THP-1 cell line, a human macrophage-like system. The addition of proteins and agitation into the system used for THP-1 studies will more closely simulate physiological conditions where factors such pH and enzymatic reactions could influence NP action. This will highlight potential protein binding and immune opsonization that might influence NP functioning and localization. To enhance NP efficacy, it is possible to incorporate conventional antibiotics through surface attachments or encapsulation thus simultaneously maximizing pathogen killing and controlling inflammation. Through this multimodal approach we can deliver drugs to the specific site of infection with enhanced intracellular uptake and the sustained release of anti-TB drugs within the cell that will contribute to a reduction in daily administered dosages (Ungaro *et al.*, 2012).

We hypothesized that C-PLGA NPs have the potential to elicit an antibacterial immune response. In this study, we showed that curdlan-containing PLGA NPs stimulated TNF- α production by macrophages. Further investigation is required to determine the impact of this on intracellular bacteria, and whether this will translate to bacterial killing. This study highlights the immune stimulating potential of C-PLGA NPs and that there is potential for these NPs to be further developed into a host directed therapy for the treatment of TB."

# Supplementary material

## Chapter 3

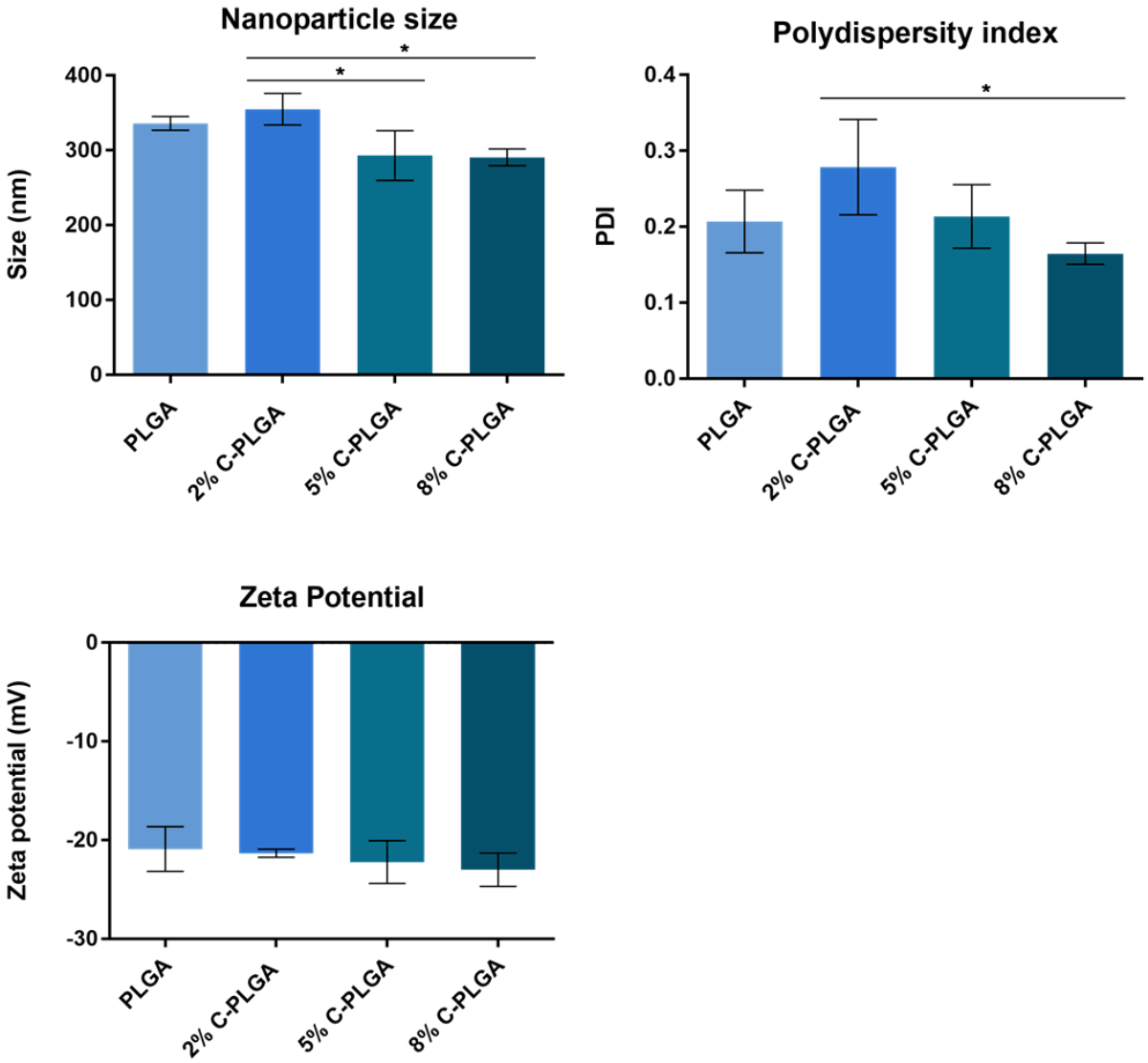


**Figure S3.1. The physiochemical parameters of the 4 different NP formulations.** The A) average size (nm), B) average PDI, C) and average zeta potential (mV) of the 1X wash PLGA, 2%, 5% and 8% C-PLGA NPs. Data represents triplicate repeats and error bars indicate ±SD. Samples were analyzed using a Malvern Zetasizer NanoZS90 at 25 ˚C. The data was analyzed using a one-way ANOVA followed by a Tukey's multiple comparisons test. A $P<0.05$ value was considered to be statistically significant. *Indicate a statistically significant difference.

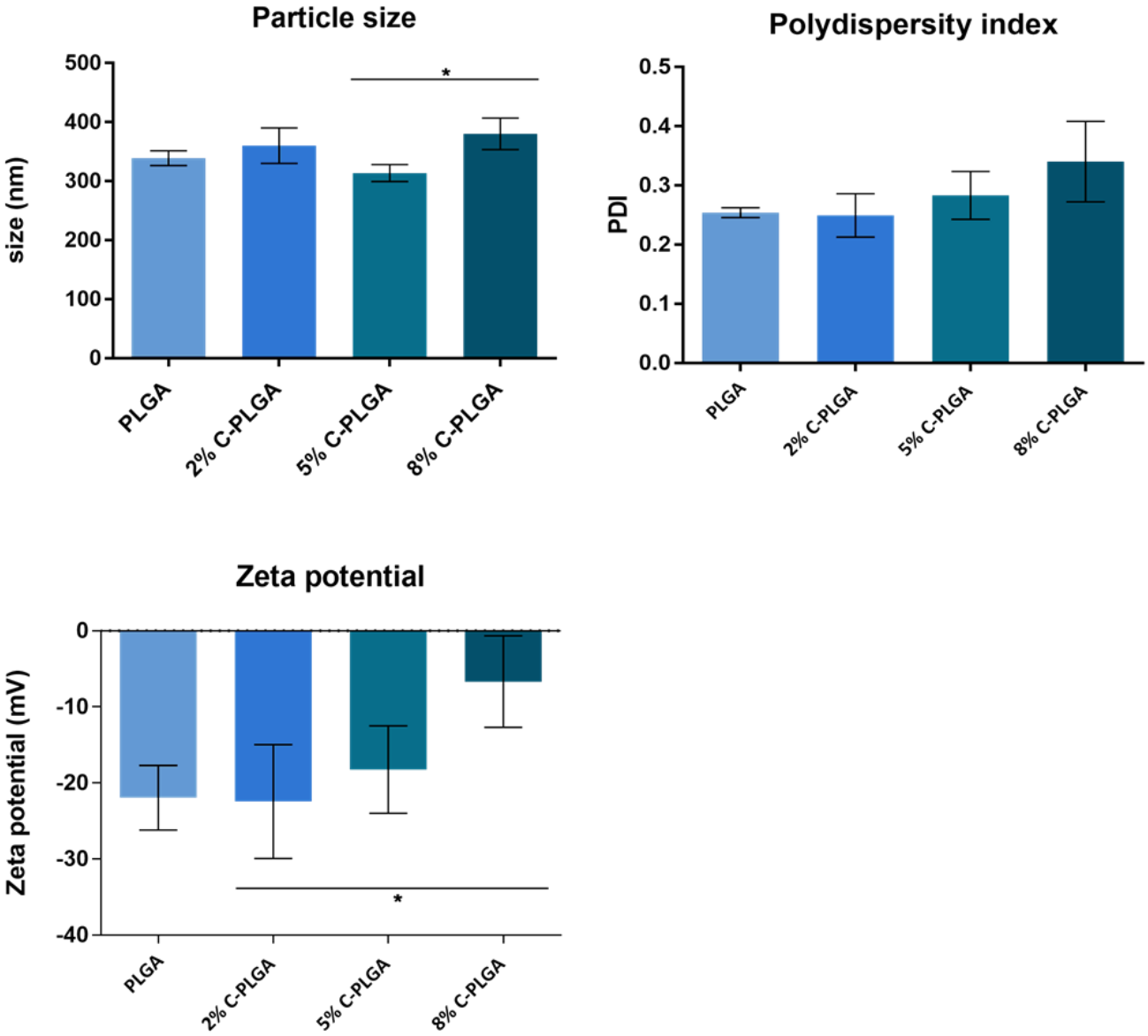


**Figure S3.2.The physiochemical parameters of the 4 different NP formulations.** The A) average size (nm), B) average PDI, C) and average zeta potential (mV) of the 2X wash PLGA, 2%, 5% and 8% C-PLGA NPs. Data represents triplicate repeats and error bars indicate ±SD. Samples were analyzed using a Malvern Zetasizer NanoZS90 at 25 ˚C. The data was analyzed using a one-way ANOVA followed by a Tukey's multiple comparisons test. A $P<0.05$ value was considered to be statistically significant. *Indicate a statistically significant difference.

# Chapter 4

**Infection 1 (Biological repeat 1)**

**A** **Bioluminescence of *in vitro M. tuberculosis* treated with NPs over 72h**

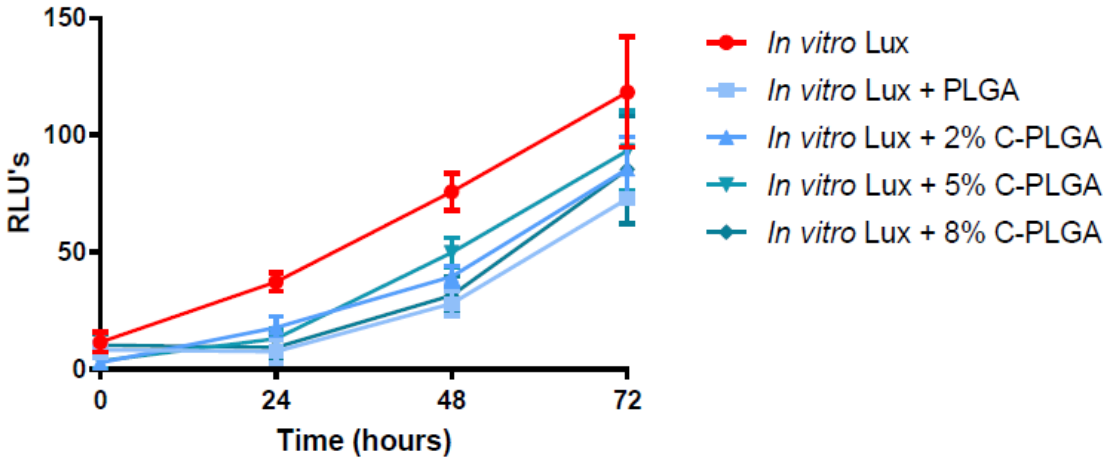


**B** **Bioluminescence of intracellular *M. tuberculosis* treated with NPs over 72h**

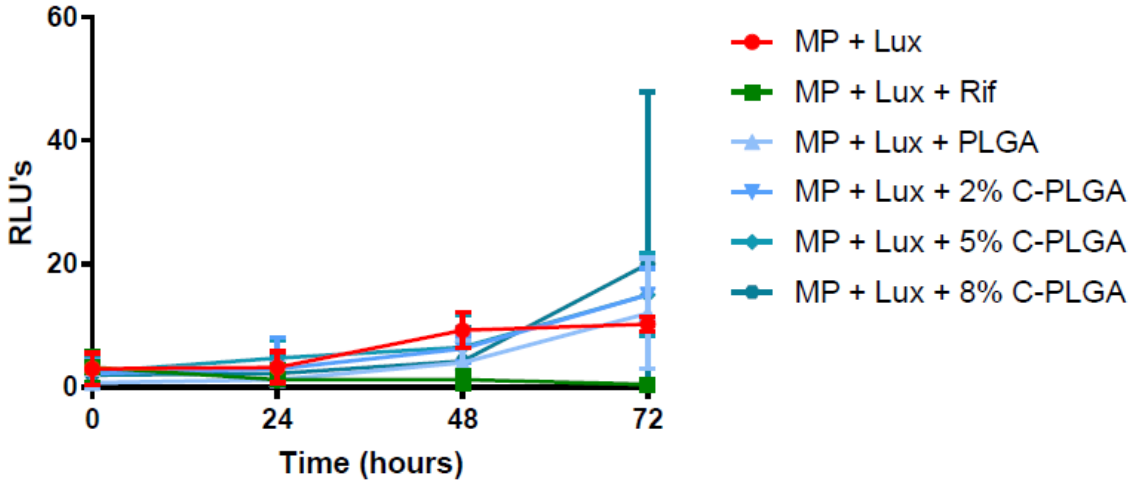

**Infection 2 (Biological repeat 2)**

**A** Bioluminescence of *in vitro M. tuberculosis* treated with NPs over 72h

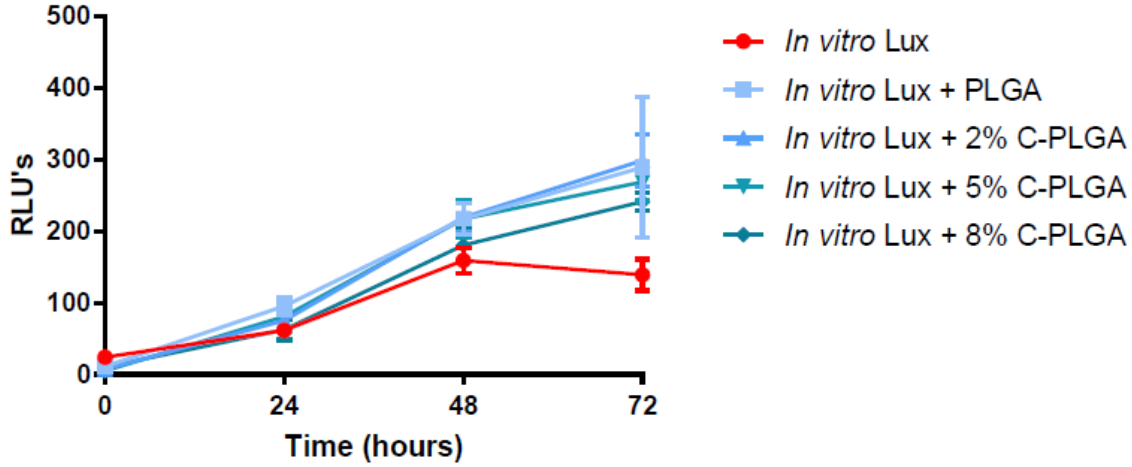


**B** Bioluminescence of intracellular *M. tuberculosis* treated with NPs over 72h

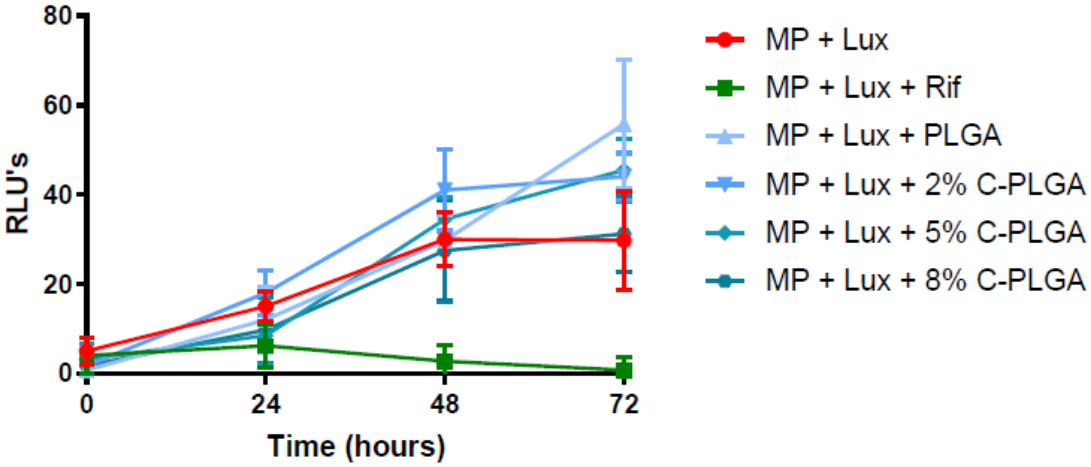

**Infection 3 (Biological repeat 3)**

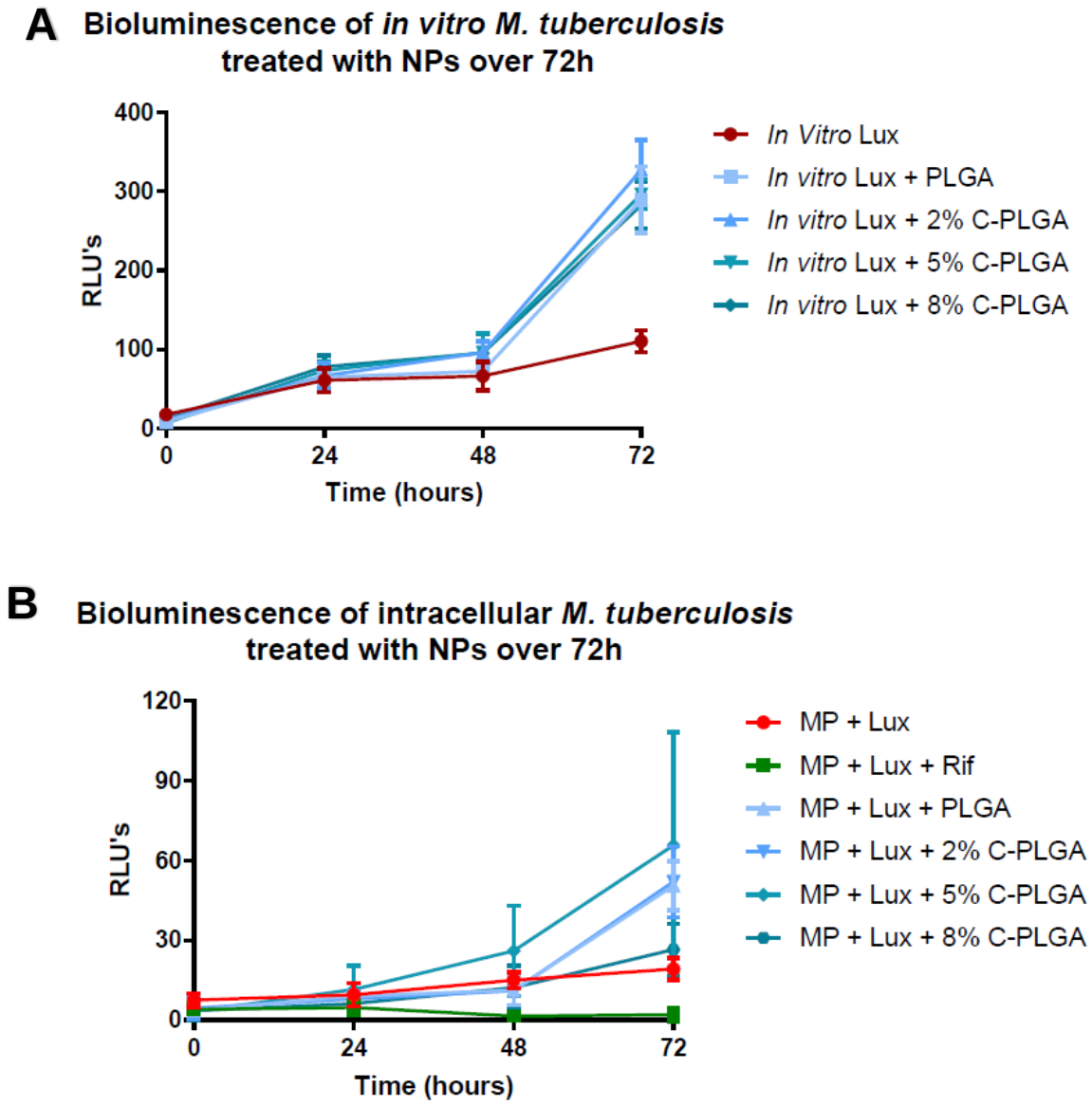


**Figure S4.1. Expression of the bacterial luciferase operon on the pMV306hsp + LuxCDABE plasmid enables us to track intracellular *M. tuberculosis* cell numbers over time.** In vitro- cultured *M. tuberculosis* Δ*leuD*Δ*panD*::pMV306hsp-lux (A) cell numbers were compared with intracellular *M. tuberculosis* Δ*leuD*Δ*panD*::pMV306hsp-lux within RAW264.7 macrophages (B), by tracking luminescence over 72h. The intracellular and in vitro cultures were treated with 1X wash PLGA, 2%, 5% and 8% C-PLGA NPs at a concentration of 5 mg/mL. Untreated controls were incorporated as well as rifampicin (2 µg/mL) treated controls for the intracellular mycobacterial cells. Data expressed as the mean of quadruplicate technical repeats with error bars indicating ±SD. A one-way ANOVA was conducted between the different treatments and a $P<0.05$ value were considered to be statistically

significant determined through a Tukey's multiple comparisons test. Each biological repeat is clustered together (A + B).

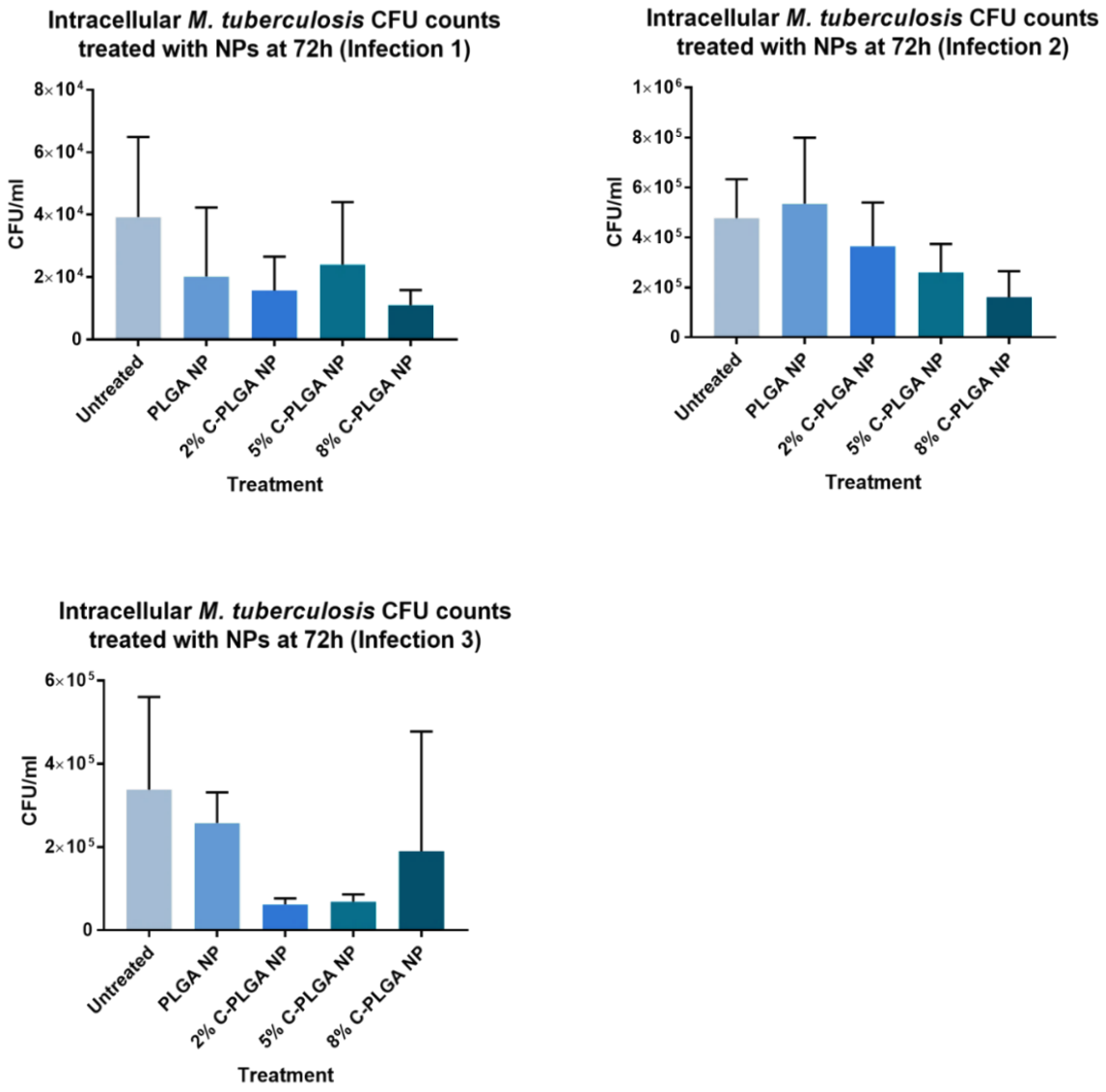


**Figure S1.2. CFU plating of *M. tuberculosis* Δ*leuD*Δ*panD*::pMV306hsp-lux.** RAW264.7 macrophages were infected with *M. tuberculosis* Δ*leuD*Δ*panD*::pMV306hsp-lux and treated with PLGA, 2%, 5% and 8% C-PLGA NPs for 72h and compared to untreated controls. Macrophages were lysed after 72h and the cells plated on 7H10 agar supplemented with leucine and pantothenate. Agar plates were incubated at 37 ˚C for 21 days. Data represents quadruplicate technical repeats with error bars indicating ±SD. A one-way ANOVA was used to analyze the data and a Tukey's multiple comparisons test confirmed no statistically significant differences between the treatments (P>0.05).

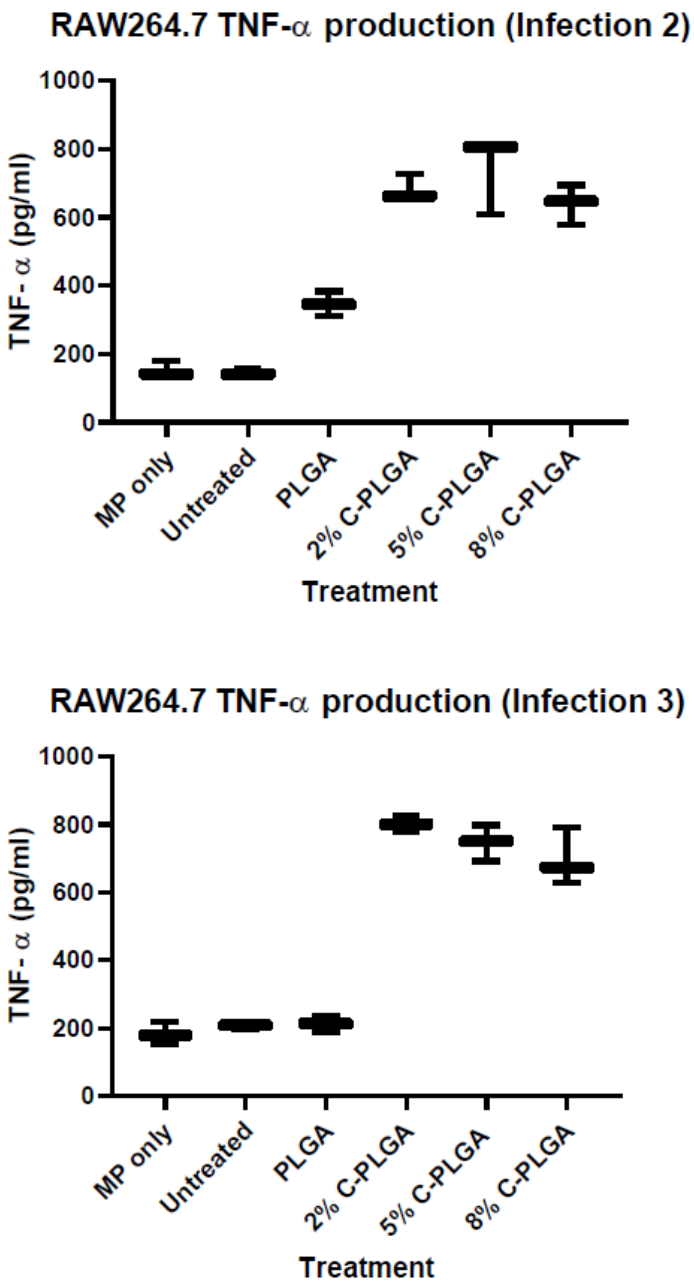


**Figure S2. TNF-α cytokine secretion by RAW264.7 murine macrophages due to NP stimulation.** RAW264.7 macrophages were infected with *M. tuberculosis* Δ*leuD*Δ*panD*::pMV306hsp-lux and treated with PLGA, 2%, 5% and 8% C-PLGA NPs at a concentration of 5 mg/mL. The supernatant of the macrophage-only controls as well as untreated controls was collected together with the NP treated wells after 72h and cytokine levels were quantified with a mouse Multiplex luminex kit. The total cytokine panel consisted out of 6 different cytokines; however, only TNF-α was within a detectable range. Data represents triplicate technical repeats and the assay was performed in duplicate. A one-way ANOVA were conducted between the different treatments followed by a Tukey's multiple comparisons test and a $P<0.05$ value was considered to be statistically significant.

# Published Literature review

Pharm Res (2019) 36:8
https://doi.org/10.1007/s11095-018-2528-9

EXPERT REVIEW

## Mycobacterium Tuberculosis and Interactions with the Host Immune System: Opportunities for Nanoparticle Based Immunotherapeutics and Vaccines

Raymonde B. Bekale[1] · Su-Mari Du Plessis[2] · Nai-Jen Hsu[3] · Jyoti R. Sharma[4] · Samantha L. Sampson[2] · Muazzam Jacobs[3,4,5] · Mervin Meyer[6] · Gene D. Morse[7] · Admire Dube[1]

Received: 23 July 2018 / Accepted: 17 October 2018


**ABSTRACT** Tuberculosis (TB) caused by *Mycobacterium tuberculosis* remains a deadly infectious disease. The thin pipeline of new drugs for TB, the ineffectiveness in adults of the only vaccine available, i.e. the Bacillus Calmette-Guerin vaccine, and increasing global antimicrobial resistance, has reinvigorated interest in immunotherapies. Nanoparticles (NPs) potentiate the effect of immune modulating compounds (IMC), enabling cell targeting, improved transfection of antigens, enhanced compound stability and provide opportunities for synergistic action, via delivery of multiple IMCs. In this review we describe work performed in the application of NPs towards achieving immune modulation for TB treatment and vaccination. Firstly, we present a comprehensive review of *M. tuberculosis* and how the bacterium modulates the host immune system. We find that current work suggest great promise of NP based immunotherapeutics as novel treatments and vaccination systems. There is need to intensify research efforts in this field, and rationally design novel NP immunotherapeutics based on current knowledge of the mycobacteriology and immune escape mechanisms employed by *M. tuberculosis*.

**KEY WORDS** immunotherapeutic nanoparticles · immunotherapy for tuberculosis · *Mycobacterium tuberculosis* · nanoparticle based host directed therapy · nanoparticles and vaccination

### ABBREVIATIONS

| | |
|---|---|
| AA | Arachidonic acid |
| AG | Arabinogalactan |
| APCs | Antigen presenting cells |
| BCG | Bacillus Calmette-Guerin |
| CaM | Calmodulin |
| CLRs | C-type lectin receptors |
| CORVET | Core vacuole/endosome tether |
| DCs | Dendritic cells |
| EEA1 | Early endosomal antigen 1 |
| ER | Endoplasmic reticulum |
| HBHA | Heparin binding hemagglutinin adhesion protein |
| HIV | Human immunodeficiency virus |

Raymonde B. Bekale and Su-Mari Du Plessis contributed equally to this work.

✉ Admire Dube
adube@uwc.ac.za

[1] Discipline of Pharmaceutics, School of Pharmacy, University of the Western Cape, Cape Town, South Africa

[2] NRF-DST Centre of Excellence for Biomedical Tuberculosis Research, South African Medical Research Council Centre for Tuberculosis Research, Division of Molecular Biology and Human Genetics, Faculty of Medicine and Health Sciences, Stellenbosch University, Cape Town, South Africa

[3] Division of Immunology, Department of Pathology, Institute of Infectious Disease and Molecular Medicine, Faculty of Health Sciences, University of Cape Town, Cape Town, South Africa

[4] National Health Laboratory Service, Johannesburg, South Africa

[5] Immunology of Infectious Disease Research Unit, South African Medical Research Council, Cape Town, South Africa

[6] DST/Mintek Nanotechnology Innovation Centre (NIC), Biolabels Unit, Department of Biotechnology, University of the Western Cape (UWC), Cape Town, South Africa

[7] AIDS Clinical Trials Group Pharmacology Specialty Laboratory, New York State Center of Excellence in Bioinformatics and Life Sciences, School of Pharmacy and Pharmaceutical Sciences, University at Buffalo, Buffalo, New York, USA

Published online: 28 November 2018

# Chapter 6

# References

Abate, G. and Hoft, D. (2016) 'Immunotherapy for tuberculosis: future prospects', *ImmunoTargets and Therapy*, p. 37. doi: 10.2147/itt.s81892.

Abdelghany, S. *et al.* (2019) 'Alginate modified-PLGA nanoparticles entrapping amikacin and moxifloxacin as a novel host-directed therapy for multidrug-resistant tuberculosis', *Journal of Drug Delivery Science and Technology*. Elsevier, 52(May), pp. 642–651. doi: 10.1016/j.jddst.2019.05.025.

Achkar, J. M., Chan, J. and Casadevall, A. (2015) 'B cells and antibodies in the defense against Mycobacterium tuberculosis infection', *Immunological Reviews*, 264(1), pp. 167–181. doi: 10.1111/imr.12276.

Ahmad, S. *et al.* (2017) 'Targeting dendritic cells through gold nanoparticles: A review on the cellular uptake and subsequent immunological properties', *Molecular Immunology*. Elsevier, 91(January), pp. 123–133. doi: 10.1016/j.molimm.2017.09.001.

Amaral, E. P., Lasunskaia, E. B. and D'Império-Lima, M. R. (2016) 'Innate immunity in tuberculosis: How the sensing of mycobacteria and tissue damage modulates macrophage death', *Microbes and Infection*, pp. 11–20. doi: 10.1016/j.micinf.2015.09.005.

Andreu, N. *et al.* (2010) 'Optimisation of Bioluminescent Reporters for Use with Mycobacteria', 5(5). doi: 10.1371/journal.pone.0010777.

Andreu, N. *et al.* (2012) 'Rapid measurement of antituberculosis drug activity in vitro and in macrophages using bioluminescence', *Journal of Antimicrobial Chemotherapy*, 67(2), pp. 404–414. doi: 10.1093/jac/dkr472.

Andreu, N. *et al.* (2013) 'Rapid in vivo assessment of drug efficacy against Mycobacterium tuberculosis using an improved firefly luciferase', (April), pp. 2118–2127. doi: 10.1093/jac/dkt155.

Baer, D. R. (2018) 'The Chameleon effect: Characterization challenges due to the variability of nanoparticles and their surfaces', *Frontiers in Chemistry*, 6(MAY), pp. 1–7. doi: 10.3389/fchem.2018.00145.

Ballester, M. *et al.* (2011) 'Nanoparticle conjugation and pulmonary delivery enhance the protective efficacy of Ag85B and CpG against tuberculosis', *Vaccine*. Elsevier Ltd, 29(40), pp. 6959–6966. doi: 10.1016/j.vaccine.2011.07.039.

Barberis, I. *et al.* (2017) 'The history of tuberculosis: From the first historical records to the isolation of Koch's bacillus', *Journal of Preventive Medicine and Hygiene*, 58(1), pp. E9–E12.

Barry, C. E. *et al.* (2009) 'The spectrum of latent tuberculosis: Rethinking the biology and intervention strategies', *Nature Reviews Microbiology*, pp. 845–855. doi: 10.1038/nrmicro2236.

Basha, Y. ., Kumar, T. S. S. and Doble, M. (2019) 'Dual delivery of tuberculosis drugs via cyclodextrin conjugated curdlan nanoparticles to infected macrophages', *Carbohydrate Polymers*. Elsevier, 218(January), pp. 53–62. doi: 10.1016/j.carbpol.2019.04.056.

Belyakov, I. M. and Ahlers, J. D. (2009) 'What Role Does the Route of Immunization Play in the

Generation of Protective Immunity against Mucosal Pathogens?', *The Journal of Immunology*, 183(11), pp. 6883–6892. doi: 10.4049/jimmunol.0901466.

Bhattacharjee, S. (2016) 'DLS and zeta potential - What they are and what they are not?', *Journal of Controlled Release*. Elsevier B.V., 235, pp. 337–351. doi: 10.1016/j.jconrel.2016.06.017.

Bivas-Benita, M. *et al.* (2009) 'Pulmonary delivery of DNA encoding Mycobacterium tuberculosis latency antigen Rv1733c associated to PLGA-PEI nanoparticles enhances T cell responses in a DNA prime/protein boost vaccination regimen in mice', *Vaccine*, 27(30), pp. 4010–4017. doi: 10.1016/j.vaccine.2009.04.033.

Bouchemal, K. *et al.* (2019) 'β-Glucan grafted microcapsule, a tool for studying the immunomodulatory effect of microbial cell wall polysaccharides', *Bioconjugate Chemistry*, p. acs.bioconjchem.9b00304. doi: 10.1021/acs.bioconjchem.9b00304.

Brown, R. M. *et al.* (2003) 'Lipoarabinomannan-Reactive Human Secretory Immunoglobulin A Responses Induced by Mucosal Bacille Calmette-Guérin Vaccination', *The Journal of Infectious Diseases*, 187(3), pp. 513–517. doi: 10.1086/368096.

Cambau, E. and Drancourt, M. (2014) 'Steps towards the discovery of Mycobacterium tuberculosis by Robert Koch, 1882', *Clinical Microbiology and Infection*. European Society of Clinical Infectious Diseases, 20(3), pp. 196–201. doi: 10.1111/1469-0691.12555.

Cambier, C. J., Falkow, S. and Ramakrishnan, L. (2014) 'Host evasion and exploitation schemes of Mycobacterium tuberculosis', *Cell*. Elsevier Inc., 159(7), pp. 1497–1509. doi: 10.1016/j.cell.2014.11.024.

Canaday, D. H. *et al.* (2001) ' CD4 + and CD8 + T Cells Kill Intracellular Mycobacterium tuberculosis by a Perforin and Fas/Fas Ligand-Independent Mechanism ', *The Journal of Immunology*, 167(5), pp. 2734–2742. doi: 10.4049/jimmunol.167.5.2734.

Carlétti, D. *et al.* (2013) 'A single dose of a DNA vaccine encoding Apa coencapsulated with 6,6=-trehalose dimycolate in microspheres confers long-term protection against tuberculosis in Mycobacterium bovis BCG-primed mice', *Clinical and Vaccine Immunology*, 20(8), pp. 1162–1169. doi: 10.1128/CVI.00148-13.

Caruso, A. M. *et al.* (1999) 'Mice deficient in CD4 T cells have only transiently diminished levels of IFN-gamma, yet succumb to tuberculosis.', *Journal of immunology (Baltimore, Md. : 1950)*, 162(9), pp. 5407–16. Available at: http://www.ncbi.nlm.nih.gov/pubmed/10228018.

Caux, C. *et al.* (1992) 'GM-CSF and TNF-alpha coorperate in the generation of denritic Langerhans cells', *Nature*, 360.

Cavalcanti, Y. V. N. *et al.* (2012) 'Role of TNF-alpha, IFN-gamma, and IL-10 in the development of pulmonary tuberculosis', *Pulmonary Medicine*. doi: 10.1155/2012/745483.

Chan, G. C.-F., Chan, W. K. and Sze, D. M. (2009) 'The effects of beta-glucan on human immune and cancer cells.', *Journal of hematology & oncology*, 2, p. 25. doi: 10.1186/1756-8722-2-25.

Chen, X. and Gao, C. (2018) 'Influences of Surface Coating of PLGA Nanoparticles on Immune Activation of Macrophages', *Journal of Materials Chemistry B*. doi: 10.1039/C7TB03080K.

Chen, Y. *et al.* (1995) 'Peripheral deletion of antigen-reactive T cells in oral tolerance', *Nature*, pp. 177–180. doi: 10.1038/376177a0.

Chiang, C. *et al.* (2018) 'Mitigating the Impact of Antibacterial Drug Resistance through Host-Directed Therapies: Current Progress, Outlook, and Challenges', *American Society for Microbiology*, 9(1).

Chua, J. and Deretic, V. (2004) 'Mycobacterium tuberculosis Reprograms Waves of Phosphatidylinositol 3-Phosphate on Phagosomal Organelles', *JOURNAL OF BIOLOGICAL CHEMISTRY*, 279(35), pp. 36982–36992. doi: 10.1074/jbc.M405082200.

Churchyard, G. J. *et al.* (2009) 'Advances in Immunotherapy for Tuberculosis Treatment', *Clinics in Chest Medicine*. Elsevier Ltd, pp. 769–782. doi: 10.1016/j.ccm.2009.08.009.

Cook, G. M. *et al.* (2009) 'Physiology of mycobacteria', *Adv. Microb Physiol.*, 55, pp. 81–319. doi: 10.1016/S0065-2911(09)05502-7.Physiology.

Cooper, A. M. *et al.* (1993) 'Disseminated tuberculosis in interferon gamma gene-distrupted mice', *J.Exp.Med.*, 178(December), pp. 2243–2247.

Dambuza, I. M. *et al.* (2016) 'Persistent p55TNFR expression impairs T cell responses during chronic tuberculosis and promotes reactivation', *Scientific Reports*. Nature Publishing Group, 6(December), pp. 1–17. doi: 10.1038/srep39499.

Danaei, M. *et al.* (2018) 'Impact of Particle Size and Polydispersity Index on the Clinical Applications of Lipidic Nanocarrier Systems', *Pharmaceutics*, 10(2), p. 57. doi: 10.3390/pharmaceutics10020057.

Danhier, F. *et al.* (2012) 'PLGA-based nanoparticles: An overview of biomedical applications', *Journal of Controlled Release*. Elsevier B.V., 161(2), pp. 505–522. doi: 10.1016/j.jconrel.2012.01.043.

Delogu, G., Sali, M. and Fadda, G. (2013) 'The biology of mycobacterium tuberculosis infection', *Mediterranean Journal of Hematology and Infectious Diseases*, 5(1). doi: 10.4084/mjhid.2013.070.

Dheda, K. *et al.* (2016) 'Tuberculosis', pp. 1211–1226.

van Dissel, J. T. *et al.* (2011) 'Ag85B-ESAT-6 adjuvanted with IC31® promotes strong and long-lived Mycobacterium tuberculosis specific T cell responses in volunteers with previous BCG vaccination or tuberculosis infection', *Vaccine*. Elsevier Ltd, 29(11), pp. 2100–2109. doi: 10.1016/j.vaccine.2010.12.135.

Dissel, J. T. Van (no date) 'Immunotherapy of Infectious Diseases : A Future for Long Forgotten Cures ?'

Dongowski, G. *et al.* (2012) 'Factors influencing β-glucan levels and molecular weight in cereal based products', *Journal of Cereal Science*, 46(4), pp. 131–141. doi: 10.1080/10408398.2013.854733.

Dube, A. *et al.* (2013) 'Multimodal nanoparticles that provide immunomodulation and intracellular drug delivery for infectious diseases', *Nanomedicine: Nanotechnology, Biology, and Medicine*. Elsevier Inc., 10(4), pp. 831–838. doi: 10.1016/j.nano.2013.11.012.

Dube, A. *et al.* (2014) 'State of the art and future directions in nanomedicine for tuberculosis', pp. 1725–1734.

Dube, A. and Reynolds, J. L. (2016) 'Modulation of Innate Immune Responses Using Nanoparticles for Infectious Disease Therapy', *Current biotechnology*, 2, pp. 60–65. doi: 10.2174/2213529402666160601120 7.

Duque, G. A. and Descoteaux, A. (2014) 'Macrophage cytokines: Involvement in immunity and infectious diseases', *Frontiers in Immunology*, pp. 1–12. doi: 10.3389/fimmu.2014.00491.

Fauci, A. S. (2018) 'Addressing the Tuberculosis Epidemic 21st Century Research for an Ancient Disease', *JAMA*, 320(13), pp. 1315–1316. doi: 10.1001/jama.2018.12852.

Fenaroli, F., Westmoreland, D., Benjaminsen, J., Kolstad, T., Skjeldal, F. M., Meijer, Annemarie H., *et al.* (2014) 'Nanoparticles as drug delivery system against tuberculosis in zebrafish embryos: Direct visualization and treatment', *ACS Nano*, 8(7), pp. 7014–7026. doi: 10.1021/nn5019126.

Fenaroli, F., Westmoreland, D., Benjaminsen, J., Kolstad, T., Skjeldal, F. M., Meijer, Annemarie H, *et al.* (2014) 'Nanoparticles as drug delivery system against tuberculosis in zebrafish embryos: Direct visualization and treatment', *ACS Nano*, 8(7), pp. 7014–7026. doi: 10.1021/nn5019126.

Flynn, J. A. L. *et al.* (1993) 'An essential role for interferon γ in resistance to mycobacterium tuberculosis infection', *Journal of Experimental Medicine*, 178(6), pp. 2249–2254. doi: 10.1084/jem.178.6.2249.

Forrellad, M. A. *et al.* (2013) 'Virulence factors of the Mycobacterium tuberculosis complex.', *Virulence*, 4(1), pp. 3–66. doi: 10.4161/viru.22329.

Frick, M. (2015) *2015 Report on Tuberculosis Research Funding Trends, 2005–2014: a Decade of Data, Treatment Action Group, New ork*. Available at: https://www.sexrightsafrica.net/wp-content/uploads/2016/12/TB-RD-Funding-Trends-2015.pdf.

Gartner, T. *et al.* (2008) 'Immunogenicity and protective efficacy of a tuberculosis DNA vaccine co-expressing pro-apoptotic caspase-3', *Vaccine*, 26(11), pp. 1458–1470. doi: 10.1016/j.vaccine.2007.12.056.

Gengenbacher, M. and Kaufmann, S. H. E. (2012) 'Mycobacterium tuberculosis: success through dormancy.', *FEMS microbiology reviews*. NIH Public Access, 36(3), pp. 514–32. doi: 10.1111/j.1574-6976.2012.00331.x.

Gengenbacher, M. and Kaufmann, S. H. E. (2013) 'Mycobacterium tuberculosis : Success through dormancy', 36(3), pp. 514–532. doi: 10.1111/j.1574-6976.2012.00331.x.Mycobacterium.

Ghosh, K. *et al.* (2013) 'Successful Therapy of Visceral Leishmaniasis With Curdlan Involves T-Helper 17 Cytokines', 207. doi: 10.1093/infdis/jis771.

Gideon, H. P. and Flynn, J. L. (2011) 'Latent tuberculosis: what the host "sees"?', *Immunologic research*, 50(2–3), pp. 202–12. doi: 10.1007/s12026-011-8229-7.

Giri, P. K., Verma, I. and Khuller, G. K. (2006) 'Enhanced immunoprotective potential of Mycobacterium tuberculosis Ag85 complex protein based vaccine against airway Mycobacterium tuberculosis challenge following intranasal administration', *FEMS Immunology and Medical Microbiology*, 47(2), pp. 233–241. doi: 10.1111/j.1574-695X.2006.00087.x.

Goodridge, H. S., Wolf, A. J. and Underhill, D. M. (2009) 'b -glucan recognition by the innate immune system', 230, pp. 38–50.

Greco, E. *et al.* (2012) 'Janus-faced liposomes enhance antimicrobial innate immune response in Mycobacterium tuberculosis infection', 109(21). doi: 10.1073/pnas.1200484109.

Griffiths, K. L. *et al.* (2016) 'Targeting dendritic cells to accelerate T-cell activation overcomes a bottleneck in tuberculosis vaccine efficacy', *Nature Communications*. Nature Publishing Group, 7, pp. 1–13. doi: 10.1038/ncomms13894.

Gülbay, B. E. *et al.* (2006) 'Side effects due to primary antituberculosis drugs during the initial phase of

therapy in 1149 hospitalized patients for tuberculosis', *Respiratory Medicine*, 100(10), pp. 1834–1842. doi: 10.1016/j.rmed.2006.01.014.

Guler, R. and Brombacher, F. (2015) 'Host-directed drug therapy for tuberculosis', *Nature Chemical Biology*. Nature Publishing Group, 11(10), pp. 748–751. doi: 10.1038/nchembio.1917.

Gustafson, H. H. *et al.* (2016) 'Nanoparticle Uptake : The Phagocyte Problem', *Nano Today.*, 10(4), pp. 487–510. doi: 10.1016/j.nantod.2015.06.006.Nanoparticle.

Harari, A. *et al.* (2011) 'disease', 17(3), pp. 372–376. doi: 10.1038/nm.2299.Dominant.

Hetland, G., Løvik, M. and Wiker, H. G. (1998) 'Protective effect of beta-glucan against mycobacterium bovis, BCG infection in BALB/c mice.', *Scandinavian journal of immunology*, 47(6), pp. 548–53. Available at: http://www.ncbi.nlm.nih.gov/pubmed/9652822.

Hett, E. C. and Rubin, E. J. (2008) 'Bacterial Growth and Cell Division: a Mycobacterial Perspective', *Microbiology and Molecular Biology Reviews*, 72(1), pp. 126–156. doi: 10.1128/MMBR.00028-07.

Hoshyar, N. *et al.* (2016) 'The effect of nanoparticle size on in vivo pharmacokinetics and cellular interaction', *Nanomedicine*, 11(6), pp. 673–692. doi: 10.2217/nnm.16.5.

Hsu, N. J. *et al.* (2017) 'Myeloid and T cell-derived TNF protects against central nervous system tuberculosis', *Frontiers in Immunology*, 8(FEB), pp. 1–12. doi: 10.3389/fimmu.2017.00180.

Hussein, J. *et al.* (2018) 'A phase I, open-label trial on the safety and immunogenicity of the adjuvanted tuberculosis subunit vaccine H1/IC31® in people living in a TB-endemic area', *Trials*. Trials, 19(1), pp. 1–10. doi: 10.1186/s13063-017-2354-0.

Hwang, J. *et al.* (2018) 'Functional silica nanoparticles conjugated with beta-glucan to deliver anti-tuberculosis drug molecules', *Journal of Industrial and Engineering Chemistry*. The Korean Society of Industrial and Engineering Chemistry, 58, pp. 376–385. doi: 10.1016/j.jiec.2017.09.051.

Jauregui-amezaga, A. *et al.* (2013) 'Risk of developing tuberculosis under anti-TNF treatment despite latent infection screening', *Journal of Crohn's and Colitis*. European Crohn's and Colitis Organisation, 7(3), pp. 208–212. doi: 10.1016/j.crohns.2012.05.012.

Jayachandran, R. *et al.* (2007) 'Survival of Mycobacteria in Macrophages Is Mediated by Coronin 1-Dependent Activation of Calcineurin', *Cell*, 130(1), pp. 37–50. doi: 10.1016/j.cell.2007.04.043.

John Chan, Simren Mehtaa, Sushma Bharrhana, Yong Chena, Jacqueline M. Achkara, Arturo Casadevalla, and J. F. (2014) 'The role of B cells and humoral immunity in Mycobacterium tuberculosis infection', *Semin Immunol.*, 26(6), pp. 588–600. doi: 10.1016/j.smim.2014.10.005.The.

Jouanguy, E. *et al.* (1997) 'Partial interferon-γ receptor 1 deficiency in a child with tuberculoid bacillus Calmette-Guerin infection and a sibling with clinical tuberculosis', *Journal of Clinical Investigation*, 100(11), pp. 2658–2664. doi: 10.1172/JCI119810.

Kaufmann, S. H. E. (2000) 'Is the development of a new tuberculosis vaccine possible?', *Nature Medicine*, 6(9), pp. 955–960. doi: 10.1038/79631.

Keeton, R. *et al.* (2014) 'Soluble TNFRp75 regulates host protective immunity against Mycobacterium tuberculosis', *Journal of Clinical Investigation*, 124(4), pp. 1537–1551. doi: 10.1172/JCI45005.

Keren, I. *et al.* (2004) 'Persister cells and tolerance to antimicrobials', *FEMS Microbiology Letters*, 230(1), pp. 13–18. doi: 10.1016/S0378-1097(03)00856-5.

Khademi, F. *et al.* (2018) 'Potential of polymeric particles as future vaccine delivery systems/adjuvants for parenteral and non-parenteral immunization against tuberculosis: A systematic review', *Iranian Journal of Basic Medical Sciences*, 21(2), pp. 116–123. doi: 10.22038/ijbms.2017.22059.5648.

Khader, S. A. *et al.* (2006) 'Interleukin 12p40 is required for dendritic cell migration and T cell priming after Mycobacterium tuberculosis infection', *Journal of Experimental Medicine*, 203(7), pp. 1805–1815. doi: 10.1084/jem.20052545.

Khoshnood, S. *et al.* (2018) 'Novel vaccine candidates against Mycobacterium tuberculosis', *International Journal of Biological Macromolecules*. Elsevier B.V., 120, pp. 180–188. doi: 10.1016/j.ijbiomac.2018.08.037.

Kirby, D. J. *et al.* (2008) 'PLGA microspheres for the delivery of a novel subunit TB vaccine', *Journal of Drug Targeting*, 16(4), pp. 282–293. doi: 10.1080/10611860801900462.

Kleinnijenhuis, J. *et al.* (2011a) 'Innate Immune Recognition of *Mycobacterium tuberculosis*', *Clinical and Developmental Immunology*, 2011, pp. 1–12. doi: 10.1155/2011/405310.

Kleinnijenhuis, J. *et al.* (2011b) 'Innate Immune Recognition of Mycobacterium tuberculosis', *Clinical and Developmental Immunology*, 2011, pp. 1–12. doi: 10.1155/2011/405310.

Kolloli, A. and Subbian, S. (2017a) 'Host-Directed Therapeutic Strategies for Tuberculosis', 4(October). doi: 10.3389/fmed.2017.00171.

Kolloli, A. and Subbian, S. (2017b) 'Host-Directed Therapeutic Strategies for Tuberculosis', *Frontiers in Medicine*, 4(October). doi: 10.3389/fmed.2017.00171.

Kusner, D. J. (2005) 'Mechanisms of mycobacterial persistence in tuberculosis', *Clinical Immunology*, pp. 239–247. doi: 10.1016/j.clim.2004.07.016.

Lahey, T. *et al.* (2013) 'Recurrent tuberculosis risk among HIV-infected adults in Tanzania with prior active tuberculosis', *Clinical Infectious Diseases*, 56(1), pp. 151–158. doi: 10.1093/cid/cis798.

Langermans, J. A. M. *et al.* (2005) 'Protection of macaques against Mycobacterium tuberculosis infection by a subunit vaccine based on a fusion protein of antigen 85B and ESAT-6', *Vaccine*, 23(21), pp. 2740–2750. doi: 10.1016/j.vaccine.2004.11.051.

Lemmer, Y. *et al.* (2015) 'Mycolic acids, a promising mycobacterial ligand for targeting of nanoencapsulated drugs in tuberculosis', *Journal of Controlled Release*. Elsevier B.V., 211, pp. 94–104. doi: 10.1016/j.jconrel.2015.06.005.

Levin, R., Grinstein, S. and Canton, J. (2016a) 'The life cycle of phagosomes : formation , maturation , and resolution', 273, pp. 156–179.

Levin, R., Grinstein, S. and Canton, J. (2016b) 'The life cycle of phagosomes: formation, maturation, and resolution', *Immunological Reviews*, 273(1), pp. 156–179. doi: 10.1111/imr.12439.

Lewis, K. (2010) 'Persister Cells', *Annual Review of Microbiology*, 64(1), pp. 357–372. doi: 10.1146/annurev.micro.112408.134306.

Li, C. *et al.* (2016) 'Gold Nanoparticles Promote Proliferation of Human Periodontal Ligament Stem Cells and Have Limited Effects on Cells Differentiation', 2016.

Lin, P. L. and Flynn, J. L. (2010) 'Understanding Latent Tuberculosis: A Moving Target', *The Journal of Immunology*. doi: 10.4049/jimmunol.0903856.

Long, W. *et al.* (2019) 'High risk of activation of latent tuberculosis infection in rheumatic disease patients High risk of activation of latent tuberculosis infection in rheumatic disease patients', *Infectious Diseases*. Taylor & Francis, 0(0), pp. 1–7. doi: 10.1080/23744235.2019.1682187.

Louw, G. E. and Sampson, S. L. (2017) 'Implications of chromosomal mutations for mycobacterial drug resistance', in *Drug Resistance in Bacteria, Fungi, Malaria, and Cancer*, pp. 233–262. doi: 10.1007/978-3-319-48683-3_10.

Lyadova, I. V and Panteleev, A. V (2015) 'Th1 and Th17 Cells in Tuberculosis : Protection , Pathology , and Biomarkers', 2015.

Makadia, H. K. and Siegel, S. J. (2011) 'Poly Lactic-co-Glycolic Acid (PLGA) as Biodegradable Controlled Drug Delivery Carrier', *Polymers*, 3(3), pp. 1377–1397. doi: 10.3390/polym3031377.

Malik, Z. A. *et al.* (2003) 'Cutting Edge: Mycobacterium tuberculosis Blocks Ca2+ Signaling and Phagosome Maturation in Human Macrophages Via Specific Inhibition of Sphingosine Kinase', *The Journal of Immunology*, 170(6), pp. 2811–2815. doi: 10.4049/jimmunol.170.6.2811.

Malik, Zulfiqar A *et al.* (2003) 'Cutting Edge: Mycobacterium tuberculosis Blocks Ca2+ Signaling and Phagosome Maturation in Human Macrophages Via Specific Inhibition of Sphingosine Kinase', *The Journal of Immunology*, 170(6), pp. 2811–2815. doi: 10.4049/jimmunol.170.6.2811.

Marrakchi, H., Lanéelle, M. A. and Daffé, M. (2014) 'Mycolic acids: Structures, biosynthesis, and beyond', *Chemistry and Biology*, 21(1), pp. 67–85. doi: 10.1016/j.chembiol.2013.11.011.

McCall, R. L. and Sirianni, R. W. (2013) 'PLGA Nanoparticles Formed by Single- or Double-emulsion with Vitamin E-TPGS', *Journal of Visualized Experiments*, (82), pp. 1–8. doi: 10.3791/51015.

Meena, L. S. and Rajni, T. (2010) 'Survival mechanisms of pathogenic Mycobacterium tuberculosis H 37Rv', *FEBS Journal*, pp. 2416–2427. doi: 10.1111/j.1742-4658.2010.07666.x.

Mei, F. *et al.* (2015) 'Synthesis and Characterization of Biodegradable Poly ( lactic-co-glycolic acid ) Synthesis and Characterization of Biodegradable', 2348. doi: 10.1080/00222348.2014.1002325.

Mercy Eleanor, G; Aditya, T; Kumar, A; Dan, M. (2016) 'Review on Mycobacterium tuberculosis', *Research and Reviews: Journal of Microbiology and Biotechnology*, 2(1), pp. 9–18. Available at: http://www.rroij.com/open-access/review-on-mycobacterium-tuberculosis-.pdf%0Ahttps://www.rroij.com/open-access/review-on-mycobacterium-tuberculosis-.pdf.

Merget, B. *et al.* (2013) 'MycPermCheck: The Mycobacterium tuberculosis permeability prediction tool for small molecules', *Bioinformatics*, 29(1), pp. 62–68. doi: 10.1093/bioinformatics/bts641.

Mouton, J. *et al.* (2019) 'Comprehensive Characterization of the Attenuated Double Auxotroph Mycobacterium tuberculosis?leuD?panCD as an Alternative to H37Rv', *Frontiers in Microbiology*, 10.

Mouton, J. M. *et al.* (2016) 'Elucidating population-wide mycobacterial replication dynamics at the single-cell level', *Microbiology (United Kingdom)*, 162(6), pp. 966–978. doi: 10.1099/mic.0.000288.

Nasiruddin, M., Neyaz, M. K. and Das, S. (2017) 'Nanotechnology-Based Approach in Tuberculosis Treatment', *Tuberculosis Research and Treatment*, 2017(Table 1), pp. 1–12. doi: 10.1155/2017/4920209.

Ndlovu, H. and Marakalala, M. J. (2016) 'Granulomas and inflammation: Host-directed therapies for tuberculosis', *Frontiers in Immunology*, 7(OCT). doi: 10.3389/fimmu.2016.00434.

Negi, S. *et al.* (2019) 'Curdlan Limits Mycobacterium tuberculosis Survival Through STAT-1 Regulated Nitric Oxide Production', 10(May), pp. 1–16. doi: 10.3389/fmicb.2019.01173.

Niederweis, M. *et al.* (2010) 'Mycobacterial outer membranes: in search of proteins', *Trends in Microbiology*, 18(3), pp. 109–116. doi: 10.1016/j.tim.2009.12.005.

O'Hogan, D. T. and Singh, M. (2003) 'Microparticles as vaccine adjuvants and delivery systems', *Expert Review of Vaccines*, 2(2), pp. 269–283. doi: 10.1586/14760584.2.2.269.

O'Leary, S., O'Sullivan, M. P. and Keane, J. (2011) 'IL-10 blocks phagosome maturation in Mycobacterium tuberculosis-infected human macrophages', *American Journal of Respiratory Cell and Molecular Biology*, 45(1), pp. 172–180. doi: 10.1165/rcmb.2010-0319OC.

Okada, M. *et al.* (2007) 'Evaluation of a novel vaccine (HVJ-liposome/HSP65 DNA + IL-12 DNA) against tuberculosis using the cynomolgus monkey model of TB', *Vaccine*, 25(16 SPEC. ISS.), pp. 2990–2993. doi: 10.1016/j.vaccine.2007.01.014.

Opitz, B. *et al.* (2013) 'Adjuvant immunotherapies as a novel approach to bacterial infections R eview Adjuvant immunotherapies as a novel approach to bacterial infections', (April). doi: 10.2217/imt.13.17.

Pagan, A. J. and Ramakrishnan, L. (2018) 'The Formation and Function of Granulomas', 63, pp. 639–665. doi: 10.1104/pp.113.222737.

Pauwels, A. M. *et al.* (2017a) 'Patterns, Receptors, and Signals: Regulation of Phagosome Maturation', *Trends in Immunology*. Elsevier Ltd, 38(6), pp. 407–422. doi: 10.1016/j.it.2017.03.006.

Pauwels, A. M. *et al.* (2017b) 'Patterns, Receptors, and Signals: Regulation of Phagosome Maturation', *Trends in Immunology*. Elsevier Ltd, pp. 407–422. doi: 10.1016/j.it.2017.03.006.

Penn-Nicholson, A. *et al.* (2018) 'Safety and immunogenicity of the novel tuberculosis vaccine ID93 + GLA-SE in BCG-vaccinated healthy adults in South Africa: a randomised, double-blind, placebo-controlled phase 1 trial', *The Lancet Respiratory Medicine*. Elsevier Ltd, 6(4), pp. 287–298. doi: 10.1016/S2213-2600(18)30077-8.

Pethe, K. *et al.* (2001) 'The heparin-binding haemagglutinin of *M. tuberculosis* is required for extrapulmonary dissemination', *Nature*, 412(6843), pp. 190–194. doi: 10.1038/35084083.

Pieters, J. (2008) 'Mycobacterium tuberculosis and the Macrophage: Maintaining a Balance', *Cell Host and Microbe*, 3(6), pp. 399–407. doi: 10.1016/j.chom.2008.05.006.

Poerio, N. *et al.* (2017) 'Liposomes loaded with bioactive lipids enhance antibacterial innate immunity irrespective of drug resistance', *Scientific Reports*. Nature Publishing Group, 7(March), pp. 1–14. doi: 10.1038/srep45120.

Prados-Rosales, R. *et al.* (2017) 'Enhanced control of Mycobacterium tuberculosis extrapulmonary dissemination in mice by an arabinomannan-protein conjugate vaccine', *PLoS Pathogens*, 13(3), pp. 1–28. doi: 10.1371/journal.ppat.1006250.

Prax, M. and Bertram, R. (2014) 'Metabolic aspects of bacterial persisters', *Frontiers in Cellular and Infection Microbiology*, 4(October), pp. 1–6. doi: 10.3389/fcimb.2014.00148.

Prendergast, K. A. and Kirman, J. R. (2013) 'Dendritic cell subsets in mycobacterial infection: Control of bacterial growth and T cell responses', *Tuberculosis*. Elsevier Ltd, 93(2), pp. 115–122. doi: 10.1016/j.tube.2012.10.008.

Queval, C. J. *et al.* (2017) 'Mycobacterium tuberculosis Controls Phagosomal Acidification by Targeting CISH-Mediated Signaling', *Cell Reports*, 20(13), pp. 3188–3198. doi: 10.1016/j.celrep.2017.08.101.

Queval, C. J., Brosch, R. and Simeone, R. (2017) 'The macrophage: A disputed fortress in the battle against Mycobacterium tuberculosis', *Frontiers in Microbiology*, 8(NOV), pp. 1–11. doi: 10.3389/fmicb.2017.02284.

RESIST-TB (2019) 'DRUG-RESISTANT TUBERCULOSIS CLINICAL TRIALS PROGRESS REPORT', (November 2019), pp. 2019–2021.

Riss, T. L. *et al.* (2017) 'Cell Viability Assays', 1601. doi: 10.1007/978-1-4939-6960-9.

Rittershaus, E. S. C., Baek, S. H. and Sassetti, C. M. (2013) 'The normalcy of dormancy: Common themes in microbial quiescence', *Cell Host and Microbe*. Elsevier Inc., 13(6), pp. 643–651. doi: 10.1016/j.chom.2013.05.012.

Rodriguez-Rivera, F. P. *et al.* (2017) 'Visualization of mycobacterial membrane dynamics in live cells', *Journal of the American Chemical Society*, 139(9), pp. 3488–3495. doi: 10.1021/jacs.6b12541.

Rosada, R. S. *et al.* (2008) 'Protection against tuberculosis by a single intranasal administration of DNA-hsp65 vaccine complexed with cationic liposomes', *BMC Immunology*, 9, pp. 1–13. doi: 10.1186/1471-2172-9-38.

Rose, F. *et al.* (2015) 'Engineering of a novel adjuvant based on lipid-polymer hybrid nanoparticles: A quality-by-design approach', *Journal of Controlled Release*. Elsevier B.V., 210, pp. 48–57. doi: 10.1016/j.jconrel.2015.05.004.

Sallusto, F. and Lanzavecchi, A. (1994) 'Efficient presentation of soluble antigen by cultured human dendritic cells is maintained by granulocyte/macrophage colony-stimulating factor plus iuterleukin 4 and downregulated by tumor necrosis factor α', *Journal of Experimental Medicine*, 179(4), pp. 1109–1118. doi: 10.1084/jem.179.4.1109.

Sampson, S. L. *et al.* (2004) 'Protection Elicited by a Double Leucine and Pantothenate Auxotroph of Mycobacterium tuberculosis in Guinea Pigs', 72(5), pp. 3031–3037. doi: 10.1128/IAI.72.5.3031.

Savic, R. M. *et al.* (2017) 'Defining the optimal dose of rifapentine for pulmonary tuberculosis: Exposure–response relations from two phase II clinical trials', *Clinical Pharmacology and Therapeutics*, 102(2), pp. 321–331. doi: 10.1002/cpt.634.

Scanga, C. A. *et al.* (2000) 'Depletion of CD4+ T cells causes reactivation of murine persistent tuberculosis despite continued expression of interferon γ and nitric oxide synthase 2', *Journal of Experimental Medicine*, 192(3), pp. 347–358. doi: 10.1084/jem.192.3.347.

Schnippel, K. *et al.* (2018) 'Effect of bedaquiline on mortality in South African patients with drug-resistant tuberculosis: a retrospective cohort study', *The Lancet Respiratory Medicine*. Elsevier Ltd, 6(9), pp. 699–706. doi: 10.1016/S2213-2600(18)30235-2.

Selwyn, P. A. *et al.* (1989) 'The New England Journal of Medicine Downloaded from nejm.org at UC SHARED JOURNAL COLLECTION on February 14, 2011. For personal use only. No other uses without permission. Copyright © 1993 Massachusetts Medical Society. All rights reserved.', *The New England journal of medicine*, 320(9). doi: 10.1056/NEJM199311113292002.

Seung, K. J. and Hewison, C. (2019) 'Now is the time for shorter all-oral regimens for multidrug-resistant tuberculosis', *The Lancet Global Health*. The Author(s). Published by Elsevier Ltd. This is an Open

Access article under the CC BY 4.0 license, 7(6), p. e706. doi: 10.1016/S2214-109X(19)30186-X.

Sharma, G. *et al.* (2010) 'Polymer particle shape independently influences binding and internalization by macrophages', *Journal of Controlled Release*. Elsevier B.V., 147(3), pp. 408–412. doi: 10.1016/j.jconrel.2010.07.116.

Shim, Y.-H. *et al.* (2006) 'Effect of cryoprotectants on the reconstitution of surfactant-free nanoparticles of poly(DL-lactide-co-glycolide)', *Journal of Microencapsulation*, 22(6), pp. 593–601. doi: 10.1080/02652040500162659.

Sikri, K. and Tyagi, J. S. (2013) 'The evolution of Mycobacterium tuberculosis dormancy models', *Current Science*, 105(5), pp. 607–616.

Silva Miranda, M. *et al.* (2012) 'The tuberculous granuloma: An unsuccessful host defence mechanism providing a safety shelter for the bacteria?', *Clinical and Developmental Immunology*, 2012. doi: 10.1155/2012/139127.

Sinha, P. *et al.* (2016) 'Differentiation of Mycobacterium tuberculosis complex from non-tubercular mycobacteria by nested multiplex PCR targeting IS6110, MTP40 and 32kD alpha antigen encoding gene fragments', *BMC Infectious Diseases*. BMC Infectious Diseases, 16(1), pp. 1–10. doi: 10.1186/s12879-016-1450-1.

Sirianni, R. W. *et al.* (2013) 'Highly penetrative, drug-loaded nanocarriers improve treatment of glioblastoma', *Proceedings of the National Academy of Sciences*, 110(29), pp. 11751–11756. doi: 10.1073/pnas.1304504110.

Smith, T., Wolff, K. A. and Nguyen, L. (2013) 'Molecular Biology of Drug Resistance in Mycobacterium tuberculosis', *Curr Top Microbiol Immunol.*, 374, pp. 53–80. doi: 10.1007/82.

Snapper, S. B. *et al.* (1990) 'Isolation and characterization of efficient plasmid transformation mutants of Mycobacterium smegmatis', *Molecular Microbiology*, 4(11), pp. 1911–1919. doi: 10.1111/j.1365-2958.1990.tb02040.x.

Spampinato, V. *et al.* (2016) 'Surface analysis of gold nanoparticles functionalized with thiol-modified glucose SAMs for biosensor applications', *Frontiers in Chemistry*, 4(FEB), pp. 1–12. doi: 10.3389/fchem.2016.00008.

Steingart, K. R. *et al.* (2009) 'Performance of purified antigens for serodiagnosis of pulmonary tuberculosis: A meta-analysis', *Clinical and Vaccine Immunology*, 16(2), pp. 260–276. doi: 10.1128/CVI.00355-08.

Stetefeld, J., McKenna, S. A. and Patel, T. R. (2016) 'Dynamic light scattering: a practical guide and applications in biomedical sciences', *Biophysical Reviews*. Biophysical Reviews, 8(4), pp. 409–427. doi: 10.1007/s12551-016-0218-6.

Stockert, J. C. *et al.* (2012) 'MTT assay for cell viability: Intracellular localization of the formazan product is in lipid droplets', *Acta Histochemica*, 114(8), pp. 785–796. doi: 10.1016/j.acthis.2012.01.006.

Stylianou, E. *et al.* (2014) 'Mucosal delivery of antigen-coated nanoparticles to lungs confers protective immunity against tuberculosis infection in mice', *European Journal of Immunology*, 44(2), pp. 440–449. doi: 10.1002/eji.201343887.

Tallieux, L. *et al.* (2003) 'DC-SIGN is the major Mycobacterium tuberculosis receptor on human dendritic cells', *Journal of Experimental Medicine*, 197(1), pp. 121–127. doi: 10.1084/jem.20021468.

Tian, T. *et al.* (2005) ' In Vivo Depletion of CD11c + Cells Delays the CD4 + T Cell Response to Mycobacterium tuberculosis and Exacerbates the Outcome of Infection ', *The Journal of Immunology*, 175(5), pp. 3268–3272. doi: 10.4049/jimmunol.175.5.3268.

Tiberi, S. *et al.* (2018) 'Tuberculosis: progress and advances in development of new drugs, treatment regimens, and host-directed therapies', *The Lancet Infectious Diseases*, 3099(18), pp. 1–16. doi: 10.1016/S1473-3099(18)30110-5.

Tobin, D. M. (2015) 'Host-Directed Therapies for Tuberculosis', *Cold Spring Harb Perspect Med*. doi: 10.1101/cshperspect.a021196.

Torrado, E. and Cooper, A. M. (2011) 'NIH Public Access', 21(6), pp. 455–462. doi: 10.1016/j.cytogfr.2010.10.004.IL-17.

Torrey, H. L. *et al.* (2016) 'High persister mutants in mycobacterium tuberculosis', *PLoS ONE*, 11(5), pp. 1–28. doi: 10.1371/journal.pone.0155127.

Tukulula, M. *et al.* (2015) 'Curdlan-conjugated PLGA nanoparticles possess macrophage stimulant activity and drug delivery capabilities', *Pharmaceutical Research*, 32(8), pp. 2713–2726. doi: 10.1007/s11095-015-1655-9.

Tukulula, M. *et al.* (2018) 'Functionalization of PLGA Nanoparticles with 1 , 3- β -glucan Enhances the Intracellular Pharmacokinetics of Rifampicin in Macrophages'. Pharmaceutical Research.

Ungaro, F. *et al.* (2012) 'Engineered PLGA nano- and micro-carriers for pulmonary delivery: Challenges and promises', *Journal of Pharmacy and Pharmacology*, pp. 1217–1235. doi: 10.1111/j.2042-7158.2012.01486.x.

De Vallière, S. *et al.* (2005) 'Enhancement of innate and cell-mediated immunity by antimycobacterial antibodies', *Infection and Immunity*, 73(10), pp. 6711–6720. doi: 10.1128/IAI.73.10.6711-6720.2005.

Vauthier, C. and Ponchel, G. (no date) *Polymer Nanoparticles for Nanomedicines*.

Velásquez, G. E. *et al.* (2018) 'Efficacy and safety of high-dose rifampin in pulmonary tuberculosis a randomized controlled trial', *American Journal of Respiratory and Critical Care Medicine*, 198(5), pp. 657–666. doi: 10.1164/rccm.201712-2524OC.

Venkateswaran, K. *et al.* (2003) 'ATP as a biomarker of viable microorganisms in clean-room facilities', *Journal of Microbiological Methods*, 52(3), pp. 367–377. doi: 10.1016/S0167-7012(02)00192-6.

Wagener, M. *et al.* (2018) 'Dectin-1-Syk-CARD9 signaling pathway in TB immunity', *Frontiers in Immunology*, pp. 1–7. doi: 10.3389/fimmu.2018.00225.

Wang, N., Liang, H. and Zen, K. (2014) 'Molecular mechanisms that influence the macrophage M1-M2 polarization balance', *Frontiers in Immunology*, 5(NOV), pp. 1–9. doi: 10.3389/fimmu.2014.00614.

Wayne, L. G. and Sohaskey, C. D. (2001) 'NONREPLICATING PERSISTENCE OF MYCOBACTERIUM TUBERCULOSIS', *Annual Review of Microbiology*, 55, pp. 139–163.

Weiss, G. and Schaible, U. E. (2015) 'Macrophage defense mechanisms against intracellular bacteria', *Immunological Reviews*, 264(1), pp. 182–203. doi: 10.1111/imr.12266.

WHO (2018) *Global tuberculosis report 2018*. Available at: https://www.who.int/tb/publications/global_report/en/.

WHO (2019) *Tuberculosis report 2019*.

WHO World Health Organization (2017) *Tuberculosis Report 2017 Global*. Available at: file:///C:/Users/hp/Downloads/9789241565516-eng.pdf%0Ahttp://apps.who.int/bookorders.%0Ahttp://apps.who.int/iris/bitstream/10665/259366/1/9789241565516-eng.pdf?ua=1.

Williams, A. *et al.* (2005) 'An assay to compare the infectivity of Mycobacterium tuberculosis isolates based on aerosol infection of guinea pigs and assessment of bacteriology', *Tuberculosis*, 85(3), pp. 177–184. doi: 10.1016/j.tube.2004.11.001.

Wolf, A. J. *et al.* (2008) 'Initiation of the adaptive immune response to Mycobacterium tuberculosis depends on antigen production in the local lymph node, not the lungs', *Journal of Experimental Medicine*, 205(1), pp. 105–115. doi: 10.1084/jem.20071367.

Wong, D. *et al.* (2011) 'Mycobacterium tuberculosis protein tyrosine phosphatase (PtpA) excludes host vacuolar-H+-ATPase to inhibit phagosome acidification', *Proceedings of the National Academy of Sciences*, 108(48), pp. 19371–19376. doi: 10.1073/pnas.1109201108.

Xu, S. *et al.* (2009) 'Phospholipase Cγ2 is critical for Dectin-1-mediated Ca2+ flux and cytokine production in dendritic cells', *Journal of Biological Chemistry*, 284(11), pp. 7038–7046. doi: 10.1074/jbc.M806650200.

Yadav, K. *et al.* (2016) 'Noscapine Loaded PLGA Nanoparticles Prepared Using Oil-in-Water Emulsion Solvent Evaporation Method', *Journal of Nanopharmaceutics and Drug Delivery*, 3(1), pp. 97–105. doi: 10.1166/jnd.2015.1074.

Yu, F. *et al.* (2012) 'Nanoparticle-based adjuvant for enhanced protective efficacy of DNA vaccine Ag85A-ESAT-6-IL-21 against Mycobacterium tuberculosis infection', *Nanomedicine: Nanotechnology, Biology, and Medicine*. Elsevier Inc., 8(8), pp. 1337–1344. doi: 10.1016/j.nano.2012.02.015.

Zainuddin, Z. F. and Dale, J. W. (1990) 'Does Mycobacterium tuberculosis have plasmids?', *Tubercle*, 71(1), pp. 43–49. doi: 10.1016/0041-3879(90)90060-L.

Zazo, H., Colino, C. I. and Lanao, J. M. (2016) 'Current applications of nanoparticles in infectious diseases', *Journal of Controlled Release*. Elsevier B.V., 224, pp. 86–102. doi: 10.1016/j.jconrel.2016.01.008.

Zhang, R. and Edgar, K. J. (2014) 'Properties, chemistry, and applications of the bioactive polysaccharide curdlan', *Biomacromolecules*, pp. 1079–1096. doi: 10.1021/bm500038g.

Zhang, W. *et al.* (2003) 'Tumour necrosis factor-α (TNF-α) transgene-expressing dendritic cells (DCs) undergo augmented cellular maturation and induce more robust T-cell activation and anti-tumour immunity than DCs generated in recombinant TNF-α', *Immunology*, 108(2), pp. 177–188. doi: 10.1046/j.1365-2567.2003.01489.x.

Zhang, Y. (2014) 'Persisters, persistent infections and the Yin-Yang model', *Emerging Microbes and Infections*, 3(November 2013), pp. 1–10. doi: 10.1038/emi.2014.3.

Zhu, C.-C. *et al.* (2015) 'Dectin-1 agonist curdlan modulates innate immunity to Aspergillus fumigatus in human corneal epithelial cells.', *International journal of ophthalmology*, 8(4), pp. 690–696. doi: 10.3980/j.issn.2222-3959.2015.04.09.